Universitat Autònoma de Barcelona

Characterization of the movement of a circadian protein in the temperature-dependent root synchronization of Arabidopsis thaliana

Weiwei Chen

Characterization of the movement of a circadian protein in the temperature-dependent root synchronization of *Arabidopsis thaliana*

PhD Thesis

Weiwei Chen

Barcelona, 2020

Facultad de Biociencias

Departamento de Biología Animal, Biología Vegetal y Ecología

Programa de Doctorado en Biología y Biotecnología Vegetal

Characterization of the movement of a circadian protein in the temperature-dependent root synchronization of *Arabidopsis thaliana*

Memoria presentada por Weiwei Chen para optar al título de doctor por la Universidad Autónoma de Barcelona

La Directora de Tesis:

Dra. Paloma Más Martínez

La Tutora de Tesis:

Dra. Roser Tolrà

El candidato a Doctor:

Weiwei Chen

Table of contents

Introduction

1. Overview of the circadian clock function

An endogenous time-keeping mechanism has been observed in almost every organism studied to date. This endogenous clock maintains robust rhythms of approximately 24 hours even under constant environmental conditions, thus the name circadian (from Latin for “about a day”). The circadian clock provides a competitive advantage in fitness and survival, regulates daily rhythms of physiology and behavior, and can be re-entrained to match the environmental conditions (Doherty and Kay, 2010).

The classical view of the circadian clock function consists of three main components: input pathways, central oscillators, and output pathways (Figure 1). The input pathways refer to all the external environmental cues and molecular components that pass time-of-day information to the central oscillator. Several environmental conditions, including light, temperature or feeding and social cues, act as main *Zeitgebers* (from the German for “time givers”) able to reset the clock every day (Crosthwaite et al., 1995). In most organisms, the central oscillator is composed of a variety of core clock components that regulated each other through several multiple transcriptional/translational interlocked feedback loops (Bell-Pedersen et al., 2005). The core clock components are genes whose protein products are important for generating and sustaining the circadian rhythms (Ko and Takahashi, 2006). The clock components receive the information from the input pathways to generate the biological rhythms in multiple output pathways including among many other, sleep-wake cycles, feeding-fasting cycles, blood pressure, hormone release, energy metabolism, locomotor activity (Kalsbeek et al., 2011; Matsuo and Ishiura, 2010). The circadian regulation ensures that all the rhythmic biological processes occur at suitable time-of-day, thus improving the organism´s fitness (Green et al., 2002; Ouyang et al., 1998).

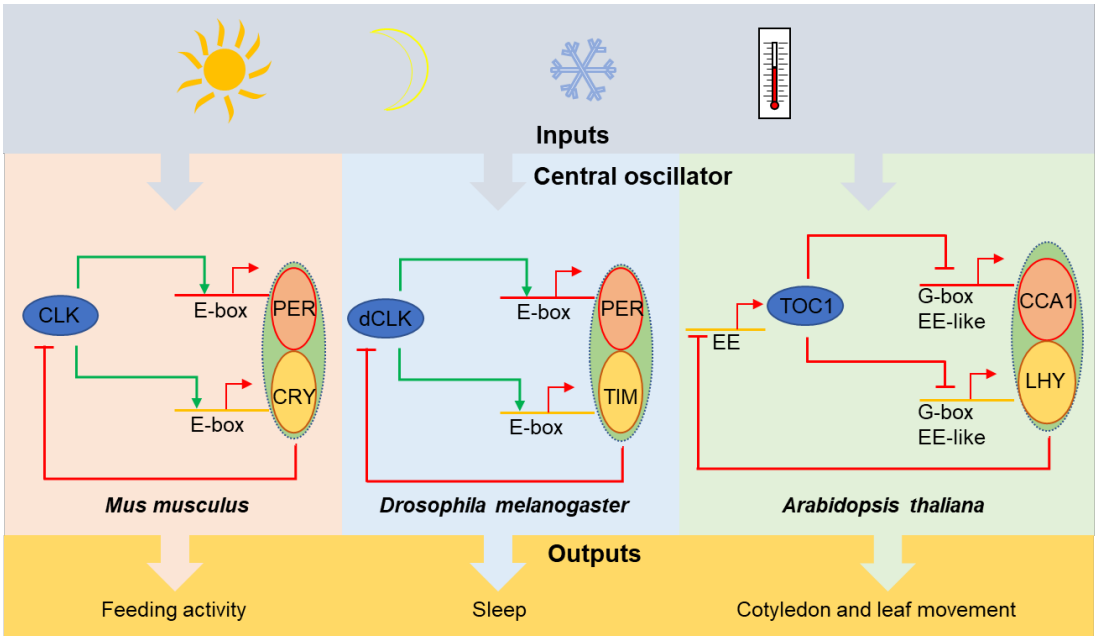

Figure 1. A simplified schematic of the similarities of the different compartments of the circadian clock among different species (*Mus musculus, Drosophila melanogaster,* and *Arabidopsis thaliana).* The simplified model consists of inputs (light, temperature), the central oscillator, and outputs. Abbreviations: CCA1, CIRCADIAN CLOCK ASSOCIATED 1; CLK, circadian locomotor output cycles protein kaput; CRY, cryptochrome; dCLK, *Drosophila* circadian locomotor output cycles protein kaput; EE, evening element; LHY, late elongated hypocotyl; PER, period; TIM, timeless; TOC1, timing of CAB expression 1. Modified from (Doherty and Kay, 2010).

The clock in most organisms shares a remarkable property known as temperature compensation, whereby the period length of the biological rhythms remains nearly unaltered over a wide range of physiological changes in temperature. The phenomenon of temperature compensation was first observed in *Drosophila* pseudoobscura pupae (Pittendrigh, 1954). The clock also exhibits a property known as nutritional compensation, whereby the period length of the biological rhythms remains the same over different nutritional supplements (Iwasaki and Dunlap, 2000). Temperature and nutritional compensation are crucial for organisms to sustain the internal 24 hours rhythms independently of the temperature or nutritional variations in the environment. The circadian clocks from different species also share other properties: the circadian clock can be re-entrained each day to match the environmental conditions; and the circadian rhythmicity driven by the circadian clock is able to maintain the 24 hours rhythmicity in the absence of changes in

environmental cues, i.e. under constant free-running conditions (Harmer, 2009; Más, 2008).

In many multicellular organisms, circadian clocks are able to generate self-sustaining and cell-autonomous oscillations in every single cell (Doherty and Kay, 2010; Jolma et al., 2010). These cellular circadian rhythms need to be integrated into a tissue or organismal level to accomplish coordinated and balanced physiological responses. It has become widely accepted in mammals the existence of hierarchical and tissue-specific functions of networked circadian clocks. The circadian clock in the suprachiasmatic nucleus (SCN) is known as a master oscillator, whereas clocks in peripheral tissues, including liver lung heart and muscle, are termed slaver oscillators (Barclay et al., 2012; Schibler and Sassone-Corsi, 2002).

2. The Plant Circadian Clock

As sessile organisms, plants cannot elude unfavorable environmental conditions. They have to cope with the changing external cues (for example, light and temperature oscillations) to properly adapt their growth and development (Sanchez and Kay, 2016). The circadian clock is the endogenous cellular mechanism that temporally coordinates this adaptation. From a simplified point of view, and as mentioned above for other organisms, the circadian system in *Arabidopsis* also consists of three main components: inputs, central oscillators, and outputs. External environmental signals (inputs) are responsible for synchronizing the internal timekeeper or the molecular mechanism responsible for tracking time (central oscillator) and generating the rhythms in multiple biological processes (outputs) (Harmer, 2009). Research over the last years has shown that this is a rather simplified organization as the circadian system is much more complex. Clock inputs could directly regulate clock output pathways and the core clock components could play some roles in the central oscillator as well as clock inputs and outputs (Harmer, 2009).

2.1 The central oscillator

The components of the central oscillator are regulated by transcriptional feedback loops (Figure 2) (Huang et al., 2016; McClung, 2019) in conjunction with additional mechanisms including post-transcriptional and post-translational regulation, and chromatin modifications (Seo and Mas, 2014). The central loop has been initially defined to be composed of two morning-expressed MYB-related transcription factors, *LATE ELONGATED HYPOCOTYL* (*LHY*) (Schaffer et al., 1998) and *CIRCADIAN CLOCK ASSOCIATED 1* (*CCA1*) (Wang and Tobin, 1998) and the dusk-expressed *TIMING OF CAB2 EXPRESSION1* (*TOC1*) or *PSEUDO RESPONSE REGULATOR1* (*PRR1*) (Makino et al., 2002; Strayer et al., 2000). CCA1 and LHY are partially redundant (Mizoguchi et al., 2002) and heterodimerize (Lu et al., 2009; Yakir et al., 2009) to perform their circadian function. Over-expression of either gene leads to arrhythmia, whereas single loss-of-function *CCA1* or *LHY* mutations exhibit a shortened period and advance phase (Green and Tobin, 1999; Mizoguchi et al., 2002; Schaffer et al., 1998; Wang and Tobin, 1998). On the other hand, the *cca1/lhy* double mutant is arrhythmic under free-running conditions (Alabadí et al., 2002). CCA1 and LHY function as negative regulators that contribute to the repression of *TOC1* (Alabadí et al., 2001) by binding to the Evening Element (EE) motif present at the *TOC1* promoter (Alabadí et al., 2002). TOC1 in turn represses *CCA1* and *LHY* expression (Gendron et al., 2012; Huang et al., 2012) and functions as a general repressor of other morning- and evening-expressed oscillator genes (Huang et al., 2012). TOC1 mutant plants exhibit a shortened period phenotype while over-expression of TOC1 causes arrhythmia in several clock outputs (Strayer et al., 2000; (Makino et al., 2002; Más et al., 2003a).

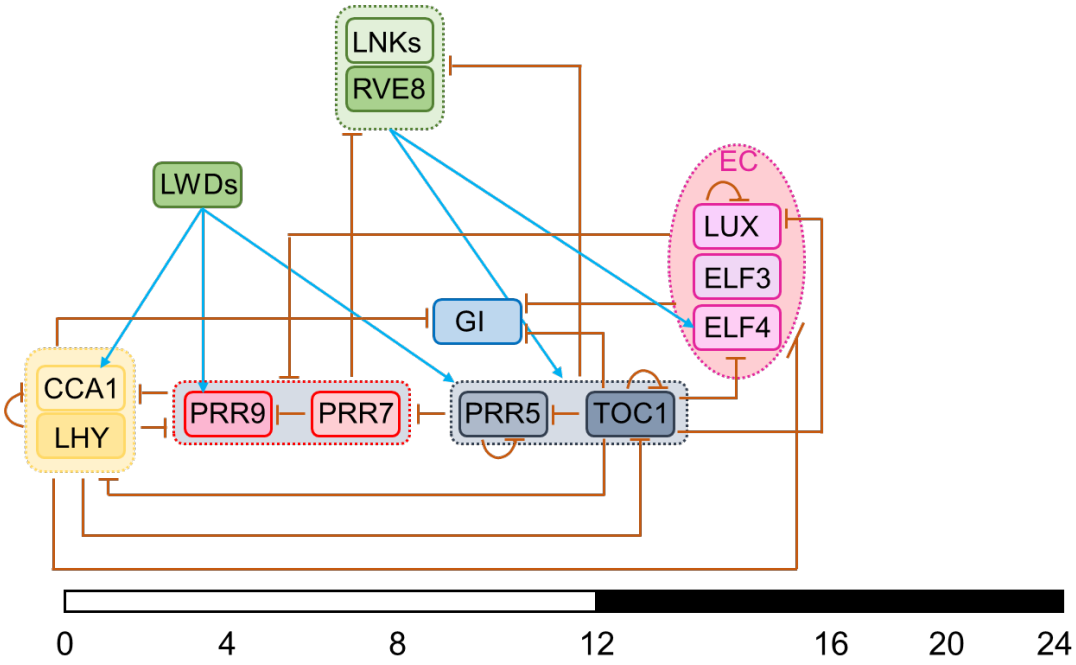

Figure 2. A simplified schematic of the transcriptional feedback loops (core circadian oscillator) in *Arabidopsis thaliana*. The sequential expression of each clock main component during a light/dark cycle is shown from left to right. The time of activity (each clock component) is displayed in hours after dawn (below the white (light) and black(dark) bar on the bottom). Clock components within a colored dashed box belong to the same circadian function group. Brown bars suggest repression of transcription, and blue arrows suggest activation. Modified from (Nohales and Kay, 2016).

TOC1 belongs to the PRR (PSEUDO-RESPONSE REGULATOR) family composed of four additional components (along with TOC1). The *PRR* genes are expressed sequentially: the *PRR9* transcript peaks close to dawn, followed by *PRR7*, *PRR5*, *PRR3*, and lastly *PRR1* at dusk (Makino et al., 2001; Mizuno and Nakamichi, 2005). *PRR9, PRR7* and *PRR5* are direct transcriptional targets repressed by CCA1 and LHY (Adams et al., 2015; Kamioka et al., 2016). PRR9 and PRR7 in conjunction with PRR5 in turn repress *CCA1* and *LHY* (Nakamichi et al., 2010).

In addition to TOC1, other circadian factors are also expressed during the night. For instance, the components of the evening complex (EC), which include the MYB-like transcription factor LUX ARRHYTHMO (LUX, also known as PHYTOCLOCK1), EARLY FLOWERING 3 (ELF3) and ELF4, two plant-specific nuclear proteins with unidentified domains (Herrero et al., 2012; Nusinow et al., 2011). The EC functions as a

transcriptional negative regulator and is directly recruited to the promoters of *PRR9*, *PRR7* and *GIGANTEA* (*GI*), and to the *LUX* promoter itself (Chow et al., 2012; Dixon et al., 2011; Helfer et al., 2011; Mizuno et al., 2014).The functions of the EC and ELF4 are further described in sections 2.5 and 2.6.

GI is a large plant-specific protein without well-characterized functional domains (Martin-Tryon et al., 2007). This gene is inhibited in the morning by CCA1 and LHY (Lu et al., 2012a), and conversely, *CCA1* and *LHY* appear to be induced by GI (Martin-Tryon et al., 2007). In the evening, TOC1 and the EC both participate in *GI* repression (Huang et al., 2012; Mizuno et al., 2014). The *gi-1* mutant exhibits a shortened period of the rhythmic reporter (*CHLOROPHYLL A/B-BINDING PROTEIN 2*, *CAB2*) and leaf movement, whereas *gi-2* mutant causes a similar shortened period of leaf movement but a lengthened period of the rhythmic reporter (*CAB2*) (Park et al., 1999). Besides, over-expression of *GI* leads to a shortened circadian period and a delayed circadian phase (measured for *COLD CIRCADIAN REGULATED2* (*CCR2*) rhythmic reporter), suggesting that *GI* plays a significant role in controlling circadian rhythms (Mizoguchi et al., 2005).

A number of transcriptional activators are observed to play important roles in the plant circadian clock. LIGHT-REGULATED WD1 (LWD1) and LWD2 are transcriptional co-activators recruited to the promoters of a set of clock genes, including *CCA1*, *PRR9*, *PRR5*, and *TOC1* (Wu et al., 2008, 2016). Three CCA1/LHY homologs, REVEILLE8 (RVE8), RVE4, and RVE6 protein form complexes with transcriptional coactivators, NIGHT LIGHT-INDUCIBLE AND CLOCK-REGULATED1 (LNK1), and LNK2 to activate expression of *PRR5*, *TOC1*, and *ELF4* (Pérez-García et al., 2015; Rugnone et al., 2013; Xie et al., 2014). Latest results show that the MYB domain of RVE8 has the DNA binding specificity, whereas the LCL domain of RVE8 could recruit LNKs to target promoters. Besides, the LNKs could recruit RNA Polymerase II and the transcript elongation FACT complex to activate rhythmically the transcription of *TOC1* and *PRR5* (Ma et al., 2018).

2.2 Input pathways

Environmental signals such as light and temperature convey time information and are required to synchronize the internal clock. The impact of light controlling the pace of the plant circadian clock is very important, and multiple regulatory levels are affected by the light intensity and quality (Nohales and Kay, 2016). Light perceived through a set of photoreceptors has been shown to be involved in setting the pace of the clock (Fankhauser and Staiger, 2002; Fehér et al., 2011; Ito et al., 2012; Jones et al., 2015). The speed of the clock increases with higher light intensity, whereas the speed of the clock slows down at lower light intensity (following the so-called Aschoff's rule) (Aschoff, 1979).

Light has the ability to acutely induce the expression of multiple core-clock genes (Farré et al., 2005; Lu et al., 2009; Rugnone et al., 2013; Wang and Tobin, 1998). Etiolated plants irradiated with light with different wavelengths for around 2 hours present an rapid response, inducing the transcription of several core clock genes including *CCA1*, *LHY*, *PRR9*, *LNK1*, *LNK3*, *ELF4*, and *TOC1* (Makino et al., 2001; Shikata et al., 2014; Tepperman et al., 2001). LWD1 and LWD2 seem to participate in the activation and light input to the plant circadian system (Wang et al., 2011; Wu et al., 2008). Light can also induce the expression of *PRR7* and *GI* (Farré et al., 2005; Park et al., 1999). This acute effect of light on the accumulation of core clock components could affect proper resetting and the regulation of expression of target genes, which would eventually affect the transcriptome.

In Arabidopsis, there are at least five families of photoreceptors: PHYTOCHROMES, CRYPTOCHROMES, the ZEITLUPE (ZTL) family, phototropins, and UV Resistance Locus 8 (UVR8) (Figure3).

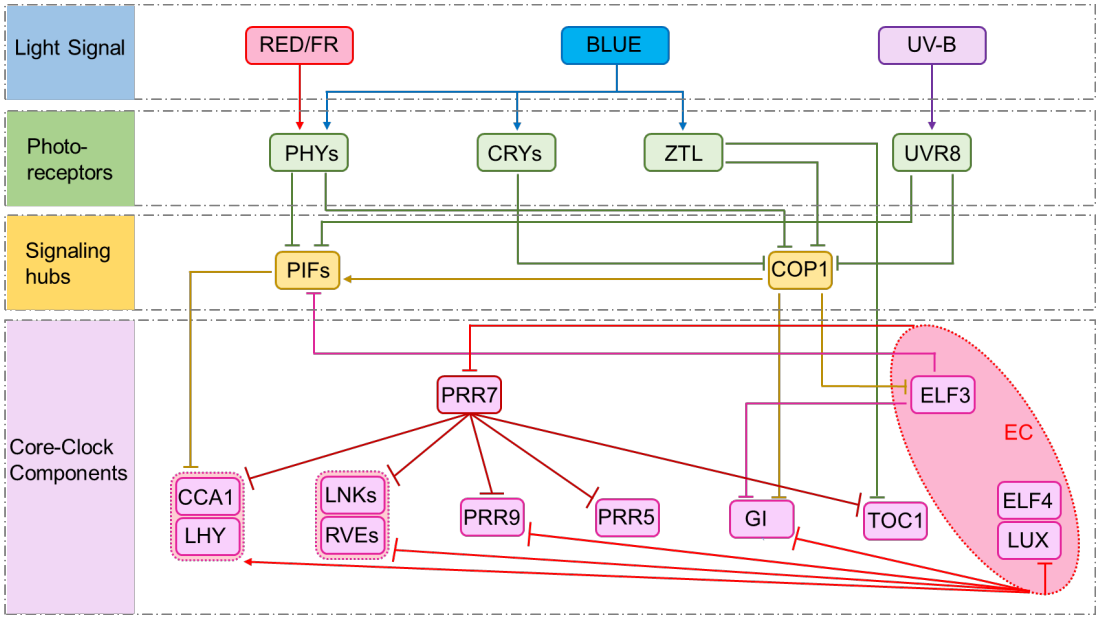

Figure 3. A simplified schematic of the crosstalk among light-signals and their integration into the circadian clock network in plants. Light signals (RED/FAR RED, BLUE, UV-B) are sensed by different groups of photoreceptors (PHYs, CRYs, ZTL, UVR8), which pass the external environmental signals to molecular signaling hubs. Core-circadian clock components are downstream targets of regulation of photoreceptors and signaling hubs. Lines with blunt ends and arrows indicate repression and activation of transcription, respectively. Abbreviations: FR, far-red; UV-B, ultraviolet-B; EC, evening complex. Modified from (Sanchez et al., 2020).

The PHYTOCHROME protein family (red and far-red light receptors) has five members, PHYA-PHYE (PHYA and PHYB play dominant Roles) (Franklin and Quail, 2010; Wang and Wang, 2015). PHYB (main red light sensor) is a major PHYTOCHROME member in light-grown seedlings, whereas PHYA (main far-red sensor that also participates in blue-light signaling) is highly abundant in dark-grown plants (Sanchez et al., 2020; Sharrock and Clack, 2002). PHYB interacts with CRY2 in the control of flowering time, hypocotyl elongation and circadian period length by the clock (Más et al., 2000). The interaction of PHYB and CONSTITUTIVE PHOTOMORPHOGENIC 1 (COP1, one E3 ubiquitin ligase) provides a direct link between ELF3 and light-signaling pathways (Liu et al., 2001a; Yu et al., 2008a). The interaction of ELF3 and COP1 enables the link between light input signaling and the circadian clock through targeted destabilization of GI (Yu et al., 2008a). Recent evidence has further revealed that PHYB plays a major role in this molecular connection, because it mediates ELF3's interaction with other

light-signaling components (Huang et al., 2016). PHYB also appears to directly interact with various clock components (CCA1, LHY, LUX, TOC1) and the interaction is differential under red and far-red light (Yeom et al., 2014).

The connection between light-signaling pathways and clock components for proper oscillator function is best demonstrated by the transcriptional regulation of the clock gene *ELF4*, whose rhythmic expression is affected by the coordination of light and the clock (Li et al., 2011a). Three positive regulators of PHYA signaling, ELONGATED HYPOCOTYL 5 (HY5), FAR RED IMPAIRED RESPONSE 1 (FAR1) and FAR RED ELONGATED HYPOCOTYL 3 (FHY3), directly bind the *ELF4* promoter and stimulate its expression (Li et al., 2011a). This binding is later repressed by the core clock proteins CCA1 and LHY, which repress *ELF4* expression in the morning (Li et al., 2011a).

PHYTOCHROMES also interact with PHYTOCHROME INTERACTING FACTORS (PIFs), which are basic helix-loop-helix (bHLH)-motif-containing transcription factors (Shin et al., 2013). PIFs are able to directly bind to the DNA G-box (CACGTG) motif to subsequently regulate the transcription of their target genes. Several clock genes (such as *LHY*, *CCA1*, *PRR9*, *PRR7*, *PRR5*, and *LUX*) have G-box motifs in their promoter region. Indeed, PIF3 has been shown to bind to *CCA1* and *LHY* promoters in vitro (Martínez-García et al., 2000). On the other hand, circadian clock proteins could regulate PIFs. TOC1 has the ability to directly repress the transcriptional-activator activity of the PIF protein (Soy et al., 2016). PIF3 protein and TOC1 protein can directly interact in plants (Soy et al., 2016).

CRYPTOCHROME 1 (CRY1) and CRY2 (members of the CRYPTOCHROME protein family) are involved in a set of blue-light-mediated physiological responses (including photomorphogenesis, de-etiolation, entrainment of the circadian clock, and flowering) (Yang et al., 2017). The mechanism linking CRYPTOCHROMES to the core of the clock components is still not fully understood but several findings provide evidence that the

circadian clock is regulated by blue light. Under constant blue light condition, *cry1* mutants exhibit a lengthened period phenotype compared with wild type (Somers et al., 1998), whereas *cry2* mutants show a more subtle phenotype (Devlin and Kay, 2000; Somers et al., 1998; Yanovsky et al., 2001). However, the double *cry1/cry2* mutant seedlings show a longer period phenotype compared with wild type or single mutant under continuous blue light (Devlin and Kay, 2000). Blue light is also able to stabilize COLD REGULATED GENE 27 (COR27) and COR28 proteins, which bind to the promoters of several clock components (such as *PRR5* and *TOC1*) and repress their transcription (Li et al., 2016). Similarly, blue light has the ability to induce HY5 and HY5-HOMOLOG (HYH) gene expression and protein abundance. HY5 has been found to associate with the promoter of several main clock genes including *CCA1*, *PRR9*, and *LUX* in a light-quality-dependent manner (Hajdu et al., 2018; Li et al., 2011a). Under blue light, the association of HY5 to the promoters of several clock genes (*PRR5*, *LUX*, and *BROTHER OF LUX ARRHYTHMO* (*BOA*) is increased and correlated with changes in their expression (Hajdu et al., 2018; Li et al., 2011a).

Blue-light perception can be also achieved through the ZTL family of photoreceptors, composed of three members: ZTL, FKF1 (FLAVIN-BINDING, KELCH REPEAT, F-BOX 1), and LKP2 (LOV KELCH PROTEIN 2) (Nelson et al., 2000; Schultz et al., 2001; Somers et al., 2000). ZTL, FKF1, and LKP2 have partially overlapping functions in the regulation of the circadian function. ZTL is involved in the targeted degradation of PRR5 and TOC1 protein (Kiba et al., 2007; Más et al., 2003b), and similarly, ZTL has been shown to mediates ubiquitylation of CCA1 HIKING EXPEDITION (CHE) and regulate its stability in a light-dependent and ubiquitin proteasome system-dependent manner (Lee et al., 2018; Pruneda-Paz et al., 2009).

Ultraviolet-B (UV-B) light (280–315 nm) is sensed by UV Resistance Locus 8 (UVR8) (Rizzini et al., 2011). UVR8 interacts with COP1 in a UV-B-dependent manner, promoting the nuclear accumulation of UVR8 (Favory et al., 2009; Rizzini et al., 2011).

It has been shown that UV-B reduces *PIF4* expression, hence reducing the abundance of PIF4. Regardless of the well-characterized roles of ELF3 and HY5 as transcriptional regulators of PIF4, these two regulators have not been found to involve in the UV-B-mediated inhibition of PIF4 levels (Delker et al., 2014; Hayes et al., 2017; Nusinow et al., 2011).

The plant circadian system can also be reset by temperature changes. The predictable cold/warm cycles during the day and night with differences as small as 4°C (12 hour 18°C:12hour 22°C) are capable of entraining the clock (Michael et al., 2003). Low temperature treatments can cause a considerable dampening of amplitude of rhythms (Bieniawska et al., 2008). The circadian regulation of *C-REPEAT BINDING FACTOR1-3* (*CBF1-3,* cold-induced transcription factors) genes is disrupted in *cca1/lhy* double mutant, probably owing to the loss of both CCA1 and LHY binding to the promoters of these genes (Dong et al., 2011). A complex circadian clock model simulation has predicted negative regulation of *CBF3* through TOC1, which binds to the *CBF3* promoter and contributes to its gated response to cold conditions (Keily et al., 2013). PRR7 and PRR9 clearly play an important role in responding to external environment temperature signals. *prr7/prr9* double mutant plants cannot be entrained through temperature cycles and cannot respond properly to external temperature pulses (Salome and McClung, 2005), suggesting an important role in response to temperature signaling. The EC is also required for changes in transcript abundance in response to varying temperatures (Box et al., 2015; Ezer et al., 2017a). Temperature is known to input to the clock through regulating the EC function through LUX transcriptional activity (Chow et al., 2014). The connection of the EC with temperature is further described in section 2.5.2.

Temperature is also known to input to the clock at several different levels including alternative splicing of multiple core-clock genes. The alternative splicing of CCA1 (temperature-responsive) is thought to give rise to a non-functional version of the

CCA1 protein (CCA1β, lacks the MYB domain) that can compete with the full-length CCA1 (CCA1α) and LHY in the formation of homo- and heterodimers, resulting then in the formation of non-functional complexes (Seo et al., 2012). Notably, an *LHY* splice variant with a premature stop codon accumulates under cold conditions (James et al., 2012).

As mentioned above, the circadian clock also exhibits a remarkable property known as temperature compensation, i.e. it is able to sustain circadian periods of 24 hours within a physiological range of varying temperatures. The clock thus buffers the changes in the rates of biochemical responses (Greenham and McClung, 2015). A molecular mechanism responsible for temperature compensation in Arabidopsis has been described (Portolés and Más, 2010). The mechanism relies on the balance between the CCA1 DNA binding activity and its phosphorylation by CK2: their activities are antagonistic, but both of them are enhanced by temperature (Portolés and Más, 2010). The repression of CCA1 activity increases with higher temperature, resulting in stronger repression to target genes, whereas the CK2-dependent CCA1 phosphorylation, which results in reduced promoter binding affinity by CCA1, increases with higher temperature and leads to reduced repression of CCA1 target genes. Therefore, both activities (phosphorylation and transcriptional repression) balance each other at different temperatures and the circadian period remains unchanged (Portolés and Más, 2010).

The maintenance of a similar free-running period at different temperatures might be also achieved by the temperature-dependent regulation of the expression of morning- and evening-phased circadian clock genes (Gould et al., 2006). Therefore, the circadian clock does not run slower at lower than at higher temperatures, sustaining a period close to 24-hours within a physiological range of temperatures (Chen et al., 2020). Phosphorylation of the S45 residue in ELF4 has been found to oscillate over the course of the day in a circadian manner (Choudhary et al., 2015). This phosphorylation

appears to enhance ELF4 binding to ELF3 and to be involved in temperature compensation.

2.3 Output pathways

The central oscillator generates rhythms in multiple output processes allowing organisms to anticipate and adapt to the changing environment (Huang and Nusinow, 2016). Many studies have uncovered a number of physiological, metabolic and developmental processes controlled by the clock (Gehan et al., 2015).

It has long been known that the circadian clock is able to influence plant responses to low temperature (Eriksson and Webb, 2011). The major players in plant cold acclimation are the CBF protein family (CBF1, CBF2 and CBF3) that activate downstream cold-regulated genes. Transcript abundance of *CBFs* are clock-regulated (peaking at midday) and the cold-induction of these genes is gated by the circadian clock (Eriksson and Webb, 2011). Several main clock components such as CCA1, PRR5, PRR7, and TOC1 have been reported to bind to the promoters of some or all of these *CBF* genes (Dong et al., 2011; Huang et al., 2012; Nakamichi et al., 2012). CCA1 activates *CBFs* and improves plant freezing tolerance (Dong et al., 2011) whereas PRR5 and PRR7 repress the expression of *CBFs* and inhibit freezing tolerance (Nakamichi et al., 2009).

Hypocotyl elongation is extremely sensitive to light conditions and changes in temperature (Niwa et al., 2009; Nomoto et al., 2012). The circadian clock has the ability to regulate the photoperiodic and thermoresponsive hypocotyl growth through *PIFs* (Leivar and Monte, 2014), particularly *PIF4* and *PIF5* (Mizuno et al., 2014; Nusinow et al., 2011; Raschke et al., 2015). PIF4 and PIF5 are positive regulators of hypocotyl growth, and their gene expression patterns coincide with the end-of-night phase of

elongation (Greenham and McClung, 2015). The proper circadian regulation of *PIF4* and *PIF5* gene expression depends on early night repression through the EC (Nusinow et al., 2011). The carboxy-terminal domain of the ELF3 (EC component) interacts with PIF4 to inhibit its activity as a transcriptional regulator (Nieto et al., 2015a) in the early evening (Nozue et al., 2007).

Photoperiodic flowering in higher plants relies on the oscillation of flowering-related components driven by the circadian clock in consonance with the external environmental conditions. Plants are able to use the circadian clock to measure the duration of the day (photoperiodic pathway) and consequently trigger (or not) flowering (Amasino and Michaels, 2010; Kobayashi and Weigel, 2007). Very briefly, flowering is under the control of the florigen gene FLOWERING LOCUS T (FT), which is activated by CONSTANS (CO*,* a critical transcriptional activator) (Kobayashi et al., 1999). CO is a clock regulated protein, which is stable only in the light (Putterill et al., 1995; Valverde et al., 2004). On short days, repression of *CO* transcription is relieved after dusk, but unstable CO protein fails to accumulate in the dark. Therefore, *FT* transcription is not activated. On long days, *CO* mRNA and protein accumulate before dusk, which stabilizes CO protein. Stabilized CO protein accumulates and binds to the *FT* promoter to induce transcription. FT protein moves from leaves to the shoot apex and induces the transition from vegetative to reproductive growth (Corbesier et al., 2007; Song et al., 2015). The movement of FT is further described in section 2.7.

2.4 Tissue specificity at the core of the plant clock

Regarding the circadian structure and organization of the circadian system within the plant, it is widely accepted that every plant cell harbors a clock. The plant cells are coupled by two key connections: plasmodesmata and vascular bundles (Ludewig and Frommer, 2002; Turner and Sieburth, 2003). Plasmodesmata directly connect nearest-

neighbor cells (Ding, 1998) whereas vascular bundles connect distal parts of the plant (Ludewig and Frommer, 2002; Turner and Sieburth, 2003). Plasmodesmata is relevant for short-distance while the vascular bundles are amenable for long-distance communication. Therefore, it is very possible that plasmodesmata and vasculature could contribute to the cell-to-cell (short-distance) and long-distance coupling of the oscillation networks, respectively. Consistent with this notion, tissue-specific studies have showed that the vasculature and mesophyll clocks of leaf tissues regulate each other with unequal features. The circadian clock in the vasculature has distinct properties from other leaf tissues: without external environmental cues, vasculature clock system is still robust and regulates the coupling of the circadian clock in neighbor mesophyll leaf cells (Endo et al., 2014).

The circadian clock in the shoot apex is also reported to be hierarchically dominant in the plant circadian system (Takahashi et al., 2015) with characteristics very similar to those of the Suprachiasmatic Nucleus (SCN) in mammals (Figure 4) (Schibler and Sassone-Corsi, 2002). The shoot apex clocks are tightly coupled, exhibiting a high degree of circadian communication. Signals coming from the clocks at the shoot apex have the ability to synchronize distant clocks such as the ones in roots (Takahashi et al., 2015). Indeed, the circadian rhythms in roots are altered by shoot apex excision (Takahashi et al., 2015). Analysis of root circadian rhythms in plants with excised shoot apex have shown similar results to those found in excised roots, suggesting the importance of the shoot-to-root circadian communication (Takahashi et al., 2015). The long-distance circadian signaling influence of shoot apexes on the rhythmic activity of roots has also been demonstrated by micrografting approaches. The rhythmic recovery of arrhythmic mutant rootstocks when WT shoot apexes are used as scions in grafting experiments, also confirms the long-distance communication. This notion is also supported by the observed arrhythmia in WT rootstocks when arrhythmic shoot apexes are grafted as scions (Takahashi et al., 2015). The circadian clock in roots seems to be also synchronized by photosynthesis-related signals from the shoots, suggesting

the possibility that inter-tissue coupling and long-distance shoot-to-root signaling may occur in plants (James et al., 2008a). Further research proves that light piping down the root might contribute to this entrainment (Nimmo, 2018) but only in cells very closed to the hypocotyls.

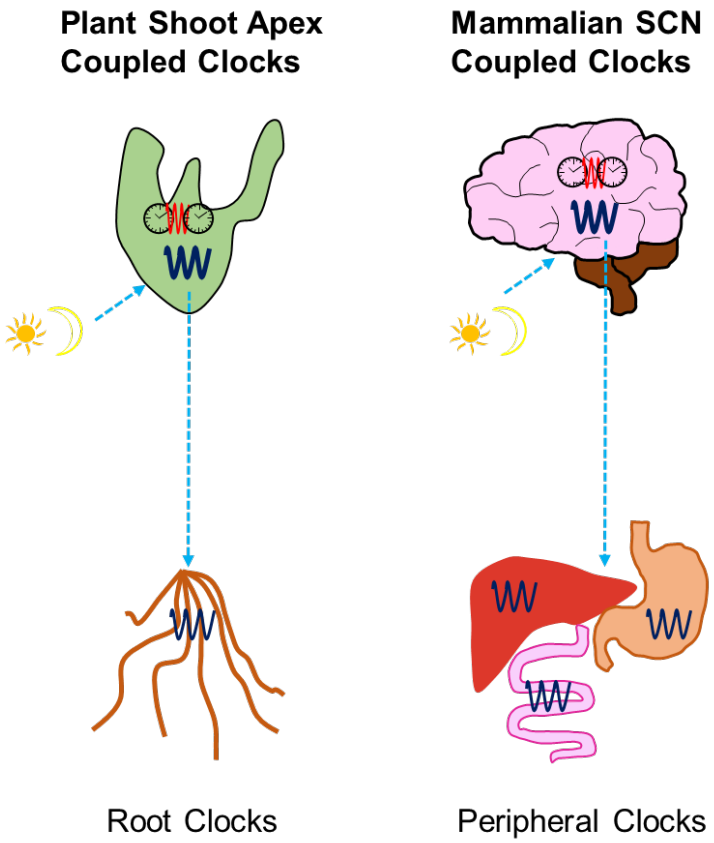

Figure 4. A simplified schematic of the similar synchronize circadian function of shoot apex (in plants) and SCN (in mammals). In mammals, the circadian clock in SCN is well coupled and could influence the circadian activity in distal organs (such as liver, intestine, and lung). The circadian clock in the shoot apex function in the same way and could influence the circadian activity in distal roots. Modified from (Takahashi et al., 2015).

Some key components of the plant circadian clock show tissue-specific expression patterns. For instance, GUS staining assays have suggested that *PRR3* shows vasculature-enriched expression patterns (Para et al., 2007). The circadian cycling of *LUX* expression in vascular tissues peaks at dusk, while in mesophyll and epidermis tissues *LUX* expression shifts to the morning (Shimizu et al., 2015). Rhythmic vasculature-enriched clock genes tend to be expressed at night, while mesophyll-

enriched clock genes are mostly expressed in the morning (Endo et al., 2014). We are only starting to unravel the cell-, tissue-and organ-specific circadian function and their integration within the whole plant.

2.5 The Evening Complex

2.5.1 Role of The Evening Complex at the central oscillator

The EC plays a major role within the plant circadian system. Loss-of-function mutation of any of the EC components (*elf3*, *elf4*, or *lux*) causes an arrhythmic phenotype (Doyle et al., 2002; Hazen et al., 2005; Hicks et al., 1996; Onai and Ishiura, 2005). The arrhythmia is accompanied by many other phenotypes such as early flowering or long hypocotyl elongation (Doyle et al., 2002; Hazen et al., 2005; Hicks et al., 2001; Khanna et al., 2003; Kim et al., 2005; Liu et al., 2001a; Nozue et al., 2007; Nusinow et al., 2011; Onai and Ishiura, 2005; Zagotta et al., 1996). Both *ELF4* and *LUX* promoters contain one evening element motif (EE, AAAATATCT), which is the binding site of CCA1 and LHY (Harmer et al., 2000). The *ELF3* promoter has one EE-like element (AATATCT) and two CCA1 binding sites (CBS, AA(A/C)AATCT) (Huang et al., 2012; Mikkelsen and Thomashow, 2009; Wang et al., 1997). CCA1 binds to the promoter of *ELF3* in the early morning to repress its expression, which supports genetic data showing that ELF3 is repressed by CCA1 (Lu et al., 2012a). A recent study identifying genome-wide targets of CCA1 using chromatin immunoprecipitation followed by high-throughput sequencing (ChIP-seq) has shown that CCA1 occupies the promoter regions of all EC components (Kamioka et al., 2016; Nagel et al., 2015). Two or more of the EC components have been shown by ChIP analysis to associate with the promoters of *PRR7*, *PRR9*, *GI*, and *LUX* (Chow et al., 2012; Dixon et al., 2011; Helfer et al., 2011). *LUX* also undergoes autoregulation by binding to its own promoter through the LUX binding site (LBS, GAT(A/T)CG), suggesting that the EC regulates its own accumulation by

suppressing *LUX* expression (Helfer et al., 2011).

Several chromatin remodeling complexes have also been found to contribute to the regulation of the EC. ELF3 interacts with the chromatin-related complex (SWI2/SNF2-RELATED, SWR1), which is responsible for the deposition of the histone variant H2A.Z. This interaction provides the means for repressive chromatin domains to repress a set of target genes in plants (Tong et al., 2020). HOS15 also forms a large protein complex with the EC components and the histone deacetylase HDA9. This HOS15–EC–HDA9 histone-modifying complex associates to the *GI* promoter and negatively regulates *GI* transcription (Park et al., 2019).

Recent studies have indicated that the EC components may also have independent functions of the EC. Indeed, a recent study has shown that the ability of LUX to bind its target genes is independent of ELF3 and ELF4 (Silva et al., 2020a). A similar finding shows that many overlapping binding sites of LUX are found among wild type background and *elf3-1* background, suggesting that the binding ability of LUX is EC-independent (Ezer et al., 2017a). ELF4 also has some EC-independent functions. For instance, the physical interaction of ELF4 with GI results in GI's sequestration from the nucleoplasm (GI binds to the *CO* promoter in the region of nucleoplasm) and its localization into nuclear bodies, thus the binding to the *CO* promoter from GI is released and photoperiodic flowering in plants is regulated (Kim et al., 2013). ELF3 also regulates hypocotyl growth via PIF4 in an EC-independent manner by directly interacting with PIF4 to limit the activation of PIF4 downstream targets (Nieto et al., 2015a). ELF3 functions as a thermosensor and the rapid shift between ELF3 active and inactive states (through phase transition) is temperature-dependent (Jung et al., 2020). Besides, the above temperature related function of ELF3 could be modulated by the amounts of ELF4, suggesting the stabilizing function of ELF3 by ELF4 (Jung et al., 2020).

2.5.2 Role of The Evening Complex in the input pathways

The EC plays significant roles integrating and transmitting multiple light and temperature signals to the plant circadian clock. Both *ELF3* and *ELF4* are regulated by light signaling pathways and are induced by light (Kikis et al., 2005; Liu et al., 2001a). FAR1, FHY3 and HY5 (positive transcriptional regulators of the PHYA signaling) bind to the promoter of *ELF4* to activate its expression during the day (Li et al., 2011a). It is known that PHYB and COP1 regulate the abundance of ELF3 protein in vivo (Liu et al., 2001a; Nieto et al., 2015a; Yu et al., 2008a). Besides, the B-BOX DOMAIN PROTEIN 19 (BBX19, a photomorphogenesis regulator) physically interacts with COP1 and ELF3 to promote the COP1-dependent degradation of ELF3 (Wang et al., 2015). The EC also regulates responses to and is regulated by UV-B light (low-intensity and non-damaging). *ELF4* abundance is highly induced by UV-B light, and null mutants of *elf3*, *lux*, or *elf4* display defects in the gating of UV-B-responsive gene abundance (Fehér et al., 2011; Takeuchi et al., 2014). Consistently, ChIP analysis shows that LUX and ELF4 are associated with the promoter of *EARLY LIGHT INDUCIBLE PROTEIN 1* (*ELIP1*), a gene involved in the UV-B signaling pathway (Takeuchi et al., 2014).

Similarly to light, the EC is also important for temperature signaling. ELF3 is required for the proper induction of several clock genes including *GI*, *LUX*, *PIF4*, *PRR7*, and *PRR9* when seedlings are moved to warmer temperature conditions. Accordingly, the temperature-responsiveness of clock gene expression is abolished in *elf4*, *elf3*, as well as *lux* null mutants (Mizuno et al., 2014). The association of the EC with the promoters of *PRR9*, *LUX*, and *PIF4* is reduced at warmer temperatures, suggesting that temperature might directly and specifically regulate EC recruitment to the promoters of the EC target genes (Box et al., 2015). This conclusion is also reinforced by ChIP-Seq analyses showing that the strength of the EC binding is increased at lower temperatures, whereas it is weaker at higher temperature (Ezer et al., 2017a).

Several studies have shown that cold signals could be integrated into the circadian

clock through different mechanisms such as transcriptional and post-transcriptional regulation. The CBF1 transcription factor has been shown to bind to the *LUX* promoter to regulate *LUX* expression (Chow et al., 2014). Besides, decreased intron retention of ELF3 has been discovered in the *gemin2-1* mutant, which is known to affect the temperature-responsive alternative splicing of *CCA1*, *RVE8*, and *TOC1* (Schlaen et al., 2015). Temperature changes may directly regulate ELF3 activity through regulating alternative splicing (Schlaen et al., 2015).

2.5.3 Role of The Evening Complex in the output pathways

As mentioned above, the EC connects the clock to several output pathways, such as the photoperiod-dependent plant growth, flowering and seed dormancy. PIF4 and PIF5 protein accumulation is post-translationally suppressed during the day, whereas *PIF4* and *PIF5* expression is transcriptionally repressed by the EC during the early night (Niwa et al., 2009; Nozue et al., 2007; Nusinow et al., 2011; Yamashino et al., 2013). As the accumulation of the EC decreases as dawn approaches, transcriptional suppression of *PIF4*/*PIF5* is abolished (Nozue et al., 2007; Nusinow et al., 2011; Yamashino et al., 2013). Therefore, the long hypocotyl phenotype of the EC mutants can be explained by the loss of transcriptional suppression at night, which leads to the premature accumulation of PIF4/PIF5 proteins (Huang and Nusinow, 2016). ELF3 also regulates hypocotyl growth via PIF4 in an EC-independent manner by directly interacting with PIF4 to limit the activation of PIF4 downstream targets (Nieto et al., 2015a).

ELF3 and ELF4 have been initially identified by their early flowering phenotype. A possible mechanism explaining their regulation of flowering is provided (Lee et al., 2007b; Mizoguchi et al., 2005; Yoshida et al., 2009; Yu et al., 2008a). GI promotes flowering by increasing the transcription of *CO* and *FT* (Mizoguchi et al., 2005). ELF3 cooperates with COP1 to destabilize GI, thereby resulting in reduced expression of *CO*

and *FT* (Yu et al., 2008a). In addition, a transcription factor known as SHORT VEGETATIVE PERIOD (SVP, a *FT* transcriptional repressor) has been shown to directly interact with ELF3 and accumulate in the ELF3 over-expression line (Lee et al., 2007b; Yoshida et al., 2009), which explains the late-flowering phenotype of ELF3 over-expressing plants (Yu et al., 2008a). The EC-target PIF4 also binds to the promoter of *FT* in a temperature-dependent manner and interacts with CO to regulate the high-temperature induced flowering under non-inductive short-day conditions (Fernández et al., 2016; Kumar et al., 2012).

A recent study has also shown that the EC together with PICKLE (PKL, a chromatin-remodeling factor) regulate the expression of *DELAY OF GERMINATION1 (DOG1*), a critical gene involved in seed dormancy during seed development (Zha et al., 2020). The germination of freshly harvested seeds is reduced in *pkl*, *lux*, or *elf3* null mutants, suggesting that *PKL*, *ELF3* and *LUX* are negative regulators of seed dormancy (Zha et al., 2020). Besides, the transcription of *DOG1* is much higher in *pkl*, *elf3*, or *lux* mutants compared with wild type (Zha et al., 2020). Further experiments have shown that PKL interacts with LUX to transmit circadian signals for directly regulating *DOG1* expression(LUX binds to the promoter of *DOG1*) (Zha et al., 2020).

2.6 EARLY FLOWERING 4

ELF4 has been identified by its function in photoperiod perception and circadian regulation (Doyle et al., 2002). ELF4 improves clock accuracy and is required for sustained robust oscillations. *ELF4* mRNA expression oscillates, displaying a peak at night (Doyle et al., 2002). Various clock components contribute to this pattern of expression. A recent study has found that RVE8, a morning-phased protein, antagonizes CCA1 and is able to activate the expression of *ELF4* through binding to the EE element (Hsu and Harmer, 2014; Hsu et al., 2013). In the afternoon, *ELF4* expression

is reduced in the double mutant of *LNK1* and *LNK2*, which integrate light input into the clock (Rugnone et al., 2013). In addition, the evening-expressed clock component TOC1 has been also found to suppress the expression of *ELF4* (Huang et al., 2012).

elf4 mutants exhibit a wide array of phenotypes, including arrhythmic circadian patterns, abnormal hypocotyl elongation, as well as early flowering (Doyle et al., 2002). Plants over-expressing ELF4 (ELF4-ox) are late flowering under inductive (long-day) photoperiods, whereas ELF4-ox plants show no delay in flowering under short days (McWatters et al., 2007). ELF4-ox PLANTS show rhythms albeit with longer circadian periods under constant light (LL) conditions following entrainment under light:dark (LD) cycles (McWatters et al., 2007). A recent study has defined the ELF4 non-annotated domain (DUF1313) and biochemically confirmed that ELF4 forms a homodimer with α-helical composition (Kolmos et al., 2009). A new isolated *elf4* mutant (through a TILLING mutagenesis screen over the *ELF4* locus) has revealed that *ELF4* is a repressor of the pace of the clock. *ELF4* achieves this function through promoting the nuclear localization of ELF3 (Herrero et al., 2012) and by repressing the expression of several circadian clock genes (*GI*, *TOC1*,*LUX, PRR9,* and *PRR7*) (Kolmos et al., 2009).

Recent results have identified a role for ELF4 as a gatekeeper, preventing the EC from associating with other proteins, including the CHLOROPLAST RNA BINDING (CRB, a chloroplast-associated protein) and the EFLs (ELF4-likes, DUF-1313 domain containing family) (Huang et al., 2016). The mechanism of the “gatekeeper” probably relies on a combination of steric interference and maintaining the complex in the nucleus and/or nuclear speckles (Herrero et al., 2012). ELF4 also displays functions independent from the EC (Kim et al., 2013). ELF4 influences GI nuclear dynamics and ELF4 physically interacts with GI in nuclear bodies (Kim et al., 2013). Through this protein interaction, ELF4 regulates the nuclear distribution of GI (Kim et al., 2013). GI binds to the promoter of *CO* in the nucleoplasm, but ELF4 sequesters GI from the nucleoplasm to nuclear bodies (Kim et al., 2013). Thus, the binding to the *CO* promoter from GI will be

released (Kim et al., 2013). The spatial regulation of GI with ELF4 in the nucleus may contribute to the regulation of photoperiodic flowering (Kim et al., 2013).

Structural studies and extensive in vitro assays have been used to understand the molecular mechanisms of the temperature-dependent EC binding to DNA and to demonstrate the critical function of ELF4 in this mechanism. In vitro DNA binding assays have shown that the full EC is able to act as a direct thermosensor (Silva et al., 2020a). The EC exhibits stronger DNA binding at 4°C than at 27°C (Silva et al., 2020a). An excess of ELF4 is able to restore the poor EC binding at 27°C, suggesting that ELF4 is a key modulator of thermosensitive EC activity (Silva et al., 2020a).

ELF4 is found to be enriched in the vasculature (Endo et al., 2014). The tissue-specific *ELF4* expression pattern strongly suggests the possibility of discrete functions of the circadian clock in vasculature (Endo, 2016). One recent research study of the shoot and root clocks in *elf3*, *elf4*, or *lux* mutants have shown specific effects on roots (Nimmo et al., 2020). The shoots of *lux* mutants have a short-period phenotype while the roots of *lux* are very weakly rhythmic under red + blue light (Nimmo et al., 2020). However, both *elf3* and *elf4* mutants show a short period in roots and abolish the differences in root period under red and blue light (Nimmo et al., 2020).

2.7 LONG DISTANCE PROTEIN MOVEMENT IN PLANTS

A number of different studies have shown that the movement of transcription factors is widespread during plant development and play significant roles in plant growth (Lee et al., 2006; Rim et al., 2011). As mentioned above, FT is a long-distance movement protein and controls the floral transition from vegetative to reproductive growth (Corbesier et al., 2007; Jaeger and Wigge, 2007). External environmental cues are sensed by the leaves. However, the responses for flowering occur at the shoot apex.

This requires the long-distance communication between leaves and the shoot apex (Jaeger and Wigge, 2007). The long-distance mobile signal has been termed as ‘‘florigen’’ and has been later discovered to be a mobile FT protein (Corbesier et al., 2007; Jaeger and Wigge, 2007; Mathieu et al., 2007a). *FT* mRNA is predominantly produced in the leaf blades and the cotyledons in response to photoperiod (Wigge et al., 2005). FT protein moves from leaves to the shoot apex through the vasculature and acts in concert with a bZIP (basic leucine zipper) transcription factor *FLOWERING LOCUS D* (*FD*) at the shoot apex to regulate flowering (Jaeger and Wigge, 2007; Wigge et al., 2005). FT interacts with FD to promote the expression of *APETALA1* (*AP1*) and *SUPPRESSOR OF CONSTANS1* (*SOC1*), which in turn promotes *LEAFY* (*LFY*) and the floral transition (Abe et al., 2005; Corbesier et al., 2007; Kardailsky et al., 1999; Kobayashi et al., 1999; Wigge et al., 2005). Thus, the movement of FT protein from leaves to shoot apex ensures the flowering occurs at the right seasonal time.

It has been also recently described that HY5 acts as a shoot- to-root mobile protein that promotes nitrate uptake and root growth (Chen et al., 2016). HY5, a member of the photomorphogenic bZIP transcription factor family (Jakoby et al., 2002) inhibits the growth of hypocotyl and the development of lateral root (Chen and Xiong, 2011; Osterlund et al., 2000; Oyama et al., 1997). HY5 also regulates a set of fundamental processes in plants related to cell elongation, cell proliferation, chloroplast development, and nutrient assimilation (Jing et al., 2013; Koornneef et al., 1980; Oyama et al., 1997). HY5 regulates the transcription of many genes by binding directly to cis-regulatory elements (Lee et al., 2007a). Indeed, genome-wide ChIP-chip experiments show that nearly one-third of the *Arabidopsis* genes are controlled by HY5, and 3000 genes of them are regulated by HY5 direct binding (Lee et al., 2007a; Zhang et al., 2011).

HY5 also acts as a shoot-to-root mobile signal. Shoot-derived HY5 protein moves from shoots to roots and activates its own expression to promote root nitrate uptake

through the activation of *NITRATE TRANSPORTER 2.1* (*NRT2.1*, a high-affinity nitrate transporter) (Cerezo et al., 2001; Chen et al., 2016). HY5 protein improves carbon assimilation and translocation (Chen et al., 2016). HY5 activation of *NRT2.1* transcription and nitrate uptake in the root is enhanced through the increase of carbon photoassimilate (sucrose) levels (Chen et al., 2016). Thus, the mobile HY5 protein mediates homeostatic regulation of carbon versus nitrate status in fluctuating environments (Chen et al., 2016).

A recent study using a set of HY5 constructs have shown that local HY5 function in specific cell types of the hypocotyl is enough to regulate hypocotyl length and can recover the primary root growth phenotypes of *hy5* mutants, without movement to the root. The authors have proposed that these functions might be due to a mobile signal downstream of HY5 (Burko et al., 2020). This study has shown that HY5 could be detected in the roots of plants expressing *HY5-GFP* under the *CAB3* (*CHLOROPHYLL A/B BINDING PROTEIN3*) promoter, a photosynthetic-tissue-specific promoter (An et al., 2004; Corbesier et al., 2007). However, HY5 protein could not be detected in the roots of plants expressing *CAB3p: HA-YFP-HA -HY5* (Burko et al., 2020; Chen et al., 2016). The different localization might be explained by the different positions of the tags or the folding of HY5 protein. Thus, the movement and determinants conditioning such movement remain to be further investigated.

Objectives

The general aim of our research project is to understand the temperature-dependent role of the clock component ELF4 in the root clock, and its function as a mobile protein. The specific objectives include:

1. Characterization of ELF4 function both in shoots and roots. We will use bioluminescence assays to examine clock gene rhythmic expression in shoots and roots of WT plants. We will also use different ELF4 mis-expressing plants.

2. Analyses of rhythms in roots after blocking ELF4 movement by shoot excision. We will explore the circadian changes in clock gene expression in roots after abolishing ELF4 trafficking by shoot excision.

3. Genome-wide view of the circadian transcriptional landscape controlled by ELF4 in roots. We will use RNA-Seq analyses of WT and *elf4-1* mutant roots as well as in WT roots in which the shoots are excised.

4. Analyses of ELF4 movement from shoots to roots. We will perform micrografting experiments with different genetic scions and rootstocks to determine the effect of ELF4 movement from shoots on the rhythms in roots.

5. Analyses of the effect of environmental conditions on ELF4 movement. We will **perform** micrografting experiments with different scions and rootstocks under different photoperiodic and temperature conditions to determine their effect on ELF4 movement.

Results

1. Prevalent function of ELF4 sustaining rhythms in roots.

We first approached the investigation of the circadian mobile signal by simultaneously following rhythms in shoots and roots of intact plants (Takahashi et al., 2015). The waveforms of the morning-expressed *CIRCADIAN CLOCK ASSOCIATED 1* (*CCA1*) and *LATE ELONGATED HYPOCOTYL* (*LHY*) promoter activities displayed a long period, slightly reduced amplitude and phase delay in roots compared with shoots (Figure 5A-C). The rhythmic messenger RNA (mRNA) accumulation assayed by quantitative PCR with reverse transcription (RT–qPCR) followed the same trend (Figure 6A). Similar patterns were observed for the promoter activity of the evening-expressed clock component *TIMING OF CAB EXPRESSION1* (*TOC1*) or *PSEUDO RESPONSE REGULATOR1* (*PRR1*) (Figure 6B and C). Therefore, the clock is fully operative in roots but its overall pace is slower and the phase is delayed compared with shoots.

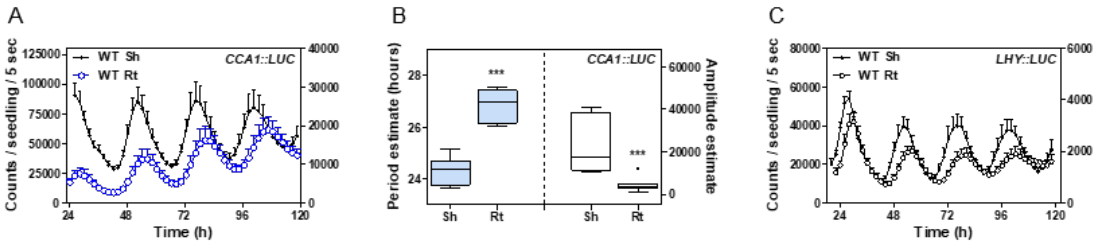

Figure 5. (A) Luminescence of *CCA1::*luciferase (*LUC*) oscillation simultaneously measured in shoots (Sh; left axis) (*n* = 9) and roots (Rt; right axis) (*n* = 9). (B) Period (left *y* axis) estimates of *CCA1::LUC* rhythms in shoots and roots (*n* = 8 for each) and amplitude (right *y* axis) estimates of *CCA1::LUC* rhythms in shoots (*n* = 7) and roots (*n* = 8). In box plots, the centre line is the median, box edges show 25th and 75th percentiles and whiskers extend to minimum and maximum values. ***P < 0.0001; two-tailed *t*-tests with 95% confidence. Luminescence of (C) *LHY::LUC* (n=6 for Sh, n=6 for Rt) rhythms simultaneously measured in shoots (Sh) and roots (Rt). Root luminescence signals in a, are represented in the right Y-axis. (A-C) Two biological replicates were performed for all experiments, with measurements taken from distinct samples grown and processed at different times.

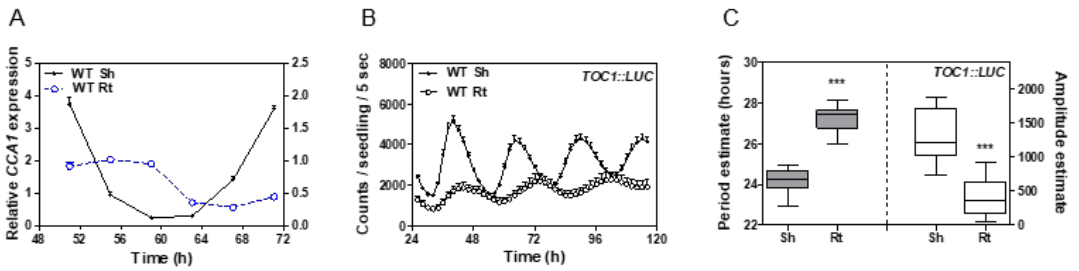

Figure 6. (A) Circadian time-course analyses of *CCA1* mRNA expression in wild-type (WT) shoots and roots. Luminescence of (B) *TOC1::LUC* (n=16 for Sh, n=15 for Rt) rhythms simultaneously measured in shoots (Sh) and roots (Rt). Root luminescence signals in (B) are represented in the right Y-axis. (C) Circadian period (left Y-axis, n=16 for Sh, n=14 for Rt) and amplitude (right Y-axis, n=16 for Sh, n=15 for Rt) estimates of *TOC1::LUC* luminescence signals (data are represented as the median ± max and min; 25-75 percentile). *** p-value<0.0001; two-tailed t-tests with 95% of confidence. (A-C) Two biological replicates were performed for all experiments, with measurements taken from distinct samples grown and processed at different times.

Under free-running conditions (in the absence of environmental time cues), the circadian clock is unable to properly run in mutant plants of any of the evening complex components (Doyle et al., 2002; Hazen et al., 2005; Hicks et al., 1996; Onai and Ishiura, 2005). We therefore examined the roles of the evening complex components in the root clock, particularly focusing on ELF4. Circadian time-course analyses showed that although some very weak oscillations could be detected (Figure 7A), the *CCA1* and *LHY* promoter activities and their mRNA expression were suppressed in *elf4-1* mutant compared with WT roots (Figure 7B-E), following a similar trend to that described in shoots (McWatters et al., 2007) (Figure 7F-H). Overexpression of ELF4 (ELF4-ox) lengthened the period of *LHY::LUC* (Figure 8A and B), indicating that increased ELF4 activity in roots slows the clock. The expression of *PSEUDO RESPONSE REGULATOR 9* (*PRR9*), a previously described direct target of the evening complex in shoots, was upregulated in *elf4-1* mutant roots (Figure 8C), suggesting that the evening complex also represses *PRR9* in roots. Thus, ELF4 has an important regulatory function in the root clock: mutation compromises rhythms, whereas overexpression lengthens the circadian period.

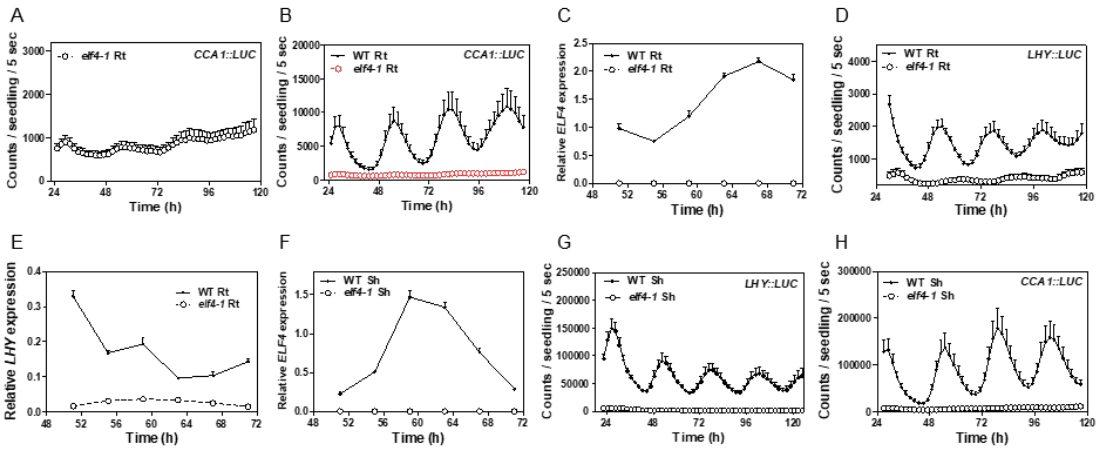

Figure 7. (A) Luminescence of *CCA1::LUC* rhythms in *elf4-1* Rt (n=8) (from Fig. 1d) showing the weak rhythms of the mutant. (B) Luminescence of *CCA1::LUC* rhythms in WT (n=9) and *elf4-1* Rt (n=8). (C) Circadian time course analyses of *ELF4* mRNA expression in WT and *elf4-1* mutant Rt. (D) Luminescence of *LHY::LUC* rhythms in WT (n=6) and *elf4-1* mutant Rt (n=6). (E) Circadian time course analyses of *LHY* mRNA expression in roots of WT and *elf4-1*. (F) Circadian time course analyses of *ELF4* mRNA expression in WT and *elf4-1* mutant Sh (also in Extended Data Fig. 3c). (G) Luminescence of *LHY::LUC* (n=6) and (H) *CCA1::LUC* (n=9) rhythms in WT and *elf4-1* mutant Sh. The "n" values refer to independent samples. (A-H) Two biological replicates were performed for all experiments, with measurements taken from distinct samples grown and processed at different times.

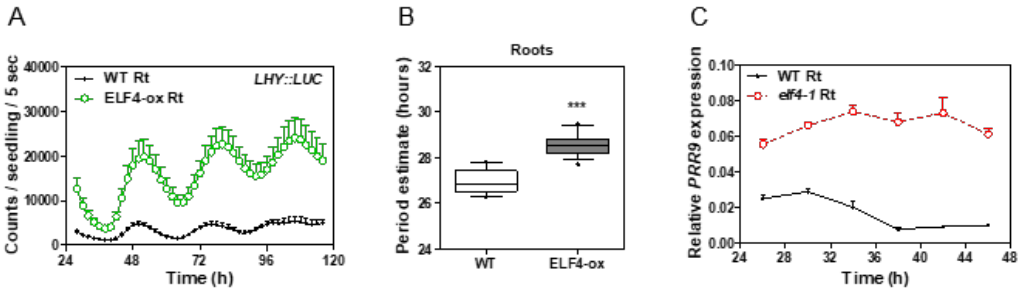

Figure 8. (A) Luminescence of *LHY::LUC* rhythms in WT (n=8) and ELF4-ox Rt (n=9). Data are represented as the means + SEM. (B) Circadian period estimates of *LHY::LUC* in WT (n=12) and ELF4-ox (n=14) roots; data are represented as the median ± max and min; 25-75 percentile). *** p-value<0.0001; two-tailed t-tests with 95% of confidence. (C) Circadian time course analyses of *PRR9* mRNA expression in roots of WT and *elf4-1*. Sampling was performed under constant light conditions (LL) following synchronization under light:dark cycles (LD). Data are represented as the means + SEM. Data for all experiments are representative of two biological replicates, with measurements taken from distinct samples grown and processed at different times.

RNA-sequencing (RNA-seq) analyses of WT and *elf4-1* mutant roots provided a

genome-wide view of ELF4 function in roots. We found that about 15% of the root genes were significantly mis-regulated in the absence of a functional ELF4, with a similar proportion of upregulated (1,297) and downregulated (1,555) genes (Figure 9). The expression of core clock genes was among the most significantly mis-regulated (Figure 10 and Figure 11) Together, the results indicate a prevalent function for ELF4 in sustaining rhythms in roots.

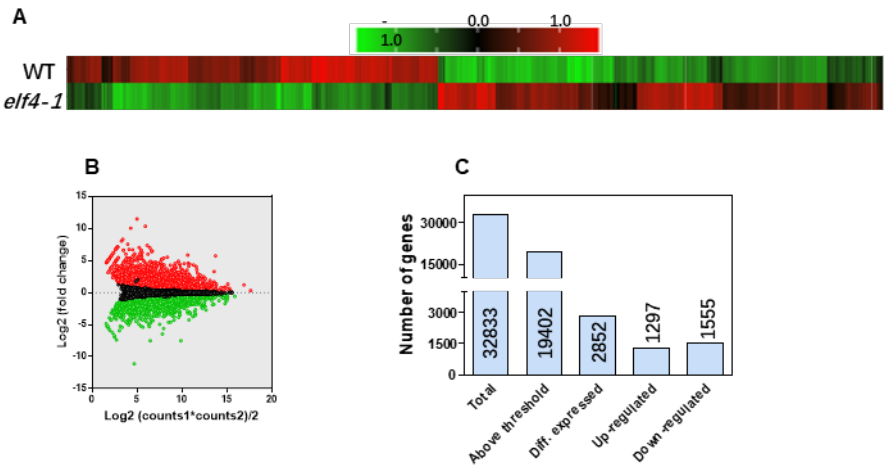

Figure 9. (A) Heatmap of the median-normalized expression (Z-scaled FPKM values) of DEGs following a hierarchical clustering using the Euclidean distance. (B) Relationship between average expression of WT (count 1) and *elf4-1* (count 2) and fold change for each gene. Black dots represent genes that are not differentially expressed, while red and green dots are the genes that are significantly up- and down-regulated, respectively. (C) Quantitative analysis of DEGs in *elf4-1* versus WT roots. The statistical analyses of the DEGs are detailed in Materials and Methods. Data for all experiments are representative of two biological replicates.

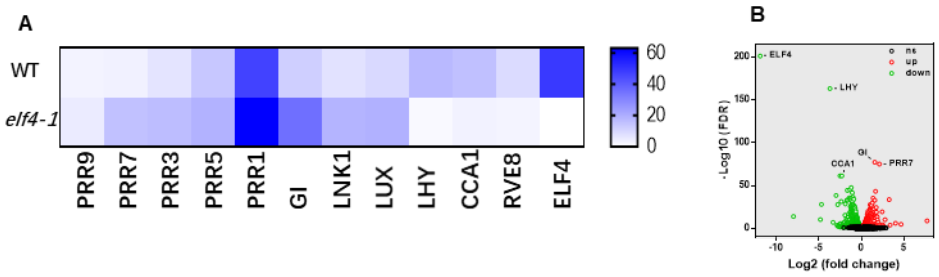

Figure 10. (A) Heatmap of the median-normalized expression (Z-scaled FPKM values) of the oscillator genes in WT and *elf4-1* roots. (B) Volcano plot showing fold-change versus significance of the differential expression test. Black dots represent genes that are not differentially expressed, while red and green dots are the genes that are significantly up- and down-regulated, respectively. Data for all experiments are representative of two biological replicates.

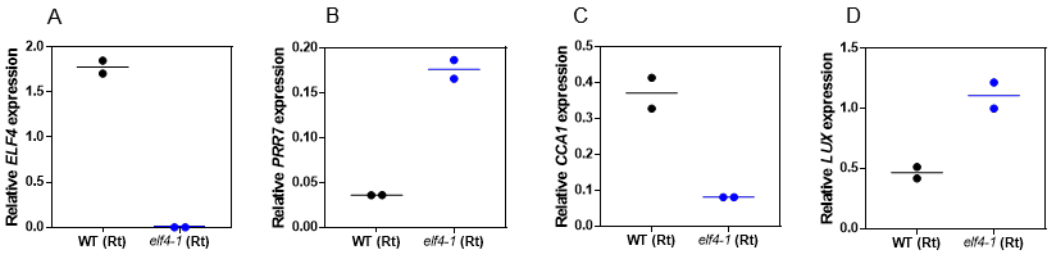

Figure 11. Analyses by RT-QPCR of (A) *ELF4*, (B) *PRR7*, (C) *CCA1* and (D) *LUX* mRNA expression in roots at CT75 after three days in LL. (A-D) Two biological replicates were performed for all experiments.

2. ELF4 moves from shoots to regulate oscillator gene expression in roots.

Our previous study showed that a signal from shoots is important for circadian rhythms in roots (Takahashi et al., 2015). Micrografting assays are a powerful tool to identify the nature of mobile signals. The grafting technique per se does not alter the rhythms in roots (Takahashi et al., 2015), as grafted WT scions into WT roots show similar rhythms as non-grafted WT plants (Figure 12A and B). By micrografting different genotypes, we found that grafts of ELF4-ox shoots into *elf4-1* rootstocks (ELF4-ox (Sh)/*elf4-1* (Rt)) (Figure 12C) were particularly efficient in recovering the rhythms in roots (Figure 12D and E). The results are noteworthy, as *CCA1::LUC* rhythms are affected in *elf4-1* mutant roots (Figure 12F). Restoration of the rhythms reflected circadian function exclusively in roots, as water instead of luciferin was applied to shoots (ELF4-ox, Sh, H_2O) to avoid luminescence signals leaking from shoots into roots of adjacent wells. Rhythms in roots were also recovered when ELF4-ox scion was grafted into *elf4-2* mutant (Figure 13A) rootstocks (Figure 13B). To exclude the possibility that the observed results were due to the high overexpression in ELF4-ox plants, we grafted WT shoots into *elf4-1* roots. Although the recovery of the rhythms was not as robust as with ELF4-ox grafts, a rhythmic pattern was observed in roots (Figure 14A). Thus, ELF4 mRNA or protein is able to move from shoots to roots. This notion was reinforced by results showing the rhythmic recovery of *elf4-1* rootstocks grafted with ELF4 minigene scion (Figure 14B and C). These results rule out the

possibility that the recovery of the rhythms was solely a result of the high overexpression of ELF4-ox scion.

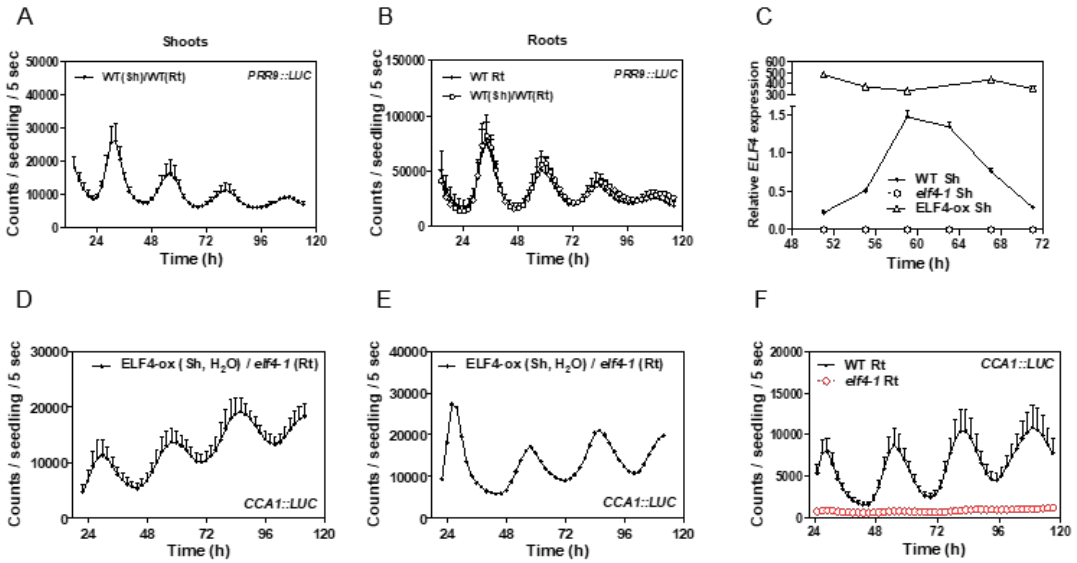

Figure 12. Luminescence of *PRR9::LUC* in (A) shoots (n=3) and (B) roots (n=3) of WT scion into WT rootstocks and its comparison with luminescence in (non-grafted) WT roots (n=4). (C) Circadian time course analyses of *ELF4* mRNA expression in shoots of WT, *elf4-1* and ELF4-ox (also in Extended Data Fig. 1h). *CCA1::LUC* luminescence in roots of ELF4-ox scion into (D) *elf4-1* (n=4) rootstocks. Water instead of luciferin was added to the wells containing ELF4-ox shoots. (E) Individual waveform of *CCA1::LUC* rhythmic recovery in roots of ELF4-ox scion and *elf4-1* rootstocks. Water instead of luciferin was added to the wells containing ELF4-ox shoots. (F) Luminescence of *CCA1::LUC* rhythms in WT (n=9) and *elf4-1* Rt (n=8). (A-F) Data are represented as the means + SEM. The mRNA expression and promoter activity analyses were performed under constant light conditions previous synchronization of plants under LD cycles at 22ºC. The "n" values refer to independent samples. (A-F) Two biological replicates were performed for all experiments.

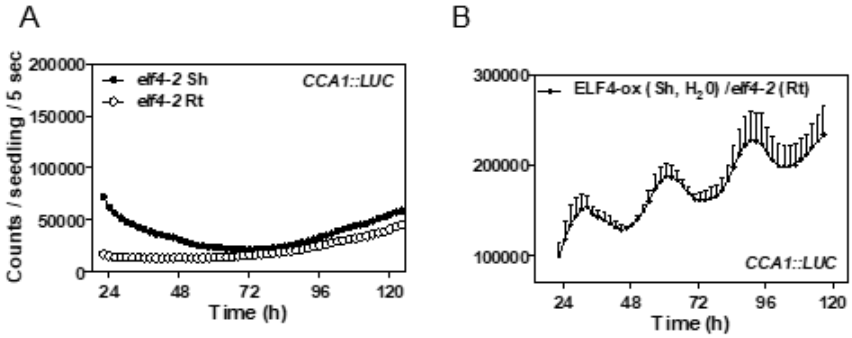

Figure 13. (A) *CCA1::LUC* luminescence in shoots and roots of *elf4-2* mutant plants (n=5 for each). *CCA1::LUC* luminescence in roots of ELF4-ox scion into (B) *elf4-2* (n=3) rootstocks. Water instead of luciferin was added to the wells containing ELF4-ox shoots. (A-B) Data are represented as the means + SEM. The promoter activity analyses were performed under constant light conditions previous synchronization of plants under LD cycles at 22ºC. The "n" values refer to independent samples. (A-B) Two biological replicates were performed for all experiments.

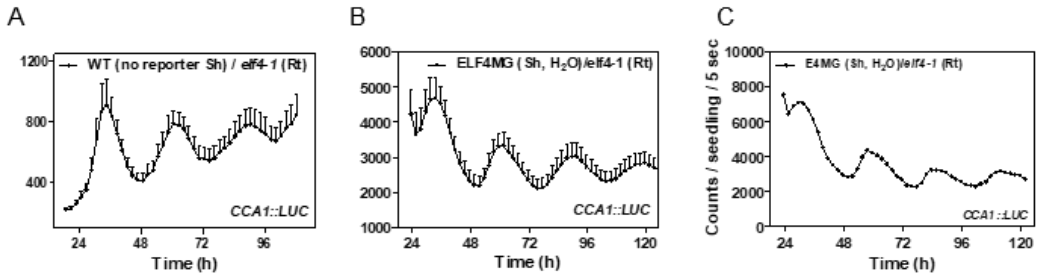

Figure 14. *CCA1::LUC* luminescence in *elf4-1* rootstocks with (A) WT (n=8) and (B) ELF4 Minigene (ELF4MG) (n=10) scions. WT scions do not express reporters and water instead of luciferin was added to the wells containing ELF4MG shoots. (C) Individual waveform of *CCA1::LUC* rhythmic recovery in roots of E4MG scion into *elf4-1* rootstocks. Water instead of luciferin was added to the wells containing E4MG shoots. (A-C) Data are represented as the means + SEM. The promoter activity analyses were performed under constant light conditions previous synchronization of plants under LD cycles at 22ºC. The "n" values refer to independent samples. (A-C) Two biological replicates were performed for all experiments, with measurements taken from distinct samples grown and processed at different times.

To investigate whether the mRNA is the mobile signal, we performed RT–qPCR time-course analyses of roots from ELF4-ox (Sh)/*elf4-1* (Rt) grafts. Our results showed no detectable amplification of *ELF4* mRNA at any time point analysed (Figure 15A), which suggests that *ELF4* mRNA did not move through the graft junctions. To confirm this notion, we injected purified ELF4 protein into *elf4-1* mutant (Figure 16A-B). Injection

of ELF4 into shoots was able to restore rhythms in roots (Figure 16C). The percentage of plants injected with ELF4 that recovered rhythms was low (5–8%) but the rhythmic recovery was observed reproducibly in different biological replicates. The restoration of root rhythms (relative amplitude error < 0.6) supports the notion that ELF4 protein moves from shoots to roots. Rhythmic recovery was not apparent when purified green fluorescent protein (GFP) was injected instead of ELF4 (Figure 16C). The movement of ELF4 protein was further assayed by using shoots of plants overexpressing ELF4–GFP grafted into *elf4-1* mutant roots. Confocal imaging showed that ELF4–GFP fluorescent signals accumulated in the vasculature of *elf4-1* mutant rootstock, across the graft junctions (Figure 17A-D). Furthermore, western blot analyses of roots from ELF4–GFP (Sh)/*elf4-1* (Rt) grafts detected ELF4 protein as a band of the expected size (arrows in Figure 18A) that was absent from protein extracts of *elf4-1* mutant roots (Figure 18A). Grafting ELF4-ox fused to three GFPs (ELF4–3×GFP) scion into *elf4-2* mutant rootstock did not lead to an obvious recovery of rhythms (Figure 19A and B), suggesting that a mobile ELF4 protein is required. The ELF4–3×GFP is still functional, as its overexpression in the *elf4-1* mutant background restored the hypocotyl phenotypes of *elf4-1* mutant plants (Figure 19C) and repressed *PRR9* gene expression (Figure 20A and B). The functional relevance of ELF4 movement was also verified in *elf4-1* (Sh)/*elf4-1* (Rt) grafts, in which roots did not recover rhythms (Figure 21A and B). Therefore, multiple lines of evidence, including the ELF4 injection data, the grafting assays showing the recovery of the rhythms, the ELF4–GFP fluorescent signals across graft junctions, the detection of ELF4 protein in roots of the grafted plants, the lack of rhythmic recovery in roots of ELF4–3×GFP grafts and in *elf4-1* scion grafts, support the notion that ELF4 protein moves from shoots to regulate rhythms in roots. Other mobile proteins such as FLOWERING LOCUS T (FT) and LONG HYPOCOTYL 5 (HY5) share features with ELF4 protein in terms of low molecular weight and high isoelectric point (Figure 22A).

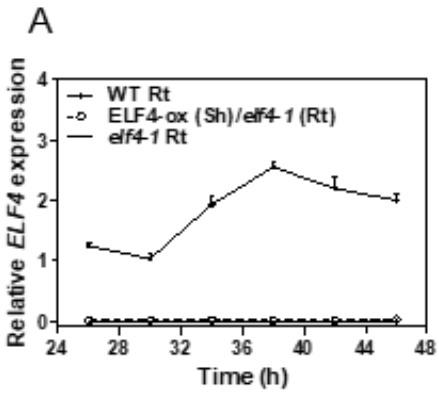

Figure 15. (A) Circadian time course analyses of *ELF4* mRNA expression in roots of WT, *elf4-1* and ELF4-ox scion and *elf4-1* rootstocks. (A) Data are represented as the means + SEM. (A) Two biological replicates were performed for all experiments.

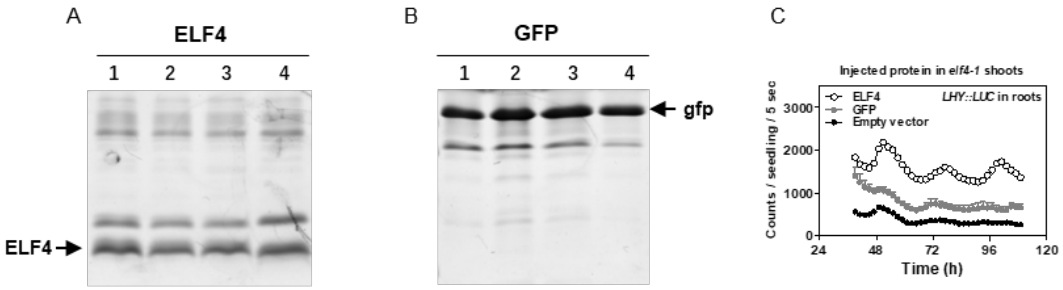

Figure 16. (A) ELF4 and (B) GFP proteins purified from bacteria and injected in shoots of *elf4-1* mutant plants to examine rhythmic recovery in roots. (C) Luminescence of *LHY::LUC* rhythms in *elf4-1* roots after injection in shoots of purified ELF4 (n=4) or GFP proteins (n=8) and *elf4-1* roots as a control (n=6). (C) Data are represented as the means + SEM. (A-C) Two biological replicates were performed for all experiments, with measurements taken from distinct samples grown and processed at different times.

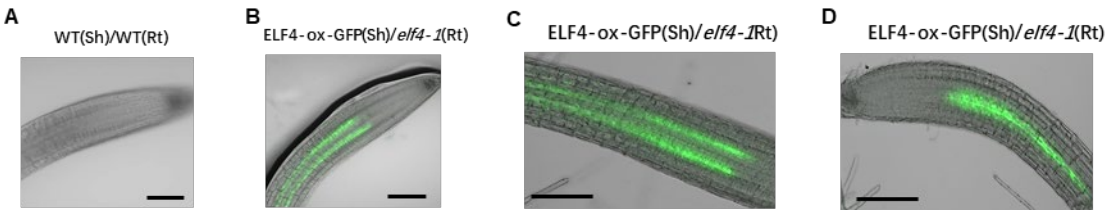

Figure 17. (A) Representative image showing the lack of fluorescence signals in roots of WT scion and WT rootstock. (B) Representative image showing fluorescence signals in roots of ELF4-ox scion into *elf4-1* rootstock. Scale bar: 100 µm. (C-D) Representative images showing fluorescence signals in roots of ELF4-ox-GFP scion and *elf4-1* rootstock. Scale bars: 100 µm. (A-D) At least two biological replicates were performed for all experiments, with measurements taken from distinct samples grown and processed at different times.

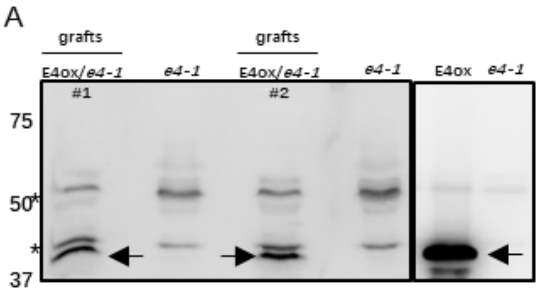

Figure 18. (A) Western-blot analysis of ELF4-GFP protein accumulation (arrows) in roots of ELF4-ox-GFP scion (E4ox) grafted into *elf4-1* rootstock (*e4-1*) (two pools of independent grafting assays, #1 and #2, are shown). Asterisks denote non-specific bands. (A) At least two biological replicates were performed for all experiments, with measurements taken from distinct samples grown and processed at different times.

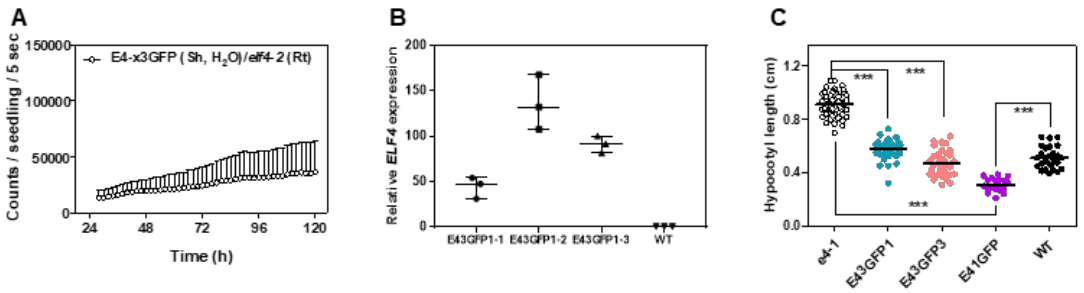

Figure 19. (A) *CCA1::LUC* luminescence in *elf4-2* rootstocks grafted with ELF4-x3GFP scions (n=5). Water instead of luciferin was added to the wells containing ELF4-x3GFP shoots. (A) Data are represented as the means + SEM. (B) Gene expression analyses of *ELF4* mRNA expression in WT and different ELF4-x3GFPs lines. Data are represented as the median ± max and min; 25-75 percentile. (C) Hypocotyl length of different lines expressing ELF4-x3GFPs (E43GFP) (E43GFP1 n=34; E43GFP3 n=35) transformed into *elf4-1* mutant plants. Hypocotyl length was also assayed for WT (n=27), *elf4-1* (n=48) and plants over-expressing ELF4 fused to 1 GFP (E41GFP) (n=19). *** p-value<0.0001; two-tailed t-tests with 95% of confidence. Data are represented as the median ± max and min; 25-75 percentile. (A-C) At least two biological replicates were performed for all experiments, with measurements taken from distinct samples grown and processed at different times.

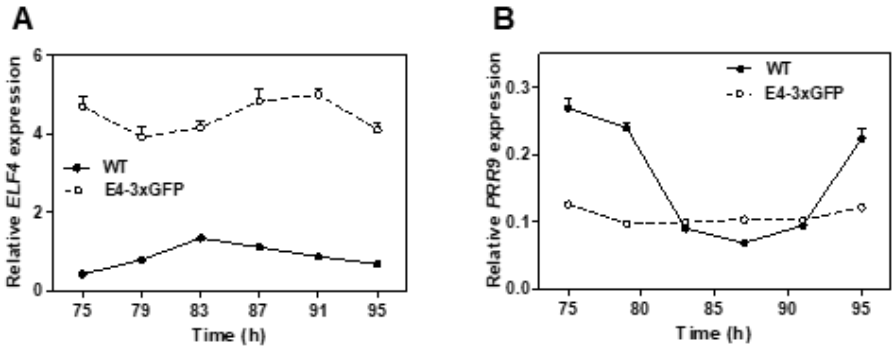

Figure 20. Circadian time course analyses of (A) *ELF4*, and (B) *PRR9* mRNA expression by RT-QPCR in shoots of WT and ELF4-x3GFPs. (A-B) Data are represented as the means + SEM. (A-B) At least two biological replicates were performed for all experiments, with measurements taken from distinct samples grown and processed at different times.

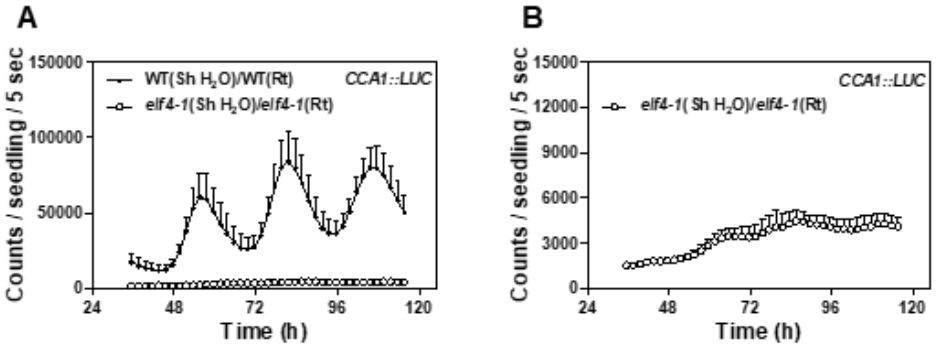

Figure 21. (A) Luminescence of *elf4-1* scion into *elf4-1* rootstocks *elf4-1* (Sh)/*elf4-1*(Rt) (n=4) and its comparison with luminescence in WT (Sh)/WT(Rt) roots (n=5). (B) Luminescence signals of *elf4-1* (Sh)/*elf4-1*(Rt) from (A) shown in a separate graph. Water instead of luciferin was added to the wells containing WT and *elf4-1* shoots. (A-B) Data are represented as the means + SEM. (A-B) At least two biological replicates were performed for all experiments, with measurements taken from distinct samples grown and processed at different times.

A

Name	Length (aa)	Mol. Weigth (Da)	Isoelectric point
FT	175	19808.4	8.05
ELF4	111	12375.5	9.16
HY5	168	18463.1	10.19

Figure 22. (A) Protein features of various plant mobile proteins.

3. Blocking ELF4 movement by shoot excision alters circadian rhythms in roots.

We next aimed to identify the function of the mobile ELF4 by blocking ELF4 movement via shoot excision. Analyses of the rhythms showed that excised roots sustained robust oscillations (Figure 23A and B) confirming that the root clock is able to run in the absence of shoots. However, comparison of intact versus excised roots uncovered a shorter period in excised roots (Figure 24A and B). As accumulation of ELF4 results in long periods in shoots (McWatters et al., 2007) and roots (Figure 8A and B), it is plausible that blocking ELF4 movement by shoot excision results in shorter periods in excised roots. If this is the case, blocking ELF4 movement should also affect ELF4 target-gene expression in excised roots. Time-course analyses by RT–qPCR revealed that the expression of *PRR9* and *PRR7* was upregulated in excised roots compared with intact roots (Figure 25A and B), which suggests that in the absence of ELF4 movement from shoots, repression of these genes is alleviated in roots. The use of ELF4-ox intact roots confirmed that *PRR9* and *PRR7* are targets of ELF4, as their expression was downregulated in intact ELF4-ox roots compared with WT intact roots (Figure 26A and B). Furthermore, ELF4-ox excised roots still showed repression of target-gene expression (Figure 27A and B) suggesting that excision per se is not responsible for the upregulation observed in WT excised roots.

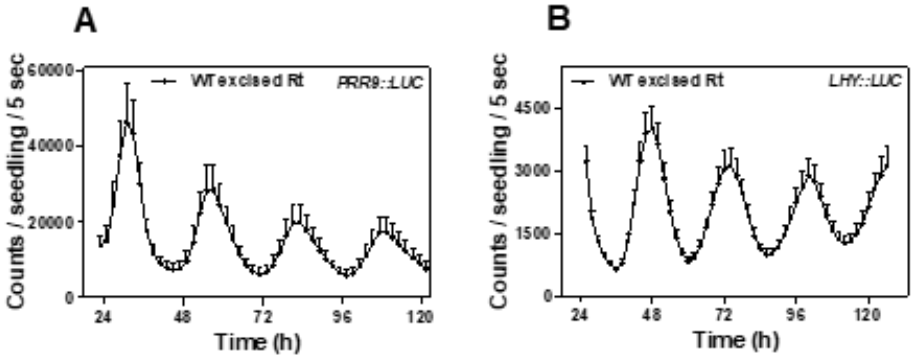

Figure 23. Luminescence of (A) *PRR9::LUC* (n=5) and (B) *LHY::LUC* (n=8) circadian rhythms in WT excised roots. Data are represented as the median ± max and min; 25-75 percentile. The "n" values refer to independent samples. (A-B) Two biological replicates were performed for all experiments, with measurements taken from distinct samples grown and processed at different times.

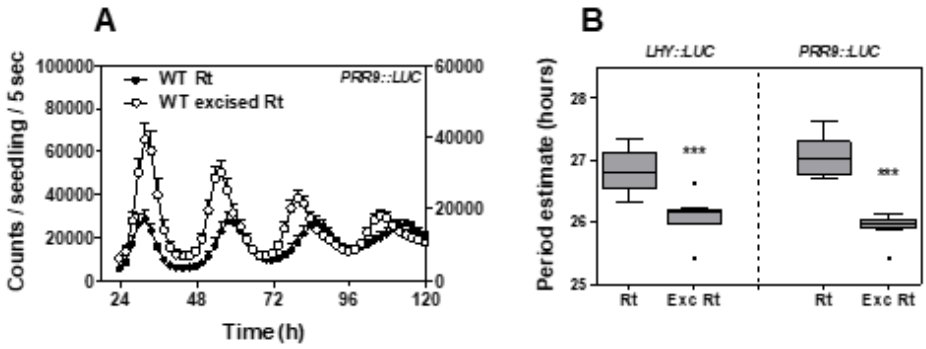

Figure 24. (A) Comparison of *PRR9::LUC* circadian rhythms in WT intact (n=6) versus excised roots (n=6). (B) Period estimates of *LHY::LUC* (left graph) (n=8) and *PRR9::LUC* (right graph) (n=8) rhythms in WT intact versus excised roots. Data are represented as the median ± max and min; 25-75 percentile. The "n" values refer to independent samples. *** p-value<0.0001; two-tailed t-tests with 95% of confidence. (A-B) Two biological replicates were performed for all experiments.

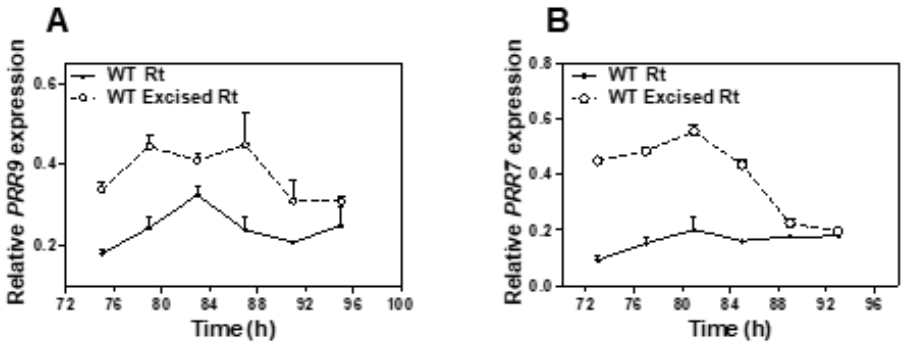

Figure 25. Circadian time course analyses of (A) *PRR9* and (B) *PRR7* mRNA expression in WT intact versus excised roots. (A-B) Data are represented as the means + SEM. (A-B) Two biological replicates were performed for all experiments, with measurements taken from distinct samples grown and processed at different times.

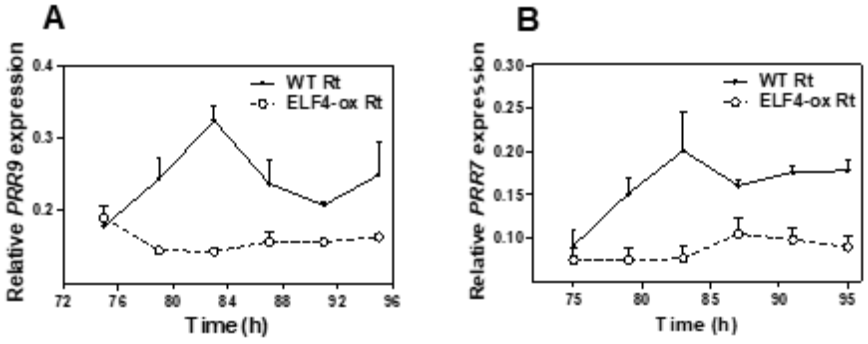

Figure 26. Circadian time course analyses of (A) *PRR9* and (B) *PRR7* mRNA expression in WT and ELF4-ox intact roots. (A-B) Data are represented as the means + SEM. (A-B) Two biological replicates were performed for all experiments, with measurements taken from distinct samples grown and processed at different times.

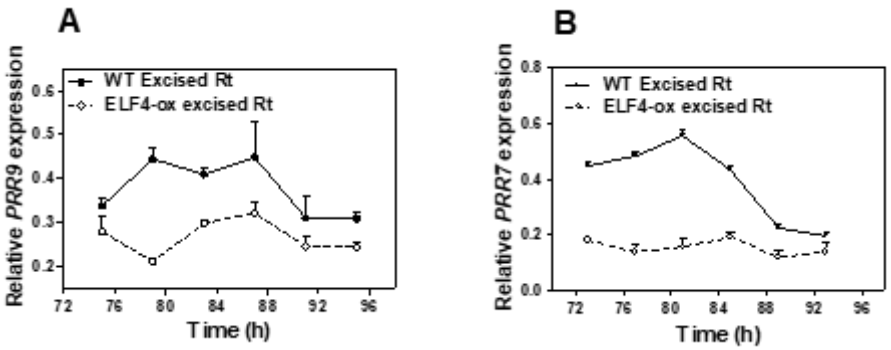

Figure. 27 Circadian time course analyses of (A) *PRR9* and (B) *PRR7* mRNA expression in WT excised and ELF4-ox excised roots. (A-B) Data are represented as the means + SEM. (A-B) Two biological replicates were performed for all experiments, with measurements taken from distinct samples grown and processed at different times.

4. Mobile ELF4 does not regulate the photoperiod-dependent phase in roots.

In aerial tissues, the circadian clock controls the photoperiodic regulation of growth and development (de Montaigu et al., 2010). To determine whether ELF4 movement is important to deliver photoperiodic information, we analysed rhythms under short day (ShD) and long day (LgD) conditions. In roots, *PRR9::LUC* waveforms displayed a subtle phase delay under LgD compared to ShD (Figure 28A) following a similar trend to that observed in shoots (Figure 28B). Time-course analyses by western blot of roots of ELF4 minigene plants (Nusinow et al., 2011) confirmed the phase delay of ELF4 protein accumulation under LgD compared with ShD (Figure 29A and B). We reasoned that if ELF4 movement is correlated with the photoperiodic-dependent phase delay, then excision of shoots might affect the phase shift in roots. In agreement with the oscillations in promoter activity (Figure 24A and B), the phase of ELF4 protein accumulation was advanced following excision under both LgD and ShD (Figure 30 A-D). Of note, under LgD conditions, excision resulted in a similar pattern of ELF4 accumulation than in intact roots under ShD (Figure 31 A and B). Thus, excision abolished the phase delay observed in intact root under LgD (compare Figure 29A and B with Figure 31 A and B). The results suggest that the photoperiod-dependent phase shift in roots is hampered by blocking ELF4 movement. However, excised roots still

showed the phase delay under LgD compared with excised roots under ShD (Figure 32 A and B). Furthermore, analyses of rhythms under LgD conditions showed that plants misexpressing ELF4 (ELF4-ox and *elf4-1* mutant) displayed very similar rhythms to WT plants both in shoots and roots (Figure 33 A and B) suggesting that ELF4 function is not essential to sustain rhythms under entraining conditions. Together, the results suggest that blocking ELF4 movement by excision advances the phase of the root clock, but the mobile ELF4 does not directly regulate the photoperiod-dependent phase shift in roots.

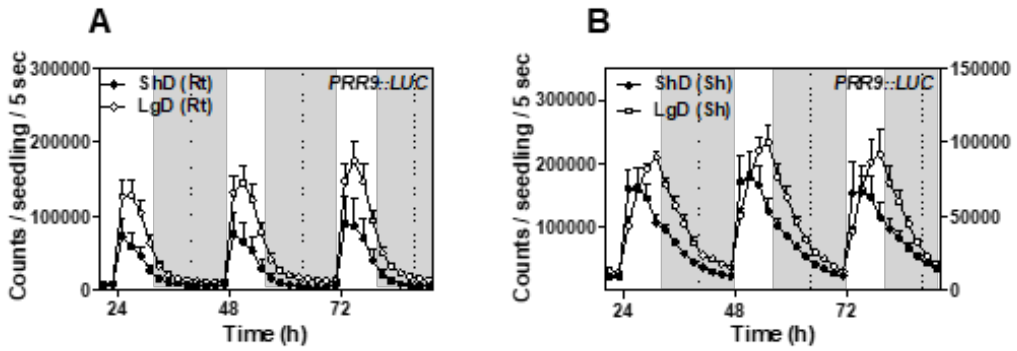

Figure 28. Luminescence analyses of *PRR9::LUC* rhythms in (A) roots (n=5 for ShD, n=6 for LgD) and (B) shoots (n=6 for ShD, n=4 for LgD) of plants grown under short day (ShD) or long day (LgD) conditions. (A-B) Data are represented as the means + SEM. The "n" values refer to independent samples. Dashed lines indicate dusk under LgD. (A-B) Two biological replicates were performed for all experiments, with measurements taken from distinct samples grown and processed at different times.

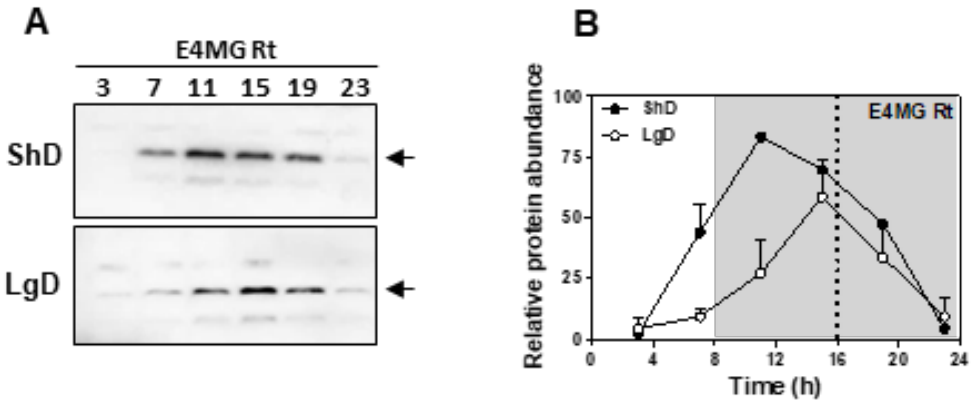

Figure 29. (A) Western-blot analyses and (B) quantification of ELF4 protein accumulation in ELF4 Minigene roots (E4MG Rt) of plants grown under ShD and LgD (also in Figure 31). (B) Data are represented as the means + SEM. Dashed lines indicate dusk under LgD. (A-B) Two biological replicates were performed for all experiments, with measurements taken from distinct samples grown and processed at different times.

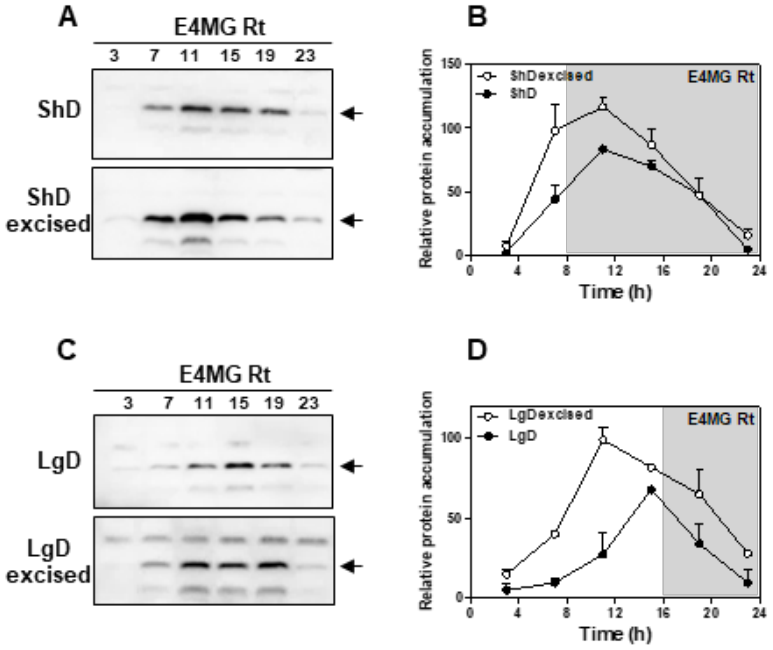

Figure 30. (A) Western-blot analysis and (B) quantification of ELF4 protein accumulation in ELF4 Minigene (E4MG) intact and excised roots under ShD (also in Figure 30). (C) Western-blot analysis and (D) quantification of ELF4 protein accumulation in E4MG intact and excised roots under LgD (also in Figure 32). (B**,** D) Data are represented as the means + SEM. (A-D**)** Two biological replicates were performed for all experiments, with measurements taken from distinct samples grown and processed at different times.

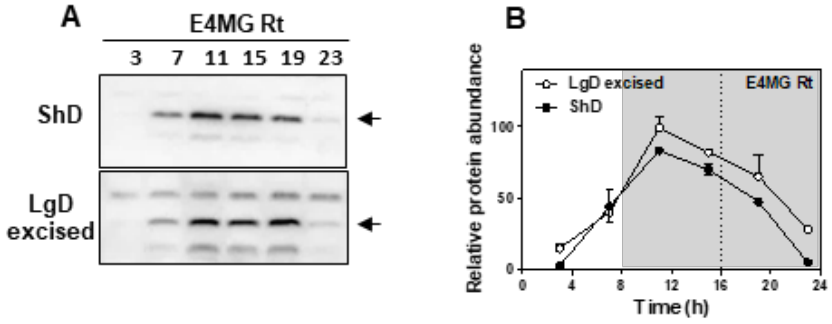

Figure 31. (A) Western-blot analyses and (B) quantification of ELF4 protein accumulation in E4MG roots of plants grown under ShD and excised roots under LgD (also in Figure 31 and Figure 33). Arrows indicate the ELF4 protein. (B) Data are represented as the means + SEM. Dashed lines indicate dusk under LgD. (A-B) Two biological replicates were performed for all experiments.

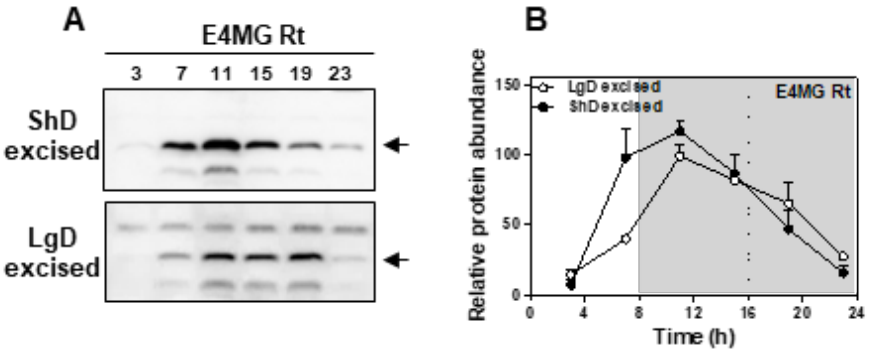

Figure 32. (A) Western-blot analysis and (B) quantification of ELF4 protein accumulation in E4MG excised roots under ShD and LgD (also in Figure 32). (B) Data are represented as the means + SEM. (A-B) Two biological replicates were performed for all experiments.

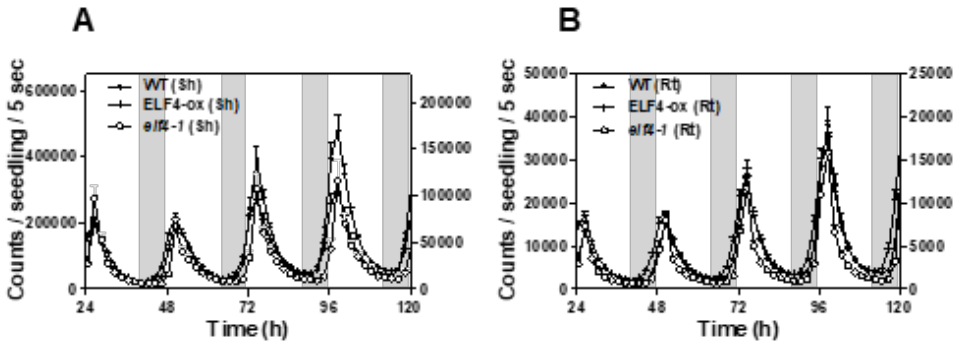

Figure 33. Luminescence of *LHY::LUC* oscillation in WT, ELF4-ox and *elf4-1* plants measured in (A) shoots (Sh) (n=12) and (B) roots (Rt) (n=12) under LgD conditions. (A-B) Data are represented as the means + SEM. Dashed lines indicate dusk under LgD. The "n" values refer to independent samples. (A-B) Two biological replicates were performed for all experiments, with measurements taken from distinct samples grown and processed at different times.

5. ELF4 movement contributes to the temperature-dependent changes in circadian period of the root clock.

As the evening complex also coordinates temperature responses, we examined whether a mobile ELF4 can convey temperature information from shoots to roots. We first examined the effect of different temperatures (28 °C, 18 °C and 12 °C) on circadian rhythms in roots. We found that the circadian period of *LHY::LUC* was shorter at higher temperatures (Figure 34 A and B). Shortening of period length with increasing temperature was also observed for other circadian reporter lines (Figure 35 A-D), indicating that at this developmental stage and under our experimental conditions, the circadian clock in roots is not able to sustain circadian period length within a range of temperatures.

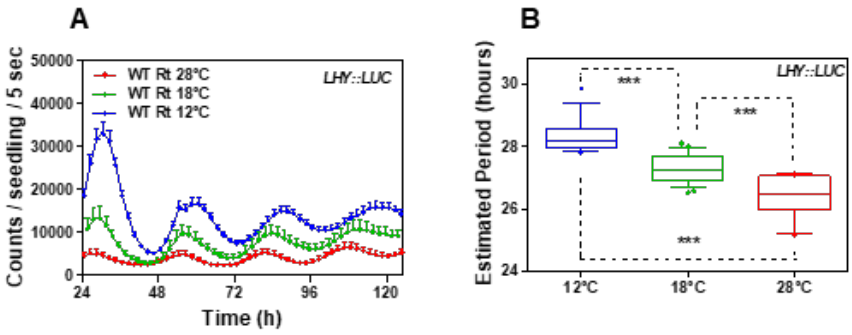

Figure 34. (A) Luminescence waveforms of *LHY::LUC* rhythmic oscillation in WT roots at 28ºC (n=8), 18ºC (n=8) and 12ºC (n=8) and (B) circadian period estimates of *LHY::LUC* rhythmic oscillation in WT roots at 28ºC (n=12), 18ºC (n=23) and 12ºC (n=14). Data are represented as the median ± max and min; 25-75 percentile. (B) *** p-value<0.0001; two-tailed t-tests with 95% of confidence. (A) Data are represented as the means + SEM. The "n" values refer to independent samples.

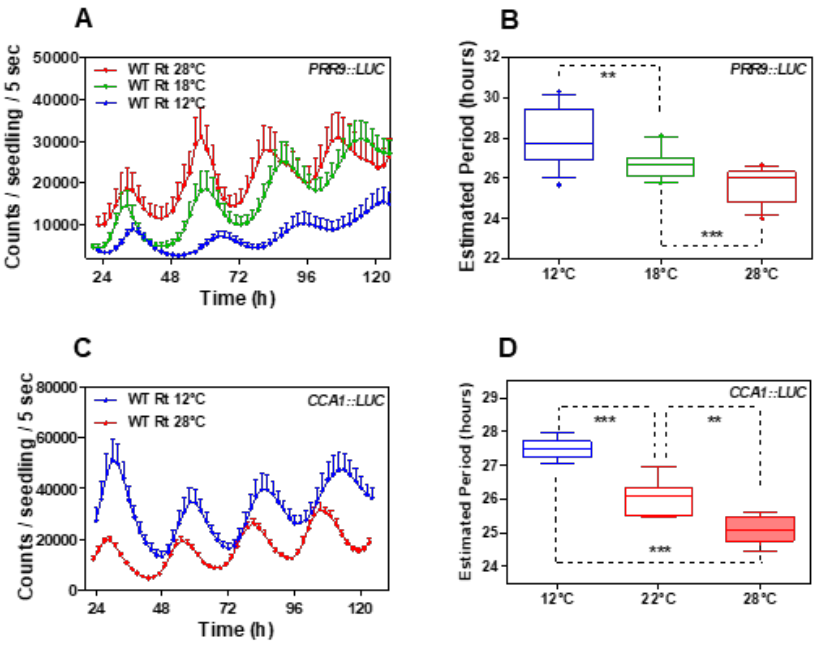

Figure 35. (A) Luminescence waveforms of *PRR9::LUC* rhythmic oscillation in roots at 28ºC (n=8), 18ºC (n=16) and 12ºC (n=8) and (B) circadian period estimates of *PRR9::LUC* rhythmic oscillation in roots at 28ºC (n=14), 18ºC (n=16) and 12ºC (n=12). (C) Luminescence waveforms and (D) circadian period estimates of *CCA1::LUC* rhythmic oscillation in roots at 28ºC (n=6), 22ºC (n=6) and 12ºC (n=6). (A, C) Data are represented as the median ± max and min; 25-75 percentile. (B, D) ** p-value<0.005; *** p-value<0.0001; two-tailed t-tests with 95% of confidence. (A, C) Data are represented as the means + SEM. The "n" values refer to independent samples.

As ELF4 accumulation increases period length, we next examined the possible contribution of ELF4 to the long period phenotype at low temperatures. Changes in period length could be mediated by increased ELF4 activity and/or by increased protein movement from shoots to roots. To examine these possibilities, we compared the effects of blocking ELF4 movement by excision at low and high temperatures. Essentially, if the long period in roots at 12 °C is independent of movement but results from the increased activity of ELF4, blocking movement from shoots by excision should not have a major effect on period length. However, if ELF4 movement contributes to the period regulation, abolishing ELF4 traffic should lead to an observable and differential effect on period length at different temperatures.

Our results showed that excision shortened the period length at 12 °C but not so markedly at 28 °C (Figure 36A-D). Therefore, blocking ELF4 movement by excision

shortens the period of WT roots at 12 °C. Analyses of other circadian reporter lines and at 18 °C also showed that excision shortened period length compared to intact roots (Figure 37A and B). The results suggest a temperature-dependent control of ELF4 movement that regulates period length in roots. To further verify this notion, we examined the rhythmic recovery in grafts of ELF4-ox scion into *elf4-1* rootstock at low and high temperatures. Our results showed an evident rhythmic recovery at 12 °C but not at 28 °C (Figure 38A and B). Furthermore, grafts of E4MG scion into *elf4-1* rootstock also efficiently recovered rhythms at 12 °C but not at 28 °C (Figure 39A and B). ELF4 was still able to delay the phase and lengthen the period at 28 °C (Figure 40A and B), suggesting that movement, rather than changes in activity, were responsible for the observed effects. ELF4 protein accumulation in roots of ELF4-ox scion into *elf4-1* rootstock was higher at 12 °C than at 28 °C (Figure 41A-C) but ELF4 protein accumulation in shoots was similar at different temperatures (Ezer et al., 2017a) (Figure 42A). Therefore, ELF4 movement, rather than protein accumulation or activity, appears to be regulated by temperature, contributing to the temperature-dependent control of circadian period in roots.

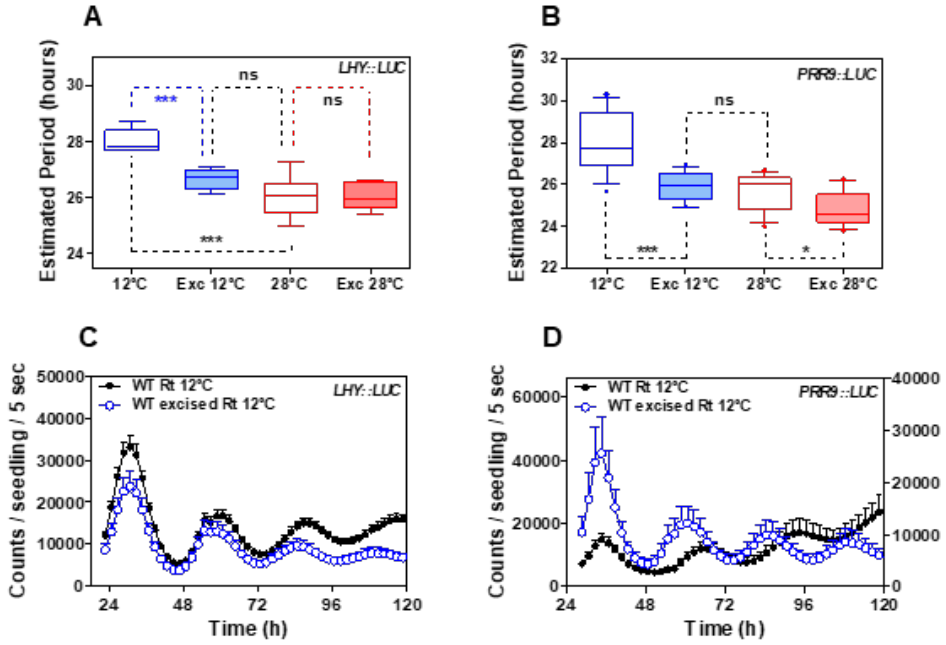

Figure 36. Circadian period estimates of (A) *LHY::LUC* in intact (n=8) versus excised WT roots (n=7) at 12ºC and 28ºC (n=8 for intact and n=8 for excised) and (B) *PRR9::LUC* in intact (n=12) versus excised WT roots (n=13) at 12ºC and 28ºC (n=14 for intact and n=16 for excised). Data are represented as the median ± max and min; 25-75 percentile. *** p-value<0.0001; * p-value<0.05; ns: non-significant p=0.369; two-tailed t-tests with 95% of confidence. Luminescence rhythmic oscillation in WT intact and excised roots (n=8 for each) at 12ºC of (C) *LHY::LUC,* (D) *PRR9::LUC* (n=8 for each). The "n" values refer to independent samples. (A-D) Two biological replicates were performed for all experiments, with measurements or analyses taken from distinct samples grown and processed at different times.

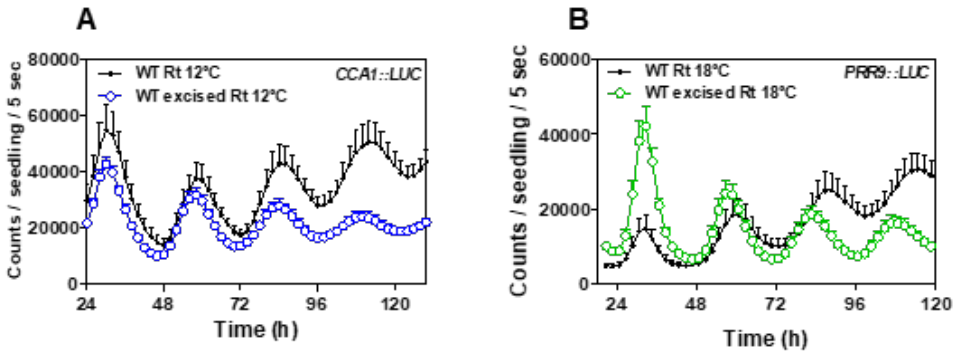

Figure 37. Luminescence rhythmic oscillation in WT intact and excised roots (n=8 for each) at 12ºC of (A) *CCA1::LUC* (n=4 for excised, n=5 for intact). (B) Luminescence of *PRR9::LUC* rhythmic oscillation in WT intact and excised roots at 18ºC (n=16 for each). (A-B) Data are represented as the means + SEM. The "n" values refer to independent samples. (A-B) Two biological replicates were performed for all experiments.

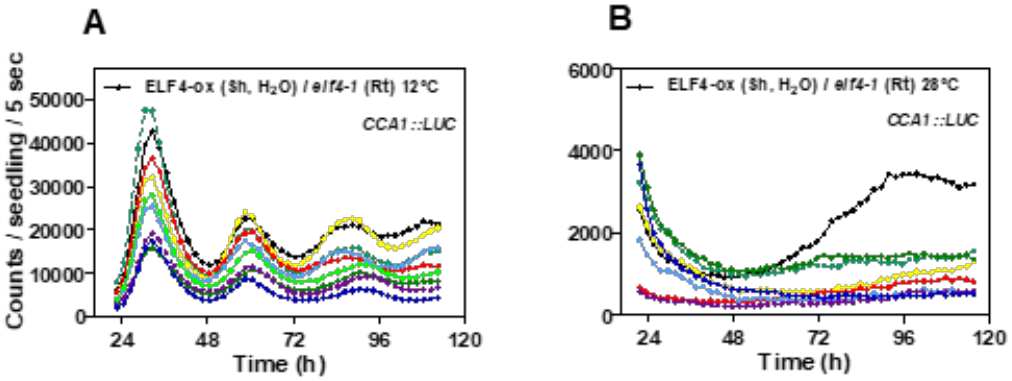

Figure 38. Individual luminescence waveforms of *CCA1::LUC* rhythmic oscillation in ELF4-ox scion into *elf4-1* rootstocks at (A) 12ºC (n=10) and (B) 28ºC (n=8). Water instead of luciferin was added to the wells containing ELF4-ox scions. Two biological replicates were performed for all experiments, with measurements taken from distinct samples grown and processed at different times.

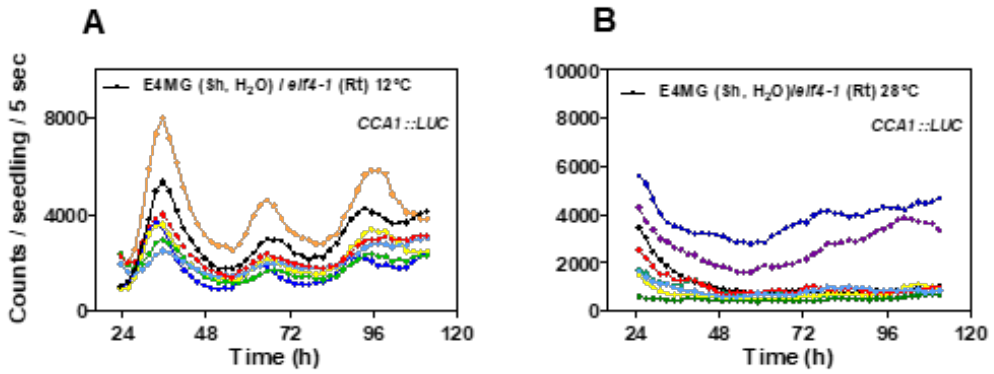

Figure 39. Individual luminescence waveforms of *CCA1::LUC* rhythmic oscillation in E4MG scion into *elf4-1* rootstocks at (A) 12ºC (n=7) and (B) 28ºC (n=8).Water instead of luciferin was added to the wells containing E4MG scions. Two biological replicates were performed for all experiments, with measurements taken from distinct samples grown and processed at different times.

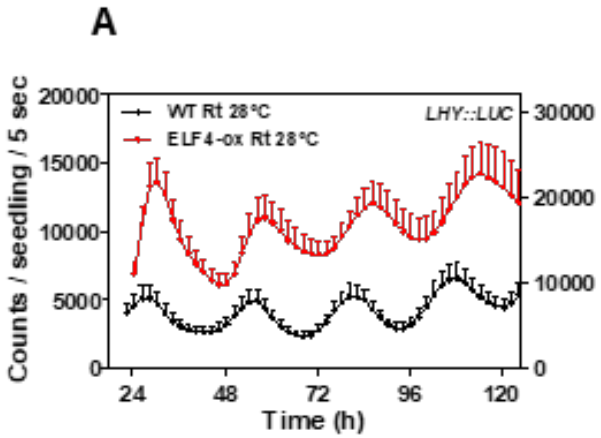

Figure 40. (A) Luminescence of *LHY::LUC* rhythmic oscillation in WT and ELF4-ox roots at 28ºC (n=8 for WT, n=5 for ELF4-ox). Data are represented as the means + SEM. (B) Circadian period estimates of *LHY::LUC* in WT (n=12) and ELF4-ox (n=17) at 28ºC. Data are represented as the median ± max and min; 25-75 percentile. Promoter activity analyses were performed under constant light conditions previous synchronization of plants under LD cycles at 22ºC. The "n" values refer to independent samples. (A-B) Two biological replicates were performed for all experiments, with measurements or analyses taken from distinct samples grown and processed at different times.

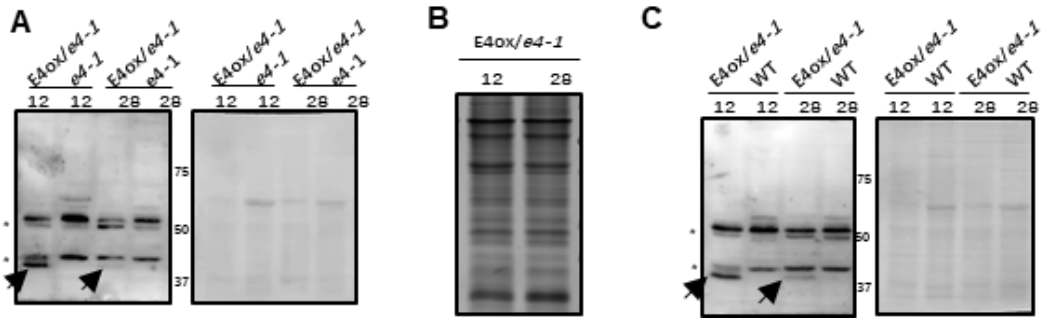

Figure 41. (A) Western-blot analysis of ELF4-GFP protein accumulation (arrow) in roots of ELF4-ox-GFP scion (E4ox) grafted into *elf4-1* rootstock (*e4-1*) at 12ºC and 28ºC. *elf4-1* mutant protein extracts were used as a control. Asterisks denote non-specific bands. Ponceau S staining of the membrane is shown in the right panel. (B) Coomassie Blue staining of protein extracts from roots of ELF4-ox-GFP scion (E4-ox) grafted into *elf4-1* rootstock (*e4-1*) at 12ºC and 28ºC. (C) Western-blot analyses of ELF4-GFP protein accumulation (arrows) in roots of ELF4-ox-GFP scion (E4-ox) grafted into *elf4-1* rootstock (*e4-1*) at 12ºC and 28ºC. WT protein extracts were used as a control. Asterisks denote non-specific bands. Ponceau S staining of the membrane is shown in the right panel.

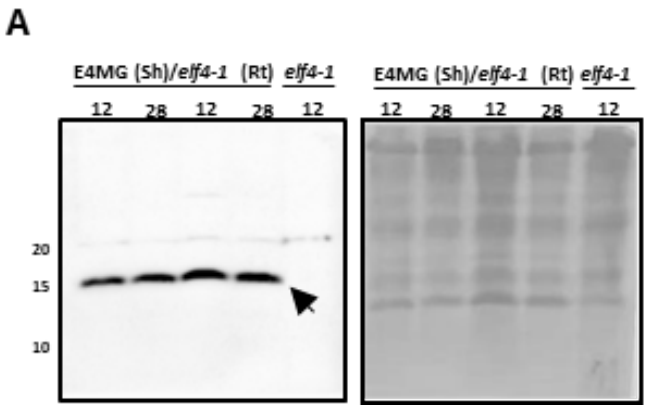

Figure 42. (A) Western-blot analyses of ELF4 protein accumulation (arrow) in shoots of ELF4 Minigene (E4MG) grafted into *elf4-1* rootstock (*e4-1*) at 12ºC and 28ºC. *elf4-1* protein extracts were used as a control. Ponceau S staining of the membrane is shown in the right panel.

We propose a model by which mobile ELF4 (MbE4) from shoots to roots defines a pool of active ELF4 protein that is competent to repress target circadian gene expression in roots. ELF4 trafficking is favoured at low temperatures, resulting in a slow-paced clock (Figure 43A), whereas high temperatures decrease the movement, leading to a faster root clock (Figure 43B). The temperature-dependent movement of ELF4 enables a shoot-to-root dialogue that controls the pace of the clock and provides a mechanism by which temperature cues from shoots set the circadian period length in roots.

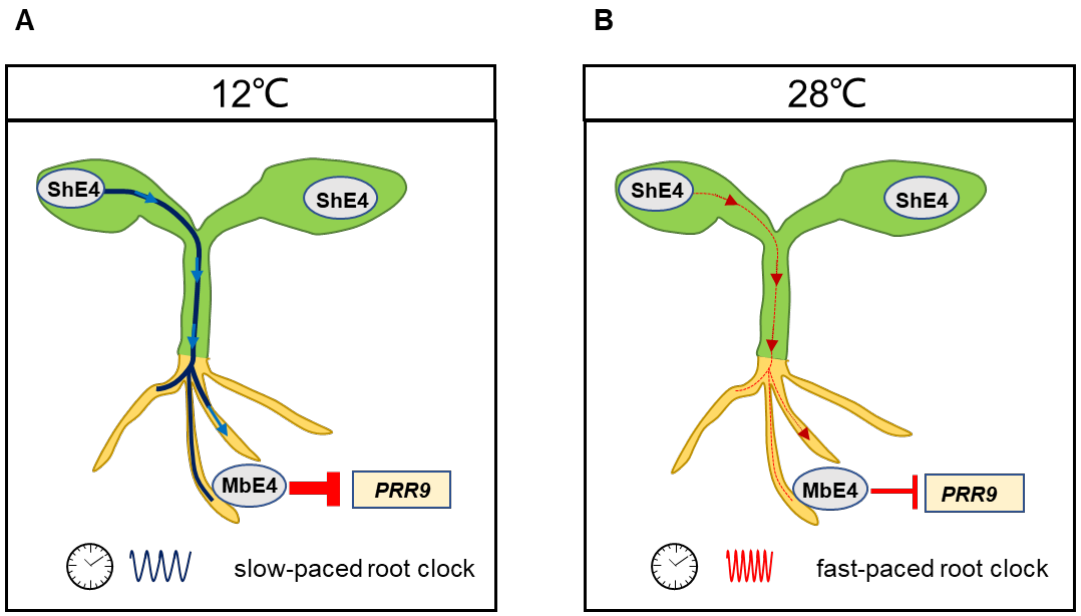

Figure 43. Schematic drawing depicting (A) the increased shoot-to-root movement of ELF4 (Sh-to-Rt mov, thick blue vertical arrows), increased *PRR9* repression and the slow pace of the root clock at low temperatures, and (B) the decreased shoot-to-root movement (Sh-to-Rt mov, thin red vertical arrows), decreased *PRR9* repression and fast-paced root clock at high temperature.

Discussion

The simultaneous examination of rhythms in shoots and roots of single individual plants shows that the promoter activities and mRNA accumulation of clock genes in roots display a longer period and delayed phase compared with shoots. A similar trend was observed for morning- and evening-expressed key oscillator genes, suggesting that the overall circadian system in roots is not as precise as in other parts of the plant for example, the shoot apex (Takahashi et al., 2015). Similar to the circadian properties in roots, hypocotyls also lack precision and robustness (displaying longer periods and arrhythmia), while leaves lack synchrony among the different samples (even though they are entrained under the same conditions) (Takahashi et al., 2015). In contrast, the shoot apex displays a high degree of precision and synchrony (with rhythms similar to the entire plants) (Takahashi et al., 2015). Besides, the shoot apex clocks are remarkable coupled and have the ability to influence rhythms in roots (Takahashi et al., 2015). Despite the long period, the rhythms persist in roots for several days under constant light conditions, which is reminiscent of a fully functional clock. The lack of precision might provide circadian flexibility for rapid adjustments and improved responses in roots.

Previous studies have reported spatial waves of clock gene expression within and among different organs (Fukuda et al., 2007; Gould et al., 2018; Greenwood et al., 2019) that might be due to differences in period length and variable local coupling. Indeed, the degree of coupling varies among different organs and different experimental conditions. The root tip shows strong cell-to-cell coupling (a stripe wave in the root tip results from a continuous resetting of the circadian oscillations in root cells) (Gould et al., 2018). Besides, the phase of hypocotyl is much more advanced than cotyledon and the top of the root or the phenotype of the wave of the clock gene expression (from shoot to root) is identified (Gould et al., 2018), which is totally match the hierarchical structure of clock (the rhythms in the roots are driven by the shoot apex) (Takahashi et al., 2015). The short period oscillations in the root tip or the

phenotype of the wave of the clock gene expression (from the root tip to above tissues) do not explain the hierarchical structure (Gould et al., 2018). In all excised tissues (shoot, root, root tip), rhythms are autonomous and the spatial waves (travel among different tissues) are not affected, thus the spatial waves are not long-distance signals dependently (Greenwood et al., 2019). The waves could be modulated in a predictable method (locally altering clock periods) through the controlling of environmental inputs (Greenwood et al., 2019). It seems that local coupling (generation of spatial waves of circadian clock gene expression across the plant) is dependent on a signal that is cell-to-cell mobile (Greenwood et al., 2019).

Many different mobile factors might contribute to the shoot-to-root synchronizing signals such as photosynthetic sugars, microRNAs, hormonal signals, mobile transcription factors and peptide ligands (Chen et al., 2016; Endo, 2016; Han et al., 2014; Inoue et al., 2018; James et al., 2008b; Katsir et al., 2011; Lee et al., 2017; Lin et al., 2008; Nimmo, 2018; Pant et al., 2008; Salisbury et al., 2007; Stahl and Simon, 2013) microRNAs contribute to the intra and inter-tissue coupling in mammals or insects (Kadener et al., 2009; Mehta and Cheng, 2013). microRNAs might play a similar role in plants.

The evening complex directly represses the expression of *PRR9* and *PRR7* (Dixon et al., 2011; Helfer et al., 2011; Herrero et al., 2012; Kolmos et al., 2011; Mizuno et al., 2014) and indirectly promotes the expression of the morning-expressed oscillator genes *CCA1* and *LHY* (Dixon et al., 2011; Kikis et al., 2005; Kolmos et al., 2011; Lu et al., 2012b). Our analyses with *elf4-1* mutant and ELF4-ox plants demonstrate that ELF4 function in roots is also important for proper repression of *PRR9* and *PRR7* and activation of *CCA1* and *LHY*. ELF4 regulatory function in roots appears to be similar to that previously described for the evening complex using whole plants. Overexpression of ELF4 lengthens the period of the root clock, suggesting that ELF4 slows the circadian period in roots, as in shoots (McWatters et al., 2007). The lengthening of the period on

accumulation of ELF4 is in agreement with the results showing that blocking ELF4 movement by shoot excision shortens the period. RNA-seq analyses revealed that the expression of oscillator genes as well as genes involved in other pathways, including responses to stimuli are affected in *elf4-1* roots. The mis-regulated genes in *elf4-1* roots might be direct targets of ELF4 and/or indirect outputs of the clock in roots.

These pathways are also consistent with the function of the evening complex in responses to environmental cues (Huang and Nusinow, 2016). The EC is regulated by external light and temperature and EC has the ability to integrate numerous environmental inputs to the circadian clock (Huang and Nusinow, 2016). The transcription of *ELF4* is regulated by three transcriptional regulators of the PHYA light signaling pathway (FHY3, FAR1, and HY5) (Li et al., 2011b). The post-translation of ELF3 is regulated by PHYB and COP1(PHYB stabilizes ELF3 protein, whereas COP1 degrades ELF3 protein by ubiquitin) (Liu et al., 2001b; Nieto et al., 2015b; Yu et al., 2008b). The strength of the EC binding ability is stronger at lower temperatures, whereas the strength of the EC binding signal is weaker at high temperatures, suggesting the binding of EC is temperature-dependent (Ezer et al., 2017b).

Several latest results discovered more functions of EC. For instance, ELF4 plays a critical role in the regulation of the temperature-dependent EC binding to DNA (Silva et al., 2020b). Under in-vitro conditions, the EC (LUX-ELF3-ELF4) acts as a direct thermosensor, with stronger DNA binding at low temperature (4 °C) and weaker binding at high temperature (27 °C) (Silva et al., 2020b). A∼20-fold molar excess of ELF4 could restore EC binding at 27 °C, indicating that ELF4 can modulate the DNA binding activity of the EC and partially overcome the temperature-dependent limitations of EC binding when present in high concentrations (at least under in-vitro conditions) (Silva et al., 2020b). It also provides the possibility to alter plant thermo-responsiveness within the ambient temperature range through modulating ELF4 expression.

Efficient micrografting has been widely used to study long-distance signaling in plants (Bainbridge et al., 2014; Turnbull et al., 2002). The movement of FT protein over longer distance was indeed confirmed through grafting experiments using the aerial parts of *SUC2p:FT-GFP ft-7* (*SUC2* (a phloem companion-cell-specific promoter (Imlau et al., 1999))) plants grafted into the roots of *ft-7* mutants (Corbesier et al., 2007). The fluorescent signal of FT-GFP protein was also detected across the graft junction and accumulated in the vasculature of the *ft-7* rootstock (Corbesier et al., 2007). The shoots of *SUC2p:FT-GFP ft-7* were also grafted as a donor to the *ft-7* shoots receiver (Corbesier et al., 2007). The distribution of the FT-GFP fusion protein was detected in the shoot apical region of the donor and receiver by confocal microscopy (Corbesier et al., 2007).

The shoot to root movement of HY5-GFP protein was also confirmed through grafting experiments using the shoots of *CAB3p:HY5-GFP hy5* (*CAB3,* a photosynthetic-tissue-specific promoter) (An et al., 2004; Corbesier et al., 2007) plants grafted into the roots of *hy5* mutants. The fluorescent signal of HY5-GFP was also detected in the roots of *hy5* mutants (Chen et al., 2016). The shoots of *HY5p:HY5-GFP hy5* plants were also grafted into the roots of *hy5* mutants, further indicating the movement of HY5 (Chen et al., 2016). HA-YFP-HA-HY5 and HY5-GFP protein could be detected at comparable levels in the shoots of different *HY5* transgenic lines (*CAB3p:HA-YFP-HA-HY5 hy5* plants, *CAB3p:HY5-GFP hy5* plants), whereas HA-YFP-HA-HY5 protein could not be detected in the roots of the *HY5* transgenic line (*CAB3p: HA-YFP-HA-HY5 hy5* plants) while HY5-GFP protein was detected in the roots of the *HY5* transgenic line (*CAB3p:HY5-GFP hy5* plants) (Burko et al., 2020; Chen et al., 2016). The position of the tags (N terminal in HA-YFP-HAtag and C terminal for the GFP tag) might affect the fold of HY5 protein and/or its movement, thus leading to different results of HY5 protein accumulation in the roots.

In this thesis, micrografts of ELF4-ox scion into *elf4-1* or *elf4-2* rootstocks enable a recovery of rhythms that is not observed when seedlings expressing ELF4–3×GFP are used as scion. These results suggest that ELF4 movement is indeed important for the rhythmic recovery. Fluorescent signals accumulating in the vasculature of *elf4-1* mutant rootstock grafted with ELF4–GFP scion and the detection of the ELF4 protein in roots of the micrografted plants also suggest that ELF4 moves from shoots to roots. This conclusion is complemented by the grafting assays of *elf4-1* (Sh)/*elf4-1* (Rt) showing the lack of rhythmic recovery in roots, and by ELF4 protein-injection assays in shoots and the subsequent rhythmic recovery in roots. Micrografts of E4MG and WT plants are also able to recover the rhythms of the *elf4-1* mutant roots, indicating that the effects are not due to excess accumulation of ELF4-ox. The results suggest that small amounts of mobile ELF4 might be required to regulate the rhythms.

Several studies have shown that mobile transcription factors and peptide ligands contribute to long-distance signaling (Chen et al., 2016; Putterill and Varkonyi-Gasic, 2016). Based on our RT-qPCR time-course analyses of roots from ELF4-ox (Sh)/*elf4-1* (Rt) grafts, the amplification of *ELF4* mRNA was barely detectable. These results suggest that the mRNA of *ELF4* does not move through the graft junctions. Further, a series of protein experiments suggest that the ELF4 protein move through the graft junctions. Injection of purified in-vitro ELF4 protein into the shoots of *elf4-1* mutant was able to restore rhythms in *elf4-1* mutant roots. The detection of ELF4 protein in roots of the ELF4-GFP (Sh)/*elf4-1* (Rt) grafts further suggest that ELF4 protein moves from shoots to roots. It would be interesting to identify other possible mobile signals and their connection, if any, with ELF4.

It is possible that veins are used as the circadian traveling ‘‘highway’’ in which the synchronizing signals circulate from plant shoot apexes to roots (Takahashi et al., 2015). Indeed, our results showed the presence of fluorescent signals accumulating in the vasculature of *elf4-1* mutant rootstock grafted with ELF4-GFP scion. These results

suggest that ELF4 moves from shoots to roots through veins. The ELF4 in leaf vasculature moves from shoots to roots through veins and plays an essential role in the physiological and molecular regulation of roots. The leaf vasculature-enriched expression pattern of *ELF4* (10-fold higher in vasculature) (Endo et al., 2014) is consistent with this possibility. It would be interesting to generate a series of transgenic lines that express *ELF4* under different tissue-specific promoters (such as mesophyll, vasculature companion cell, epidermis, shoot apical meristem, etc) and explore the phenotypes and the underlying mechanisms.

Our experiments in which we added water to the scion or used WT scion without LUC reporter exclude the possibility that rhythms in grafted roots are due to leakage from the adjacent well containing the shoot. ELF4 protein shows similar properties in terms of length, molecular weight and isoelectric point to other mobile proteins (Chen et al., 2016; Corbesier et al., 2007; Jaeger and Wigge, 2007; Mathieu et al., 2007b), which also supports the notion of ELF4 movement. We postulate that following movement, the complex regulatory feedback loops at the core of the oscillator are reset to control the pace of the clock. Further experiments at different developmental stages and under various growing conditions (for example, different light and temperature conditions) will be required to confirm whether the long-distance movement of ELF4 contributes to the spatial waves of clock gene expression observed in roots or not (Greenwood et al., 2019).

As mentioned above, other mobile transcription factors have been reported to play essential roles in plant development. For instance, the long-distance shoot-to-root movement of HY5 protein mediates coupling of light-mediated shoot growth and carbon assimilation with root growth and nitrate uptake (Chen et al., 2016). The mobile HY5 contributes to maintain the balance of carbon and nitrate metabolism in plants at varying light fluences (Chen et al., 2016). The mechanisms regulating the movement of HY5 from shoots to roots are not clear. Probably, photoperiod or

temperature could also regulate the movement of HY5 and plants reach the new balance of carbon and nitrate metabolism under different photoperiod or temperature conditions.

FT is a key regulator of the transition from vegetative to reproductive growth (Kardailsky et al., 1999; Kobayashi et al., 1999). The FT protein was identified to be mobile and was termed as ‘a ‘florigen’’ in plants. FT travels from the leaves to the shoot apex through the vasculature (Corbesier et al., 2007; Jaeger and Wigge, 2007; Mathieu et al., 2007b). FT protein acts at the shoot apical meristem in concert with the transcription factor FD (Abe et al., 2005; Corbesier et al., 2007; Kardailsky et al., 1999; Kobayashi et al., 1999; Wigge et al., 2005) to promote the expression of flowering regulators and induce plant flowering (Wu and Gallagher, 2012). The transcription of *FT* in leaves is activated by CO and this activation only occurs under long day conditions (Kobayashi et al., 1999). The molecular mechanisms controlling ELF4 in shoots remain to be elucidated. It would be interesting to identify whether other proteins in shoots regulate ELF4 transcription, translation or movement in response to changes in temperature.

Excision blocks ELF4 movement from shoots and consequently, we observe that oscillator gene expression and other output genes are affected in WT excised roots. Previous studies have also used excision to define properties of the circadian function in roots (Greenwood et al., 2019). Although many genes are affected by excision, it is noteworthy that 67% of the genes misregulated in *elf4-1* intact roots are also misexpressed in WT excised roots. Both conditions have in common a lack of ELF4 movement, suggesting that the overlapping DEGs are due to the lack of mobile ELF4 (note that the RNA-seq studies with *elf4-1* mutant were performed with intact roots). The phase shifts observed following excision prompted us to examine whether ELF4 movement contributed to the photoperiodic-dependent phase shift. However, excised roots still sustained the phase delay under LgD, suggesting that other factors

are responsible for this regulation. Light piping down the root (Nimmo, 2018) might be also important for synchronization. Regardless the mechanism, it is able to overcome the misexpression of ELF4 in shoots and roots, as ELF4-ox and *elf4-1* mutant plants displayed similar rhythms to WT. Clear alteration of circadian expression under constant light but not under entraining conditions has been reported for other clock mutant plants and plants overexpressing clock genes (Flis et al., 2015)

Previous studies have reported that temperature controls the movement of other long-distance mobile proteins. For instance, latest results show that the movement of FT protein from companion cells (Mathieu et al., 2007b) to sieve elements (the conducting cells of phloem, the region where FT moves to shoot apex (Mathieu et al., 2007b) in leaves is temperature-dependent (Liu et al., 2020). Low temperature suppresses the movement of FT in the phloem and the expression of *FT* mRNA, thus the plant reproductive success only happens under favorable temperature (Liu et al., 2020).

Cold temperatures positively regulate the transcription and post-translation accumulation of HY5 (Catalá et al., 2011; Toledo-Ortiz et al., 2014). Besides, HY5 protein is stable at 4°C even in the darkness whereas activated COP1 directly targets HY5 for ubiquitination and subsequently triggers the protein degradation of HY5 under room temperature conditions (Catalá et al., 2011; Osterlund et al., 2000). The accumulation of HY5 protein (not the amount of *HY5* mRNA) is reduced by high temperature through COP1 activity-dependent pathway, further suggesting that HY5 protein is temperature regulated (Kim et al., 2017). It will be valuable to examine whether the HY5 movement (from shoot to root) is temperature regulated.

In this thesis, we identified that shoot excision shortened the period, suggesting that ELF4 movement is important in the control of circadian period length. Period shortening is more significant at low temperatures than at high temperatures,

confirming that ELF4 movement is favoured at low temperatures. The temperature-dependent control of ELF4 movement is also supported by the increased accumulation of ELF4 protein in grafted roots at 12 °C compared to 28 °C. As ELF4 accumulation results in a longer period, the increased movement leads to a clock that runs slower at low temperatures than at high temperatures. The mobile ELF4 thus delivers temperature information and sets up a shoot-to-root long distance dialogue that regulates the pace of the clock in roots (Figure 43). It would be interesting to elucidate whether period sensitivity to temperature might provide an advantage for optimal root responsiveness to temperature variations.

Previous studies have reported higher temperature leads to increased root elongation, dependently of brassinosteroid (BR) hormone signaling and Gibberellins (GA) (Camut et al., 2019; Martins et al., 2017). Thus, plant roots grow deeper to search for water at high temperatures (the availability of water drops with warmth) (Martins et al., 2017). The transportation of root basipetal auxin and the accumulation of auxin is inhibited by cold temperature, reducing root growth, which suggest that low temperatures limit auxin transport and responses in the root (Jeon et al., 2016; Shibasaki et al., 2009; Zhu et al., 2014). Hormone signaling plays an essential role for optimal root responsiveness to temperature variations and the connection between hormone signaling and the circadian clock has been extensively reported (Singh and Mas, 2018).

The functional activity of most enzymes is higher at high temperatures. However, the pace of the circadian clock is buffer against changes in temperature within a physiological range (Hogenesch and Ueda, 2011). Thus, the circadian clock maintains a 24-hour period under different temperatures (termed as temperature compensation) (Greenham and McClung, 2015; Hogenesch and Ueda, 2011). In this thesis, we found that the circadian clock in roots is not temperature-compensated. The circadian clock in roots slows down at lower temperatures, whereas the clock

speeds up at higher temperatures. Our model shows that the different amount movement of ELF4 protein from shoot to root at different temperatures (more movement at low temperature, less movement at high temperature) breaks the overall balance of clock speed and buffering environment of the root. Indeed, ELF4 is able to delay the phase and lengthen the period of circadian clock (McWatters et al., 2007).

In whole seedlings, the protein kinase CK2 promotes the phosphorylation of CCA1 to inhibit its transcriptional activity (Portolés and Más, 2010). At high temperature, the inhibition of CCA1 to its target genes increases, whereas the phosphorylation of CCA1 from CK2 also increases (decreasing the activity of CCA1) (Portolés and Más, 2010). Thus, the clock buffers the changes from varying temperatures. In the roots, the mechanism for temperature compensation is still not clear. Probably, the balance of CK2 and CCA1 in roots is different from the shoots or not as stable as in shoots. Besides, the growing environments and energy supplements for shoots and roots are not the same. Thus, the regulation and mechanism for temperature compensation may be different. It would be very interesting to discover the mechanism for temperature compensation in roots in future.

Altogether, in this thesis, we found a shoot-to-root mobile signal ELF4 protein and ELF4 moves from shoots to regulate the pace of circadian clock in roots in a temperature-dependent manner (not photoperiodic dependently). Additionally, low temperatures favour the movement of ELF4, leading to a slower root clock, while high temperatures decrease ELF4 mobility, resulting in a fast-paced root clock. Thus, the mobile ELF4 (temperature dependent) has the ability to set a shoot-to-root dialogue that sets the speed of circadian clock in roots (Figure 43).

Conclusions

In this Doctoral thesis, we have identified the long-distance circadian communication between shoots and roots of Arabidopsis plants. The evening-expressed clock component ELF4 moves from shoots to regulate the rhythms in roots. The movement of ELF4 is not regulated by photoperiod but by temperature. Specifically:

1. The in vivo luminescence analyses and RT-QPCR assays have shown that the root clock is fully operative, but runs at a slower pace and delayed phase compared to the shoot clocks. In vivo luminescence analyses, RT-QPCR and RNA-SEQ analyses in roots of ELF4 mis-expressing plants have shown the important regulatory function of ELF4 in the root clock: mutation compromises the circadian rhythms of root clock, while overexpression lengthens the circadian period of root clock.

2. In vivo luminescence analyses of roots of grafted plants indicate that ELF4 moves from shoots to roots. RT-QPCR, confocal microscopy and western blot analyses of roots of grafted plants have shown that the shoot-to-root mobile signal is ELF4 protein.

3. In vivo luminescence analyses using roots from entire and shoot-excised plants have shown that excised roots exhibit a shorter period and advanced phase compared to the clock in entire roots. RT-QPCR analyses of entire and excised roots have also revealed that the expression of the ELF4 target genes (*PRR9* and *PRR7*) is increased in excised roots compared to entire roots, confirming that ELF4 movement is important for its regulatory circadian function in roots.

4. In vivo luminescence analyses, grafting and western blot assays under different photoperiods have shown that ELF4 movement is not prevalently regulated by photoperiod.

5. Luminescence analyses of rhythms in roots under different temperatures have

shown that root circadian clock is not able to sustain circadian period length within a range of temperatures, hence the key property of circadian rhythms, temperature compensation, is not robustly sustain in roots. In vivo luminescence analyses grafting and western blot assays have shown that the mobility of ELF4 is temperature regulated: ELF4 movement from shoots to roots is increased at lower temperatures (12ºC), whereas the movement decreases at higher temperatures (28ºC).

Summary

The circadian clock is synchronized by external environment cues, mostly through light and temperature. Explaining how the plant circadian clock responds to temperature oscillations is crucial to understanding plant responsiveness to the environment. In this thesis, we found a prevalent temperature-dependent function of the Arabidopsis clock component EARLY FLOWERING 4 (ELF4) in the root clock. The clocks in roots are able to run properly in the absence of shoots although shoot excision leads to a shorter period and advanced phase in excised roots compared to entire roots. Micrografting assays show that ELF4 moves from shoots to regulate rhythms in roots. ELF4 movement does not convey photoperiodic information, but trafficking is essential for controlling the period of the root clock in a temperature-dependent manner. Low temperatures favour ELF4 mobility, resulting in a slow paced root clock, whereas high temperatures decrease movement, leading to a faster clock. Hence, the mobile ELF4 delivers temperature information and establishes a shoot-to-root dialogue that sets the pace of the clock in roots.

Resumen

El reloj circadiano está sincronizado por señales medioambientales externas, principalmente la luz y la temperatura. Entender cómo responde el reloj circadiano de la planta a las oscilaciones de temperatura es crucial para comprender la capacidad de respuesta de la planta al medio ambiente. En esta Tesis Doctoral, encontramos una función prevalente dependiente de la temperatura del componente del reloj de Arabidopsis EARLY FLOWERING 4 (ELF4) en el reloj circadiano de la raíz. En plantas en las que el ápice aéreo se ha eliminado, el reloj puede funcionar correctamente en las raíces, aunque exhibe un período más corto y una fase avanzada en comparación con las raíces de plantas completas. Los ensayos de microinjerto muestran que ELF4 se mueve desde el ápice aéreo para regular los ritmos en las raíces. El movimiento de la proteína ELF4 no transmite información fotoperiódica, sino que es esencial para controlar el período del reloj circadiano en la raíz de una manera dependiente de la temperatura. Las bajas temperaturas favorecen la movilidad de ELF4, lo que resulta en un reloj de de ritmo lento, mientras que las altas temperaturas disminuyen el movimiento, lo que lleva a un reloj más rápido. Por lo tanto, el movimiento de la proteína ELF4 móvil proporciona información sobre la temperatura y ayuda a establecer un diálogo entre el ápice aéreo y la raíz de la planta para controlar el ritmo circadiano en la raíz.

Materials and Methods

1. Plant material, growth conditions, constructs and physiological assays.

A. thaliana seedlings were stratified at 4 °C in the dark for 2–3 d on Murashige and Skoog agar medium with 3% sucrose (MS3). Plates were transferred to chambers with controlled light and temperature conditions with 25–50 µmol m−2 s−1 of cool-white fluorescent light. Seedlings were synchronized under 12:12 h light:dark cycles at 22 °C. For experiments with different temperatures, seedlings were analysed under constant light conditions at 12 °C, 18 °C, 22 °C or 28 °C following synchronization under 12:12 h light:dark cycles at 22 °C. For experiments with different photoperiods, seedlings were grown under ShD (8:16 h light:dark) or LgD (16:8 h light:dark) conditions. Reporter lines *CCA1::LUC* (Salome and McClung, 2005), *LHY::LUC* (Herrero et al., 2012), *PRR9::LUC* (Edwards et al., 2010), *TOC1::LUC* (Portolés and Más, 2010) and *elf4-1* (Doyle et al., 2002), *elf4-2* (Huang et al., 2016), ELF4 minigene (Nusinow et al., 2011) and ELF4–GFPox (Herrero et al., 2012; Nusinow et al., 2011) plants have been described elsewhere. The ELF4–3×GFP construct was generated by PCR amplification of the *ELF4* coding sequence and subsequent subcloning into the PGWB514 gateway vector (Nakagawa et al., 2007a, 2007b). The resulting plasmid was digested with PacI and SacI restriction enzymes and ligated with the 3×GFP insert from the pBS-x3GFP vector (Addgene). The construct was transformed into *elf4-1* mutant plants. Plants were transformed using *Agrobacterium tumefaciens* (GV2260)-mediated DNA transfer (Clough and Bent, 1998). For in vitro protein-injection assays, the ELF4 coding sequence was subcloned into the pET MBP_1a vector (Novagen) after removing the GFP by digestion with NcoI and XhoI.

For hypocotyl elongation measurements, WT, *elf4-1*, ELF4–GFP-ox and ELF4–3×GFP-ox seeds transformed into the *elf4-1* mutant background were stratified on MS3 medium in the dark for 4 d at 4 °C, exposed to white light (40 µmol m^{-2} s^{-1}) for 6 h and maintained in the dark (22 °C) for 18 h before transferring to chambers under ShD

conditions. Hypocotyl length was measured using ImageJ (v.1.48 v) (https://imagej.nih.gov/ij/) 7 d after stratification. Each experiment was repeated at least twice using 20–50 seedlings per genotype. Statistical analyses were performed using GraphPad Prism (v.5.01) using two-tailed *t*-tests with 95% confidence interval.

2. In vivo luminescence assays.

In vivo luminescence assays were performed as previously described (Takahashi et al., 2015). In brief, 7- to 15-d-old seedlings synchronized under light:dark cycles at 22 °C were transferred to 96-well plates and released into the different conditions specific for each experiment. Analyses were performed with a LB960 luminometer (Berthold Technologies) using Microwin (v.4.41; Mikrotek Laborsysteme). The period, phase and amplitude were estimated using the fast Fourier transform–non-linear least squares (FFT-NLLS) suite 63 (Plautz et al., 1997) using the biological rhythms analysis software system (BRASS; v.3.0; http://www.amillar.org). For simultaneous analysis of rhythms of shoots and roots from the same plant, the connection between the two adjacent wells of the 96-well plates was serrated. Seedlings were then horizontally positioned so the shoot was placed in one well and the roots were placed in the contiguous well. For excision analyses, roots were excised from shoots and placed into the 96-well plates for luminescence analyses. Data from samples that appeared damaged or contaminated were excluded from the analysis. For analyses of grafted samples, water was applied instead of luciferin to the wells containing shoots to avoid possible leaking signals from shoots to roots, as specified. At least two biological replicates were performed per experiment, with measurements taken from independent samples grown and processed at different times. Each biological replicate included 6 to 12 independent seedlings per condition and/or genotype. Statistical analyses were performed using GraphPad Prism (v.5.01) using two-tailed *t*-tests with 95% confidence interval.

3. Protein purification and injection analyses.

Escherichia coli cells (BL21, Dh5α) were transformed and grown in LB medium (10 g l^{-1} tryptone, 5 g l^{-1} yeast extract and 10 g l^{-1} NaCl, pH 7.5) until optical density (OD600) values of 0.8–1.0. Isopropyl-β-d-1-thiogalactopyranoside (IPTG)-mediated induction of maltose-binding protein (MBP)–ELF4 and MBP–GFP was performed at 28 °C for 6 h. Bacteria resuspended in lysis buffer (50 mM Tris-HCl, pH 7–8, 5% glycerol, 50 mM NaCl) were lysed by sonication for 2–3 min (30 s on, 30 s off, high intensity) using a sonicator (Bioruptor, Diagnode). Recombinant proteins were purified using gravity-flow columns with amylose resin (New England Biolabs). MBP cleavage was performed by incubation in cleavage buffer (50 mM Trizma-HCl, pH 8.0, 0.5 mM EDTA, and 1 mM DTT) for 2 h at 30 °C with native tobacco etch virus protease (Sigma-Aldrich). The purified recombinant proteins were concentrated using Amicon centrifugal filters (Millipore) following the manufacturer's recommendations. Protein yield was estimated by measuring absorbance at 595 nm using a spectrophotometer (UV-2600, Shimadzu). Proteins were also examined by Coomassie brilliant blue staining of polyacrylamide gels to confirm protein size and integrity. Purified ELF4 was injected into leaves of 10 d old *elf4-1* mutant seedlings harbouring the *LHY::LUC* reporter line. Similar concentration of GFP protein was also injected as a negative control. Rhythms were subsequently examined in a LB960 luminometer (Berthold Technologies) as described above.

4. Time-course analyses of gene expression by RT–qPCR.

Seedlings were synchronized under light:dark cycles in MS3 medium plates for 12–14 d and subsequently transferred to constant light. Shoots and roots from intact plants were taken every 4 h over the circadian cycle. For excised roots, shoots and roots were carefully separated with a sterile razor blade and the excised roots were deposited on MS3 agar medium plates for 2 or 3 d as specified. RNA was purified using a Maxwell

RSC Plant RNA kit (Promega) following the manufacturer's recommendations. Single-stranded cDNA was synthesized using iScript Reverse Transcription Supermix for RT–qPCR (Bio-Rad). qPCR analyses were performed with cDNAs diluted 50-fold with nuclease-free water using Brilliant III Ultra-Fast SYBR Green qPCR Master Mix (Agilent) with a 96-well CFX96 Touch Real-Time PCR detection system (Bio-RAD CFX96 Manager v.3.1, Bio-Rad). Each sample was run in technical triplicates. The expression of *PP2AA3* (*PROTEIN PHOSPHATASE 2A SUBUNIT A3*, AT1G13320) or *MON1* (*MONENSIN SENSITIVITY1*, AT2G28390) (Czechowski et al., 2005) was used as a control. Crossing point (Cp) calculation was used for quantification using absolute quantification analysis by the second-derivative maximum method. At least two biological replicates were performed, with measurements taken from independent samples grown and processed at different times.

5. RNA-seq analyses.

Roots from 14-d-old intact WT, *elf4-1* mutant and excised WT plants synchronized under light:dark cycles in MS3 medium plates were transferred to constant light conditions for 3 d. Roots were excised just before transferring to constant light. Samples were collected on the fourth day under constant light at circadian time 75 (CT75). Total RNA was isolated using a Maxwell RSC Plant RNA kit. RNA sequencing was performed by IGATech. About 1–2 µg of high quality RNA (RNA integrity number > 7) was used for library preparation with a TruSeq Stranded mRNA Sample Prep kit (Illumina). Poly-A mRNA was fragmented for 3 min at 94 °C. Purification was performed with 0.8× Agencourt AMPure XP beads. RNA samples and final libraries were quantified using the Qubit 2.0 Fluorometer (Invitrogen). Quality was tested using the Agilent 2100 Bioanalyzer RNA Nano assay (Agilent). Libraries were then processed with Illumina cBot for cluster generation on the flow cell, following the manufacturer's instructions, and sequenced in paired-end mode at the multiplexing level requested on HiSeq2500 (Illumina). CASAVA (v.1.8.2) in the Illumina pipeline was used to process

raw data for both format conversion and de-multiplexing.

Sequence analysis was performed using AIR software (v.1.0) (Sequentia Biotech). In brief, raw sequence files were first subjected to quality control analysis using FastQC (v.0.10.1) before trimming and removal of adapters with BBDuk (https://jgi.doe.gov/data-and-tools/bbtools/). Reads were then mapped against the *A. thaliana* genome (TAIR10 Genome Release) with STAR (v.2.6) (Dobin et al., 2013). FeatureCounts (v.1.6.1) (Liao et al., 2014) was then used to obtain raw expression counts for each annotated gene. The differential-expression analysis was conducted with edgeR (v.3.18.1) (Robinson et al., 2010) using the TMM normalization method. Fragments per kilobase of transcript per million mapped reads (FPKM) were obtained with edgeR.

6. Western blot assays.

Approximately 50–100 mg of roots from plants grown under the specified photoperiodic condition were sampled every 4 h over a 24 h cycle. Samples were rapidly frozen with liquid nitrogen and grounded with stainless steel beads (Millipore) in a TissueLyser II (QIAGEN). Tissue was subsequently resuspended in protein extraction buffer (50 mM Tris-HCl pH 7.5, 150 mM NaCl, 0.5% NP40, 1 mM EDTA, protease inhibitor cocktail (1:100) and PMSF (1:1,000)). Protein extracts were centrifuged at 4 °C, measured for protein concentration using Bradford reagent (Bio-Rad) and normalized to 2 mg ml^{-1} in 4× SDS loading buffer (250 mM Tris-HCl, pH 6.8, 8% SDS, 0.08% bromophenol blue and 40% glycerol). Samples were run on a 12% gel and analysed by immunoblotting, fixed 30 min with 0.4% glutaraldehyde solution (Sigma-Aldrich) and detected with a haemagglutinin (HA) antibody (Roche) (1:2,000 dilution) and a goat anti-rat horseradish peroxidase-conjugated secondary antibody (Sigma-Aldrich) (1:4,000 dilution). For analyses of the grafted plants, roots from plants synchronized under light:dark cycles were subsequently transferred to constant light

for 3 d at 12 °C, 22 °C or 28 °C. Samples were collected at CT81, rapidly frozen with liquid nitrogen and grounded with stainless steel beads (Millipore) in a TissueLyser II (QIAGEN). Powder extracts were subsequently resuspended in protein extraction buffer with 100 µM MG132. Protein extracts were centrifuged at 4 °C, measured for protein concentration using Bradford reagent (Bio-Rad) and normalized to 2 µg μl^{-1} in 4× SDS loading buffer with 5 mM β-mercaptoethanol. For detection of ELF4 protein fused to GFP, samples were run on a 10% gel and detected using a GFP antibody (ab290, Abcam) (1:5,000) and goat anti-rabbit IgG (H + L chains) secondary antibody, horseradish peroxidase conjugate (Thermo Fisher Scientific, 31460 lot OG188649) (1:5,000 dilution). For detection of ELF4 protein fused to HA (ELF4 minigene) in shoots, samples were resuspended in protein extraction buffer with 100 µM MG132. Protein extracts in 4× SDS loading buffer with 5 mM β-mercaptoethanol were run on a 12% gel and analysed by immunoblotting, fixed for 30 min with 0.4% glutaraldehyde solution (Sigma-Aldrich) and detected with a HA antibody from rat IgG1 (11867423001, Sigma-Aldrich) (1:2,000) and a goat anti-rat horseradish peroxidase-conjugated secondary antibody (A9037, Sigma-Aldrich) (1:4000). Image Lab (v.5.2.1; Bio-Rad) was used to image the western blots. Membranes were stained with a Ponceau S solution following the manufacturer's recommendations (Sigma). Proteins were also run on a 10% SDS–PAGE gel and stained with Coomassie brilliant blue. At least two biological replicates were performed per experiment and/or condition, with measurements taken from independent samples grown and processed at different times.

7. Micrografting assays.

Micrografting was performed essentially as described (Takahashi et al., 2015). Data from unsuccessful grafted seedlings that failed to properly join together or grafts that were insufficiently clear to be successful were discarded. Approximately 100–150 grafting events were performed for every combination of grafts. The percentage of successfully micrografted plants was about 30-50% (possibly higher but only the

clearly successful grafted plants were taken into account). From the successfully grafted plants, 30-60% showed different degrees of recovered rhythms. For in vivo luminescence assays, shoots and roots of grafted plants were simultaneously examined using the protocol described above. Water was added instead of luciferin to wells containing shoots to exclude the possibility that recovery of rhythms in roots was due to leaking signals from shoots. As specified, some grafted shoots contained no reporter.

8. Confocal imaging.

For in vivo confocal imaging, the roots of WT and ELF4-ox-GFP-grafted shoots into *elf4-1* mutants were placed on microscope slides (Sigma). Fluorescent signals were imaged with an argon laser (transmissivity 40%; excitation 515 nm; emission range 530–630 nm) in a FV-1000 confocal microscope (Olympus) using FV-10-ASW4.2 Viewer Manager software (Olympus) with a 40×1.3 numerical aperture oil-immersion objective. Image sizes were about 640 × 640 pixels (0.497 µm per pixel) and sampling speed was 4 µs per pixel. The results are representative of at least three biological replicates for grafting and about three to four images per grafts.

List of primers

Name	Sequence	Experiment
REF1(PP2A_A3)_EXP_F	AAGCGGTTGTGGAGAACATGATACG	Expression analysis
REF1(PP2A_A3)_EXP_R	TGGAGAGCTTGATTTGCGAAATACCG	Expression analysis
MON1_EXP_F	AACTCTATGCAGCATTTGATCCACT	Expression analysis
MON1_EXP_R	TGATTGCATATCTTTATCGCCATC	Expression analysis
PRR7_EXP_F	AAGTAGTGATGGGAGTGGCG	Expression analysis
PRR7_EXP_R	GAGATACCGCTCGTGGACTG	Expression analysis
PRR9_EXP_F	ACCAATGAGGGGATTGCTGG	Expression analysis
PRR9_EXP_R	TGCAGCTTCTCTCTGGCTTC	Expression analysis
ELF4_EXP_F	GACAATCACCAATCGAGAAT	Expression analysis
ELF4_EXP_R	ATGTTTCCGTTGAGTTCTTG	Expression analysis
CCA1_EXP_F	TCGAAAGACGGGAAGTGGAACG	Expression analysis
CCA1_EXP_R	GTCGATCTTCATTGGCCATCTCAG	Expression analysis
LHY_EXP_F	AAGTCTCCGAAGAGGGTCGT	Expression analysis
LHY_EXP_R	GGCGAAAAGCTTTGAGGCAA	Expression analysis
ELF4_CLN_F	CACCATGAAGAGGAACGGCGA	Cloning
ELF4_CLN_R	AGCTCTAGTTCCGGCAGCACCA	Cloning
MBP-ELF4_CLN_F	CATGCCATGGGCATGAAGAGGAACGGCGAG	Cloning
MBP-ELF4_CLN_R	CCGCTCGAGTTAAGCTCTAGTTCCGGCAGCAC	Cloning
PacI-pBS3xGFP-F	ggttaattaacGCTGGAGGATCCATGTCTA	Generation of pGWB-c3xGFP
SacI-pBS3xGFP-R	tcgagctcTCTAGAACTAGTGGATCTTTA	Generation of pGWB-c3xGFP

References

Abe, M., Kobayashi, Y., Yamamoto, S., Daimon, Y., Yamaguchi, A., Ikeda, Y., Ichinoki, H., Notaguchi, M., Goto, K., and Araki, T. (2005). FD, a bZIP protein mediating signals from the floral pathway integrator FT at the shoot apex. Science *309*, 1052–1056.

Adams, S., Manfield, I., Stockley, P., and Carré, I.A. (2015). Revised Morning Loops of the Arabidopsis Circadian Clock Based on Analyses of Direct Regulatory Interactions. PloS One *10*, e0143943.

Alabadí, D., Oyama, T., Yanovsky, M.J., Harmon, F.G., Más, P., and Kay, S.A. (2001). Reciprocal regulation between TOC1 and LHY/CCA1 within the Arabidopsis circadian clock. Science *293*, 880–883.

Alabadí, D., Yanovsky, M.J., Más, P., Harmer, S.L., and Kay, S.A. (2002). Critical role for CCA1 and LHY in maintaining circadian rhythmicity in Arabidopsis. Curr. Biol. CB *12*, 757–761.

Amasino, R.M., and Michaels, S.D. (2010). The timing of flowering. Plant Physiol. *154*, 516–520.

An, H., Roussot, C., Suarez-Lopez, P., Corbesier, L., Vincent, C., Pineiro, M., Hepworth, S., Mouradov, A., Justin, S., Turnbull, C., et al. (2004). CONSTANS acts in the phloem to regulate a systemic signal that induces photoperiodic flowering of Arabidopsis. Dev. Camb. Engl. *131*, 3615–3626.

Aschoff, J. (1979). Circadian rhythms: influences of internal and external factors on the period measured in constant conditions. Z. Tierpsychol. *49*, 225–249.

Bainbridge, K., Bennett, T., Crisp, P., Leyser, O., and Turnbull, C. (2014). Grafting in Arabidopsis. Methods Mol. Biol. Clifton NJ *1062*, 155–163.

Barclay, J.L., Tsang, A.H., and Oster, H. (2012). Interaction of central and peripheral clocks in physiological regulation. Prog. Brain Res. *199*, 163–181.

Bell-Pedersen, D., Cassone, V.M., Earnest, D.J., Golden, S.S., Hardin, P.E., Thomas, T.L., and Zoran, M.J. (2005). Circadian rhythms from multiple oscillators: lessons from diverse organisms. Nat. Rev. Genet. *6*, 544–556.

Bieniawska, Z., Espinoza, C., Schlereth, A., Sulpice, R., Hincha, D.K., and Hannah, M.A. (2008). Disruption of the Arabidopsis circadian clock is responsible for extensive variation in the cold-responsive transcriptome. Plant Physiol. *147*, 263–279.

Box, M.S., Huang, B.E., Domijan, M., Jaeger, K.E., Khattak, A.K., Yoo, S.J., Sedivy, E.L., Jones, D.M., Hearn, T.J., Webb, A.A.R., et al. (2015). ELF3 controls thermoresponsive growth in Arabidopsis. Curr. Biol. CB *25*, 194–199.

Burko, Y., Gaillochet, C., Seluzicki, A., Chory, J., and Busch, W. (2020). Local HY5 activity mediates hypocotyl growth and shoot-to-root communication. Plant Commun. 100078.

Camut, L., Regnault, T., Sirlin-Josserand, M., Sakvarelidze-Achard, L., Carrera, E., Zumsteg, J., Heintz, D., Leonhardt, N., Lange, M.J.P., Lange, T., et al. (2019). Root-derived GA12 contributes to temperature-induced shoot growth in Arabidopsis. Nat. Plants *5*, 1216–1221.

Catalá, R., Medina, J., and Salinas, J. (2011). Integration of low temperature and light signaling during cold acclimation response in Arabidopsis. Proc. Natl. Acad. Sci. U. S. A. *108*, 16475–16480.

Cerezo, M., Tillard, P., Filleur, S., Muños, S., Daniel-Vedele, F., and Gojon, A. (2001). Major Alterations of the Regulation of Root NO_3^- Uptake Are Associated with the Mutation of Nrt2.1 and Nrt2.2 Genes in Arabidopsis. Plant Physiol. *127*, 262.

Chen, H., and Xiong, L. (2011). Genetic interaction of two abscisic acid signaling regulators, HY5 and FIERY1, in mediating lateral root formation. Plant Signal. Behav. *6*, 123–125.

Chen, W.W., Takahashi, N., Hirata, Y., Ronald, J., Porco, S., Davis, S.J., Nusinow, D.A., Kay, S.A., and Mas, P. (2020). A mobile ELF4 delivers circadian temperature information from shoots to roots. Nat. Plants *6*, 416–426.

Chen, X., Yao, Q., Gao, X., Jiang, C., Harberd, N.P., and Fu, X. (2016). Shoot-to-Root Mobile Transcription Factor HY5 Coordinates Plant Carbon and Nitrogen Acquisition. Curr. Biol. CB *26*, 640–646.

Choudhary, M.K., Nomura, Y., Wang, L., Nakagami, H., and Somers, D.E. (2015). Quantitative Circadian Phosphoproteomic Analysis of Arabidopsis Reveals Extensive Clock Control of Key Components in Physiological, Metabolic, and Signaling Pathways. Mol. Cell. Proteomics MCP *14*, 2243–2260.

Chow, B.Y., Helfer, A., Nusinow, D.A., and Kay, S.A. (2012). ELF3 recruitment to the PRR9 promoter requires other Evening Complex members in the Arabidopsis circadian clock. Plant Signal. Behav. *7*, 170–173.

Chow, B.Y., Sanchez, S.E., Breton, G., Pruneda-Paz, J.L., Krogan, N.T., and Kay, S.A. (2014). Transcriptional regulation of LUX by CBF1 mediates cold input to the circadian clock in Arabidopsis. Curr. Biol. CB *24*, 1518–1524.

Clough, S.J., and Bent, A.F. (1998). Floral dip: a simplified method for Agrobacterium-mediated transformation of Arabidopsis thaliana. Plant J. Cell Mol. Biol. *16*, 735–743.

Corbesier, L., Vincent, C., Jang, S., Fornara, F., Fan, Q., Searle, I., Giakountis, A., Farrona, S., Gissot, L., Turnbull, C., et al. (2007). FT protein movement contributes to long-distance signaling in floral induction of Arabidopsis. Science *316*, 1030–1033.

Crosthwaite, S.K., Loros, J.J., and Dunlap, J.C. (1995). Light-induced resetting of a circadian clock is mediated by a rapid increase in frequency transcript. Cell *81*, 1003–1012.

Czechowski, T., Stitt, M., Altmann, T., Udvardi, M.K., and Scheible, W.-R. (2005).

Genome-wide identification and testing of superior reference genes for transcript normalization in Arabidopsis. Plant Physiol. *139*, 5–17.

Delker, C., Sonntag, L., James, G.V., Janitza, P., Ibañez, C., Ziermann, H., Peterson, T., Denk, K., Mull, S., Ziegler, J., et al. (2014). The DET1-COP1-HY5 pathway constitutes a multipurpose signaling module regulating plant photomorphogenesis and thermomorphogenesis. Cell Rep. *9*, 1983–1989.

Devlin, P.F., and Kay, S.A. (2000). Cryptochromes Are Required for Phytochrome Signaling to the Circadian Clock but Not for Rhythmicity. Plant Cell *12*, 2499.

Ding, B. (1998). Intercellular protein trafficking through plasmodesmata. Plant Mol. Biol. *38*, 279–310.

Dixon, L.E., Knox, K., Kozma-Bognar, L., Southern, M.M., Pokhilko, A., and Millar, A.J. (2011). Temporal repression of core circadian genes is mediated through EARLY FLOWERING 3 in Arabidopsis. Curr. Biol. CB *21*, 120–125.

Dobin, A., Davis, C.A., Schlesinger, F., Drenkow, J., Zaleski, C., Jha, S., Batut, P., Chaisson, M., and Gingeras, T.R. (2013). STAR: ultrafast universal RNA-seq aligner. Bioinforma. Oxf. Engl. *29*, 15–21.

Doherty, C.J., and Kay, S.A. (2010). Circadian control of global gene expression patterns. Annu. Rev. Genet. *44*, 419–444.

Dong, M.A., Farré, E.M., and Thomashow, M.F. (2011). Circadian clock-associated 1 and late elongated hypocotyl regulate expression of the. Proc. Natl. Acad. Sci. U. S. A. *108*, 7241–7246.

Doyle, M.R., Davis, S.J., Bastow, R.M., McWatters, H.G., Kozma-Bognár, L., Nagy, F., Millar, A.J., and Amasino, R.M. (2002). The ELF4 gene controls circadian rhythms and flowering time in Arabidopsis thaliana. Nature *419*, 74–77.

Edwards, K.D., Akman, O.E., Knox, K., Lumsden, P.J., Thomson, A.W., Brown, P.E.,

Pokhilko, A., Kozma-Bognar, L., Nagy, F., Rand, D.A., et al. (2010). Quantitative analysis of regulatory flexibility under changing environmental conditions. Mol. Syst. Biol. *6*, 424.

Endo, M. (2016). Tissue-specific circadian clocks in plants. Curr. Opin. Plant Biol. *29*, 44–49.

Endo, M., Shimizu, H., Nohales, M.A., Araki, T., and Kay, S.A. (2014). Tissue-specific clocks in Arabidopsis show asymmetric coupling. Nature *515*, 419–422.

Eriksson, M.E., and Webb, A.A.R. (2011). Plant cell responses to cold are all about timing. Curr. Opin. Plant Biol. *14*, 731–737.

Ezer, D., Jung, J.-H., Lan, H., Biswas, S., Gregoire, L., Box, M.S., Charoensawan, V., Cortijo, S., Lai, X., Stöckle, D., et al. (2017a). The evening complex coordinates environmental and endogenous signals in Arabidopsis. Nat. Plants *3*, 17087.

Ezer, D., Jung, J.-H., Lan, H., Biswas, S., Gregoire, L., Box, M.S., Charoensawan, V., Cortijo, S., Lai, X., Stöckle, D., et al. (2017b). The evening complex coordinates environmental and endogenous signals in Arabidopsis. Nat. Plants *3*, 17087.

Fankhauser, C., and Staiger, D. (2002). Photoreceptors in Arabidopsis thaliana: light perception, signal transduction and entrainment of the endogenous clock. Planta *216*, 1–16.

Farré, E.M., Harmer, S.L., Harmon, F.G., Yanovsky, M.J., and Kay, S.A. (2005). Overlapping and distinct roles of PRR7 and PRR9 in the Arabidopsis circadian clock. Curr. Biol. CB *15*, 47–54.

Favory, J.-J., Stec, A., Gruber, H., Rizzini, L., Oravecz, A., Funk, M., Albert, A., Cloix, C., Jenkins, G.I., Oakeley, E.J., et al. (2009). Interaction of COP1 and UVR8 regulates UV-B-induced photomorphogenesis and stress acclimation in Arabidopsis. EMBO J. *28*, 591–601.

Fehér, B., Kozma-Bognár, L., Kevei, E., Hajdu, A., Binkert, M., Davis, S.J., Schäfer, E., Ulm, R., and Nagy, F. (2011). Functional interaction of the circadian clock and UV RESISTANCE LOCUS 8-controlled. Plant J. Cell Mol. Biol. *67*, 37–48.

Fernández, V., Takahashi, Y., Le Gourrierec, J., and Coupland, G. (2016). Photoperiodic and thermosensory pathways interact through CONSTANS to promote flowering at high temperature under short days. Plant J. Cell Mol. Biol. *86*, 426–440.

Flis, A., Fernández, A.P., Zielinski, T., Mengin, V., Sulpice, R., Stratford, K., Hume, A., Pokhilko, A., Southern, M.M., Seaton, D.D., et al. (2015). Defining the robust behaviour of the plant clock gene circuit with absolute RNA timeseries and open infrastructure. Open Biol. *5*.

Franklin, K.A., and Quail, P.H. (2010). Phytochrome functions in Arabidopsis development. J. Exp. Bot. *61*, 11–24.

Fukuda, H., Nakamichi, N., Hisatsune, M., Murase, H., and Mizuno, T. (2007). Synchronization of plant circadian oscillators with a phase delay effect of the vein network. Phys. Rev. Lett. *99*, 098102.

Gehan, M.A., Greenham, K., Mockler, T.C., and McClung, C.R. (2015). Transcriptional networks-crops, clocks, and abiotic stress. Curr. Opin. Plant Biol. *24*, 39–46.

Gendron, J.M., Pruneda-Paz, J.L., Doherty, C.J., Gross, A.M., Kang, S.E., and Kay, S.A. (2012). Arabidopsis circadian clock protein, TOC1, is a DNA-binding transcription factor. Proc. Natl. Acad. Sci. U. S. A. *109*, 3167–3172.

Gould, P.D., Locke, J.C.W., Larue, C., Southern, M.M., Davis, S.J., Hanano, S., Moyle, R., Milich, R., Putterill, J., Millar, A.J., et al. (2006). The molecular basis of temperature compensation in the Arabidopsis circadian clock. Plant Cell *18*, 1177–1187.

Gould, P.D., Domijan, M., Greenwood, M., Tokuda, I.T., Rees, H., Kozma-Bognar, L., Hall, A.J., and Locke, J.C. (2018). Coordination of robust single cell rhythms in the

Arabidopsis circadian clock via spatial waves of gene expression. ELife *7*.

Green, R.M., and Tobin, E.M. (1999). Loss of the circadian clock-associated protein 1 in Arabidopsis results in altered clock-regulated gene expression. Proc. Natl. Acad. Sci. U. S. A. *96*, 4176–4179.

Green, R.M., Tingay, S., Wang, Z.-Y., and Tobin, E.M. (2002). Circadian rhythms confer a higher level of fitness to Arabidopsis plants. Plant Physiol. *129*, 576–584.

Greenham, K., and McClung, C.R. (2015). Integrating circadian dynamics with physiological processes in plants. Nat. Rev. Genet. *16*, 598–610.

Greenwood, M., Domijan, M., Gould, P.D., Hall, A.J.W., and Locke, J.C.W. (2019). Coordinated circadian timing through the integration of local inputs in Arabidopsis thaliana. PLoS Biol. *17*, e3000407.

Hajdu, A., Dobos, O., Domijan, M., Bálint, B., Nagy, I., Nagy, F., and Kozma-Bognár, L. (2018). ELONGATED HYPOCOTYL 5 mediates blue light signalling to the Arabidopsis circadian clock. Plant J. Cell Mol. Biol. *96*, 1242–1254.

Han, X., Kumar, D., Chen, H., Wu, S., and Kim, J.-Y. (2014). Transcription factor-mediated cell-to-cell signalling in plants. J. Exp. Bot. *65*, 1737–1749.

Harmer, S.L. (2009). The circadian system in higher plants. Annu. Rev. Plant Biol. *60*, 357–377.

Harmer, S.L., Hogenesch, J.B., Straume, M., Chang, H.S., Han, B., Zhu, T., Wang, X., Kreps, J.A., and Kay, S.A. (2000). Orchestrated transcription of key pathways in Arabidopsis by the circadian clock. Science *290*, 2110–2113.

Hayes, S., Sharma, A., Fraser, D.P., Trevisan, M., Cragg-Barber, C.K., Tavridou, E., Fankhauser, C., Jenkins, G.I., and Franklin, K.A. (2017). UV-B Perceived by the UVR8 Photoreceptor Inhibits Plant Thermomorphogenesis. Curr. Biol. CB *27*, 120–127.

Hazen, S.P., Schultz, T.F., Pruneda-Paz, J.L., Borevitz, J.O., Ecker, J.R., and Kay, S.A. (2005). LUX ARRHYTHMO encodes a Myb domain protein essential for circadian rhythms. Proc. Natl. Acad. Sci. U. S. A. *102*, 10387–10392.

Helfer, A., Nusinow, D.A., Chow, B.Y., Gehrke, A.R., Bulyk, M.L., and Kay, S.A. (2011). LUX ARRHYTHMO encodes a nighttime repressor of circadian gene expression in the Arabidopsis core clock. Curr. Biol. CB *21*, 126–133.

Herrero, E., Kolmos, E., Bujdoso, N., Yuan, Y., Wang, M., Berns, M.C., Uhlworm, H., Coupland, G., Saini, R., Jaskolski, M., et al. (2012). EARLY FLOWERING4 recruitment of EARLY FLOWERING3 in the nucleus sustains the Arabidopsis circadian clock. Plant Cell *24*, 428–443.

Hicks, K.A., Millar, A.J., Carré, I.A., Somers, D.E., Straume, M., Meeks-Wagner, D.R., and Kay, S.A. (1996). Conditional circadian dysfunction of the Arabidopsis early-flowering 3 mutant. Science *274*, 790–792.

Hicks, K.A., Albertson, T.M., and Wagner, D.R. (2001). EARLY FLOWERING3 encodes a novel protein that regulates circadian clock function and flowering in Arabidopsis. Plant Cell *13*, 1281–1292.

Hogenesch, J.B., and Ueda, H.R. (2011). Understanding systems-level properties: timely stories from the study of clocks. Nat. Rev. Genet. *12*, 407–416.

Hsu, P.Y., and Harmer, S.L. (2014). Wheels within wheels: the plant circadian system. Trends Plant Sci. *19*, 240–249.

Hsu, P.Y., Devisetty, U.K., and Harmer, S.L. (2013). Accurate timekeeping is controlled by a cycling activator in Arabidopsis. ELife *2*, e00473.

Huang, H., and Nusinow, D.A. (2016). Into the Evening: Complex Interactions in the Arabidopsis Circadian Clock. Trends Genet. TIG *32*, 674–686.

Huang, H., Alvarez, S., Bindbeutel, R., Shen, Z., Naldrett, M.J., Evans, B.S., Briggs, S.P.,

Hicks, L.M., Kay, S.A., and Nusinow, D.A. (2016). Identification of Evening Complex Associated Proteins in Arabidopsis by Affinity Purification and Mass Spectrometry. Mol. Cell. Proteomics MCP *15*, 201–217.

Huang, W., Perez-Garcia, P., Pokhilko, A., Millar, A.J., Antoshechkin, I., Riechmann, J.L., and Mas, P. (2012). Mapping the core of the Arabidopsis circadian clock defines the network structure of the oscillator. Science *336*, 75–79.

Imlau, A., Truernit, E., and Sauer, N. (1999). Cell-to-cell and long-distance trafficking of the green fluorescent protein in the phloem and symplastic unloading of the protein into sink tissues. Plant Cell *11*, 309–322.

Inoue, K., Araki, T., and Endo, M. (2018). Oscillator networks with tissue-specific circadian clocks in plants. Semin. Cell Dev. Biol. *83*, 78–85.

Ito, S., Song, Y.H., and Imaizumi, T. (2012). LOV domain-containing F-box proteins: light-dependent protein degradation modules in Arabidopsis. Mol. Plant *5*, 573–582.

Iwasaki, H., and Dunlap, J.C. (2000). Microbial circadian oscillatory systems in Neurospora and Synechococcus: models for cellular clocks. Curr. Opin. Microbiol. *3*, 189–196.

Jaeger, K.E., and Wigge, P.A. (2007). FT protein acts as a long-range signal in Arabidopsis. Curr. Biol. CB *17*, 1050–1054.

Jakoby, M., Weisshaar, B., Dröge-Laser, W., Vicente-Carbajosa, J., Tiedemann, J., Kroj, T., and Parcy, F. (2002). bZIP transcription factors in Arabidopsis. Trends Plant Sci. *7*, 106–111.

James, A.B., Monreal, J.A., Nimmo, G.A., Kelly, C.L., Herzyk, P., Jenkins, G.I., and Nimmo, H.G. (2008a). The circadian clock in Arabidopsis roots is a simplified slave version of the clock in shoots. Science *322*, 1832–1835.

James, A.B., Monreal, J.A., Nimmo, G.A., Kelly, C.L., Herzyk, P., Jenkins, G.I., and Nimmo,

H.G. (2008b). The Circadian Clock in Arabidopsis Roots Is a Simplified Slave Version of the Clock in Shoots. Science *322*, 1832–1835.

James, A.B., Syed, N.H., Bordage, S., Marshall, J., Nimmo, G.A., Jenkins, G.I., Herzyk, P., Brown, J.W.S., and Nimmo, H.G. (2012). Alternative splicing mediates responses of the Arabidopsis circadian clock to temperature changes. Plant Cell *24*, 961–981.

Jeon, J., Cho, C., Lee, M.R., Van Binh, N., and Kim, J. (2016). CYTOKININ RESPONSE FACTOR2 (CRF2) and CRF3 Regulate Lateral Root Development in Response to Cold Stress in Arabidopsis. Plant Cell *28*, 1828.

Jing, Y., Zhang, D., Wang, X., Tang, W., Wang, W., Huai, J., Xu, G., Chen, D., Li, Y., and Lin, R. (2013). Arabidopsis chromatin remodeling factor PICKLE interacts with transcription factor HY5 to regulate hypocotyl cell elongation. Plant Cell *25*, 242–256.

Jolma, I.W., Laerum, O.D., Lillo, C., and Ruoff, P. (2010). Circadian oscillators in eukaryotes. Wiley Interdiscip. Rev. Syst. Biol. Med. *2*, 533–549.

Jones, M.A., Hu, W., Litthauer, S., Lagarias, J.C., and Harmer, S.L. (2015). A Constitutively Active Allele of Phytochrome B Maintains Circadian Robustness in the Absence of Light. Plant Physiol. *169*, 814–825.

Jung, J.-H., Barbosa, A.D., Hutin, S., Kumita, J.R., Gao, M., Derwort, D., Silva, C.S., Lai, X., Pierre, E., Geng, F., et al. (2020). A prion-like domain in ELF3 functions as a thermosensor in Arabidopsis. Nature.

Kadener, S., Menet, J.S., Sugino, K., Horwich, M.D., Weissbein, U., Nawathean, P., Vagin, V.V., Zamore, P.D., Nelson, S.B., and Rosbash, M. (2009). A role for microRNAs in the Drosophila circadian clock. Genes Dev. *23*, 2179–2191.

Kalsbeek, A., Yi, C.-X., Cailotto, C., la Fleur, S.E., Fliers, E., and Buijs, R.M. (2011). Mammalian clock output mechanisms. Essays Biochem. *49*, 137–151.

Kamioka, M., Takao, S., Suzuki, T., Taki, K., Higashiyama, T., Kinoshita, T., and Nakamichi,

N. (2016). Direct Repression of Evening Genes by CIRCADIAN CLOCK-ASSOCIATED1 in the Arabidopsis Circadian Clock. Plant Cell *28*, 696–711.

Kardailsky, I., Shukla, V.K., Ahn, J.H., Dagenais, N., Christensen, S.K., Nguyen, J.T., Chory, J., Harrison, M.J., and Weigel, D. (1999). Activation tagging of the floral inducer FT. Science *286*, 1962–1965.

Katsir, L., Davies, K.A., Bergmann, D.C., and Laux, T. (2011). Peptide signaling in plant development. Curr. Biol. CB *21*, R356-364.

Keily, J., MacGregor, D.R., Smith, R.W., Millar, A.J., Halliday, K.J., and Penfield, S. (2013). Model selection reveals control of cold signalling by evening-phased components of the plant circadian clock. Plant J. Cell Mol. Biol. *76*, 247–257.

Khanna, R., Kikis, E.A., and Quail, P.H. (2003). EARLY FLOWERING 4 functions in phytochrome B-regulated seedling de-etiolation. Plant Physiol. *133*, 1530–1538.

Kiba, T., Henriques, R., Sakakibara, H., and Chua, N.-H. (2007). Targeted degradation of PSEUDO-RESPONSE REGULATOR5 by an SCFZTL complex regulates clock function and photomorphogenesis in Arabidopsis thaliana. Plant Cell *19*, 2516–2530.

Kikis, E.A., Khanna, R., and Quail, P.H. (2005). ELF4 is a phytochrome-regulated component of a negative-feedback loop involving the central oscillator components CCA1 and LHY. Plant J. Cell Mol. Biol. *44*, 300–313.

Kim, S., Hwang, G., Lee, S., Zhu, J.-Y., Paik, I., Nguyen, T.T., Kim, J., and Oh, E. (2017). High Ambient Temperature Represses Anthocyanin Biosynthesis through Degradation of HY5. Front. Plant Sci. *8*, 1787.

Kim, W.-Y., Hicks, K.A., and Somers, D.E. (2005). Independent roles for EARLY FLOWERING 3 and ZEITLUPE in the control of circadian timing, hypocotyl length, and flowering time. Plant Physiol. *139*, 1557–1569.

Kim, Y., Lim, J., Yeom, M., Kim, H., Kim, J., Wang, L., Kim, W.Y., Somers, D.E., and Nam,

H.G. (2013). ELF4 regulates GIGANTEA chromatin access through subnuclear sequestration. Cell Rep. *3*, 671–677.

Ko, C.H., and Takahashi, J.S. (2006). Molecular components of the mammalian circadian clock. Hum. Mol. Genet. *15 Spec No 2*, R271-277.

Kobayashi, Y., and Weigel, D. (2007). Move on up, it's time for change--mobile signals controlling photoperiod-dependent flowering. Genes Dev. *21*, 2371–2384.

Kobayashi, Y., Kaya, H., Goto, K., Iwabuchi, M., and Araki, T. (1999). A pair of related genes with antagonistic roles in mediating flowering signals. Science *286*, 1960–1962.

Kolmos, E., Nowak, M., Werner, M., Fischer, K., Schwarz, G., Mathews, S., Schoof, H., Nagy, F., Bujnicki, J.M., and Davis, S.J. (2009). Integrating ELF4 into the circadian system through combined structural and functional studies. HFSP J. *3*, 350–366.

Kolmos, E., Herrero, E., Bujdoso, N., Millar, A.J., Tóth, R., Gyula, P., Nagy, F., and Davis, S.J. (2011). A reduced-function allele reveals that EARLY FLOWERING3 repressive action on the circadian clock is modulated by phytochrome signals in Arabidopsis. Plant Cell *23*, 3230–3246.

Koornneef, M., Rolff, E., and Spruit, C.J.P. (1980). Genetic Control of Light-inhibited Hypocotyl Elongation in Arabidopsis thaliana (L.) Heynh. Z. Für Pflanzenphysiol. *100*, 147–160.

Kumar, S.V., Lucyshyn, D., Jaeger, K.E., Alós, E., Alvey, E., Harberd, N.P., and Wigge, P.A. (2012). Transcription factor PIF4 controls the thermosensory activation of flowering. Nature *484*, 242–245.

Lee, C.-M., Feke, A., Li, M.-W., Adamchek, C., Webb, K., Pruneda-Paz, J., Bennett, E.J., Kay, S.A., and Gendron, J.M. (2018). Decoys Untangle Complicated Redundancy and Reveal Targets of Circadian Clock F-Box Proteins. Plant Physiol. *177*, 1170–1186.

Lee, H.-J., Park, Y.-J., Ha, J.-H., Baldwin, I.T., and Park, C.-M. (2017). Multiple Routes of

Light Signaling during Root Photomorphogenesis. Trends Plant Sci. *22*, 803–812.

Lee, J., He, K., Stolc, V., Lee, H., Figueroa, P., Gao, Y., Tongprasit, W., Zhao, H., Lee, I., and Deng, X.W. (2007a). Analysis of transcription factor HY5 genomic binding sites revealed its hierarchical role in light regulation of development. Plant Cell *19*, 731–749.

Lee, J.H., Yoo, S.J., Park, S.H., Hwang, I., Lee, J.S., and Ahn, J.H. (2007b). Role of SVP in the control of flowering time by ambient temperature in Arabidopsis. Genes Dev. *21*, 397–402.

Lee, J.-Y., Colinas, J., Wang, J.Y., Mace, D., Ohler, U., and Benfey, P.N. (2006). Transcriptional and posttranscriptional regulation of transcription factor expression in Arabidopsis roots. Proc. Natl. Acad. Sci. U. S. A. *103*, 6055–6060.

Leivar, P., and Monte, E. (2014). PIFs: systems integrators in plant development. Plant Cell *26*, 56–78.

Li, G., Siddiqui, H., Teng, Y., Lin, R., Wan, X., Li, J., Lau, O.-S., Ouyang, X., Dai, M., Wan, J., et al. (2011a). Coordinated transcriptional regulation underlying the circadian clock in Arabidopsis. Nat. Cell Biol. *13*, 616–622.

Li, G., Siddiqui, H., Teng, Y., Lin, R., Wan, X., Li, J., Lau, O.-S., Ouyang, X., Dai, M., Wan, J., et al. (2011b). Coordinated transcriptional regulation underlying the circadian clock in Arabidopsis. Nat. Cell Biol. *13*, 616–622.

Li, X., Ma, D., Lu, S.X., Hu, X., Huang, R., Liang, T., Xu, T., Tobin, E.M., and Liu, H. (2016). Blue Light- and Low Temperature-Regulated COR27 and COR28 Play Roles in the Arabidopsis Circadian Clock. Plant Cell *28*, 2755–2769.

Liao, Y., Smyth, G.K., and Shi, W. (2014). featureCounts: an efficient general purpose program for assigning sequence reads to genomic features. Bioinforma. Oxf. Engl. *30*, 923–930.

Lin, S.-I., Chiang, S.-F., Lin, W.-Y., Chen, J.-W., Tseng, C.-Y., Wu, P.-C., and Chiou, T.-J. (2008). Regulatory Network of MicroRNA399 and PHO2 by Systemic Signaling. Plant Physiol. *147*, 732–746.

Liu, L., Zhang, Y., and Yu, H. (2020). Florigen trafficking integrates photoperiod and temperature signals in Arabidopsis. J. Integr. Plant Biol. *n/a*.

Liu, X.L., Covington, M.F., Fankhauser, C., Chory, J., and Wagner, D.R. (2001a). ELF3 encodes a circadian clock-regulated nuclear protein that functions in an Arabidopsis PHYB signal transduction pathway. Plant Cell *13*, 1293–1304.

Liu, X.L., Covington, M.F., Fankhauser, C., Chory, J., and Wagner, D.R. (2001b). ELF3 Encodes a Circadian Clock–Regulated Nuclear Protein That Functions in an Arabidopsis PHYB Signal Transduction Pathway. Plant Cell *13*, 1293–1304.

Lu, S.X., Knowles, S.M., Andronis, C., Ong, M.S., and Tobin, E.M. (2009). CIRCADIAN CLOCK ASSOCIATED1 and LATE ELONGATED HYPOCOTYL function synergistically in the circadian clock of Arabidopsis. Plant Physiol. *150*, 834–843.

Lu, S.X., Webb, C.J., Knowles, S.M., Kim, S.H.J., Wang, Z., and Tobin, E.M. (2012a). CCA1 and ELF3 Interact in the control of hypocotyl length and flowering time in Arabidopsis. Plant Physiol. *158*, 1079–1088.

Lu, S.X., Webb, C.J., Knowles, S.M., Kim, S.H.J., Wang, Z., and Tobin, E.M. (2012b). CCA1 and ELF3 Interact in the control of hypocotyl length and flowering time in Arabidopsis. Plant Physiol. *158*, 1079–1088.

Ludewig, U., and Frommer, W.B. (2002). Genes and proteins for solute transport and sensing. Arab. Book *1*, e0092.

Ma, Y., Gil, S., Grasser, K.D., and Mas, P. (2018). Targeted Recruitment of the Basal Transcriptional Machinery by LNK Clock Components Controls the Circadian Rhythms of Nascent RNAs in Arabidopsis. Plant Cell *30*, 907.

Makino, S., Matsushika, A., Kojima, M., Oda, Y., and Mizuno, T. (2001). Light response of the circadian waves of the APRR1/TOC1 quintet: when does the quintet start singing rhythmically in Arabidopsis? Plant Cell Physiol. *42*, 334–339.

Makino, S., Matsushika, A., Kojima, M., Yamashino, T., and Mizuno, T. (2002). The APRR1/TOC1 quintet implicated in circadian rhythms of Arabidopsis thaliana: I. Characterization with APRR1-overexpressing plants. Plant Cell Physiol. *43*, 58–69.

Martínez-García, J.F., Huq, E., and Quail, P.H. (2000). Direct targeting of light signals to a promoter element-bound transcription factor. Science *288*, 859–863.

Martins, S., Montiel-Jorda, A., Cayrel, A., Huguet, S., Roux, C.P.-L., Ljung, K., and Vert, G. (2017). Brassinosteroid signaling-dependent root responses to prolonged elevated ambient temperature. Nat. Commun. *8*, 309.

Martin-Tryon, E.L., Kreps, J.A., and Harmer, S.L. (2007). GIGANTEA acts in blue light signaling and has biochemically separable roles in circadian clock and flowering time regulation. Plant Physiol. *143*, 473–486.

Más, P. (2008). Circadian clock function in Arabidopsis thaliana: time beyond transcription. Trends Cell Biol. *18*, 273–281.

Más, P., Devlin, P.F., Panda, S., and Kay, S.A. (2000). Functional interaction of phytochrome B and cryptochrome 2. Nature *408*, 207–211.

Más, P., Alabadí, D., Yanovsky, M.J., Oyama, T., and Kay, S.A. (2003a). Dual role of TOC1 in the control of circadian and photomorphogenic responses in Arabidopsis. Plant Cell *15*, 223–236.

Más, P., Kim, W.-Y., Somers, D.E., and Kay, S.A. (2003b). Targeted degradation of TOC1 by ZTL modulates circadian function in Arabidopsis thaliana. Nature *426*, 567–570.

Mathieu, J., Warthmann, N., Küttner, F., and Schmid, M. (2007a). Export of FT Protein from Phloem Companion Cells Is Sufficient for Floral Induction in Arabidopsis. Curr.

Biol. *17*, 1055–1060.

Mathieu, J., Warthmann, N., Küttner, F., and Schmid, M. (2007b). Export of FT protein from phloem companion cells is sufficient for floral induction in Arabidopsis. Curr. Biol. CB *17*, 1055–1060.

Matsuo, T., and Ishiura, M. (2010). Chapter 6 - New Insights into the Circadian Clock in Chlamydomonas. In International Review of Cell and Molecular Biology, (Academic Press), pp. 281–314.

McClung, C.R. (2019). The Plant Circadian Oscillator. Biology *8*.

McWatters, H.G., Kolmos, E., Hall, A., Doyle, M.R., Amasino, R.M., Gyula, P., Nagy, F., Millar, A.J., and Davis, S.J. (2007). ELF4 is required for oscillatory properties of the circadian clock. Plant Physiol. *144*, 391–401.

Mehta, N., and Cheng, H.-Y.M. (2013). Micro-managing the circadian clock: The role of microRNAs in biological timekeeping. J. Mol. Biol. *425*, 3609–3624.

Michael, T.P., Salome, P.A., and McClung, C.R. (2003). Two Arabidopsis circadian oscillators can be distinguished by differential temperature sensitivity. Proc. Natl. Acad. Sci. U. S. A. *100*, 6878—6883.

Mikkelsen, M.D., and Thomashow, M.F. (2009). A role for circadian evening elements in cold-regulated gene expression in Arabidopsis. Plant J. Cell Mol. Biol. *60*, 328–339.

Mizoguchi, T., Wheatley, K., Hanzawa, Y., Wright, L., Mizoguchi, M., Song, H.R., Carré, I.A., and Coupland, G. (2002). LHY and CCA1 are partially redundant genes required to maintain circadian rhythms in Arabidopsis. Dev. Cell *2*, 629–641.

Mizoguchi, T., Wright, L., Fujiwara, S., Cremer, F., Lee, K., Onouchi, H., Mouradov, A., Fowler, S., Kamada, H., Putterill, J., et al. (2005). Distinct roles of GIGANTEA in promoting flowering and regulating circadian rhythms in Arabidopsis. Plant Cell *17*, 2255–2270.

Mizuno, T., and Nakamichi, N. (2005). Pseudo-Response Regulators (PRRs) or True Oscillator Components (TOCs). Plant Cell Physiol. *46*, 677–685.

Mizuno, T., Nomoto, Y., Oka, H., Kitayama, M., Takeuchi, A., Tsubouchi, M., and Yamashino, T. (2014). Ambient temperature signal feeds into the circadian clock transcriptional circuitry through the EC night-time repressor in Arabidopsis thaliana. Plant Cell Physiol. *55*, 958–976.

de Montaigu, A., Tóth, R., and Coupland, G. (2010). Plant development goes like clockwork. Trends Genet. TIG *26*, 296–306.

Nagel, D.H., Doherty, C.J., Pruneda-Paz, J.L., Schmitz, R.J., Ecker, J.R., and Kay, S.A. (2015). Genome-wide identification of CCA1 targets uncovers an expanded clock network in Arabidopsis. Proc. Natl. Acad. Sci. U. S. A. *112*, E4802-4810.

Nakagawa, T., Kurose, T., Hino, T., Tanaka, K., Kawamukai, M., Niwa, Y., Toyooka, K., Matsuoka, K., Jinbo, T., and Kimura, T. (2007a). Development of series of gateway binary vectors, pGWBs, for realizing efficient construction of fusion genes for plant transformation. J. Biosci. Bioeng. *104*, 34–41.

Nakagawa, T., Suzuki, T., Murata, S., Nakamura, S., Hino, T., Maeo, K., Tabata, R., Kawai, T., Tanaka, K., Niwa, Y., et al. (2007b). Improved Gateway binary vectors: high-performance vectors for creation of fusion constructs in transgenic analysis of plants. Biosci. Biotechnol. Biochem. *71*, 2095–2100.

Nakamichi, N., Kusano, M., Fukushima, A., Kita, M., Ito, S., Yamashino, T., Saito, K., Sakakibara, H., and Mizuno, T. (2009). Transcript profiling of an Arabidopsis PSEUDO RESPONSE REGULATOR arrhythmic triple mutant reveals a role for the circadian clock in cold stress response. Plant Cell Physiol. *50*, 447–462.

Nakamichi, N., Kiba, T., Henriques, R., Mizuno, T., Chua, N.-H., and Sakakibara, H. (2010). PSEUDO-RESPONSE REGULATORS 9, 7, and 5 are transcriptional repressors in the Arabidopsis circadian clock. Plant Cell *22*, 594–605.

Nakamichi, N., Kiba, T., Kamioka, M., Suzuki, T., Yamashino, T., Higashiyama, T., Sakakibara, H., and Mizuno, T. (2012). Transcriptional repressor PRR5 directly regulates clock-output pathways. Proc. Natl. Acad. Sci. U. S. A. *109*, 17123–17128.

Nelson, D.C., Lasswell, J., Rogg, L.E., Cohen, M.A., and Bartel, B. (2000). FKF1, a clock-controlled gene that regulates the transition to flowering in Arabidopsis. Cell *101*, 331–340.

Nieto, C., López-Salmerón, V., Davière, J.-M., and Prat, S. (2015a). ELF3-PIF4 interaction regulates plant growth independently of the Evening Complex. Curr. Biol. CB *25*, 187–193.

Nieto, C., López-Salmerón, V., Davière, J.-M., and Prat, S. (2015b). ELF3-PIF4 interaction regulates plant growth independently of the Evening Complex. Curr. Biol. CB *25*, 187–193.

Nimmo, H.G. (2018). Entrainment of Arabidopsis roots to the light:dark cycle by light piping. Plant Cell Environ. *41*, 1742–1748.

Nimmo, H.G., Laird, J., Bindbeutel, R., and Nusinow, D.A. (2020). The evening complex is central to the difference between the circadian clocks of Arabidopsis thaliana shoots and roots. Physiol. Plant.

Niwa, Y., Yamashino, T., and Mizuno, T. (2009). The circadian clock regulates the photoperiodic response of hypocotyl elongation through a coincidence mechanism in Arabidopsis thaliana. Plant Cell Physiol. *50*, 838–854.

Nohales, M.A., and Kay, S.A. (2016). Molecular mechanisms at the core of the plant circadian oscillator. Nat. Struct. Mol. Biol. *23*, 1061–1069.

Nomoto, Y., Kubozono, S., Miyachi, M., Yamashino, T., Nakamichi, N., and Mizuno, T. (2012). A circadian clock- and PIF4-mediated double coincidence mechanism is implicated in the thermosensitive photoperiodic control of plant architectures in

Arabidopsis thaliana. Plant Cell Physiol. *53*, 1965–1973.

Nozue, K., Covington, M.F., Duek, P.D., Lorrain, S., Fankhauser, C., Harmer, S.L., and Maloof, J.N. (2007). Rhythmic growth explained by coincidence between internal and external cues. Nature *448*, 358–361.

Nusinow, D.A., Helfer, A., Hamilton, E.E., King, J.J., Imaizumi, T., Schultz, T.F., Farré, E.M., and Kay, S.A. (2011). The ELF4-ELF3-LUX complex links the circadian clock to diurnal control of hypocotyl growth. Nature *475*, 398–402.

Onai, K., and Ishiura, M. (2005). PHYTOCLOCK 1 encoding a novel GARP protein essential for the Arabidopsis circadian clock. Genes Cells Devoted Mol. Cell. Mech. *10*, 963–972.

Osterlund, M.T., Hardtke, C.S., Wei, N., and Deng, X.W. (2000). Targeted destabilization of HY5 during light-regulated development of Arabidopsis. Nature *405*, 462–466.

Ouyang, Y., Andersson, C.R., Kondo, T., Golden, S.S., and Johnson, C.H. (1998). Resonating circadian clocks enhance fitness in cyanobacteria. Proc. Natl. Acad. Sci. U. S. A. *95*, 8660–8664.

Oyama, T., Shimura, Y., and Okada, K. (1997). The Arabidopsis HY5 gene encodes a bZIP protein that regulates stimulus-induced development of root and hypocotyl. Genes Dev. *11*, 2983–2995.

Pant, B.D., Buhtz, A., Kehr, J., and Scheible, W.-R. (2008). MicroRNA399 is a long-distance signal for the regulation of plant phosphate homeostasis. Plant J. Cell Mol. Biol. *53*, 731–738.

Para, A., Farre, E.M., Imaizumi, T., Pruneda-Paz, J.L., Harmon, F.G., and Kay, S.A. (2007). PRR3 Is a vascular regulator of TOC1 stability in the Arabidopsis circadian clock. Plant Cell *19*, 3462–3473.

Park, D.H., Somers, D.E., Kim, Y.S., Choy, Y.H., Lim, H.K., Soh, M.S., Kim, H.J., Kay, S.A.,

and Nam, H.G. (1999). Control of circadian rhythms and photoperiodic flowering by the Arabidopsis GIGANTEA gene. Science *285*, 1579–1582.

Park, H.J., Baek, D., Cha, J.-Y., Liao, X., Kang, S.-H., McClung, C.R., Lee, S.Y., Yun, D.-J., and Kim, W.-Y. (2019). HOS15 Interacts with the Histone Deacetylase HDA9 and the Evening Complex to Epigenetically Regulate the Floral Activator GIGANTEA. Plant Cell *31*, 37–51.

Pérez-García, P., Ma, Y., Yanovsky, M.J., and Mas, P. (2015). Time-dependent sequestration of RVE8 by LNK proteins shapes the diurnal oscillation of anthocyanin biosynthesis. Proc. Natl. Acad. Sci. U. S. A. *112*, 5249–5253.

Pittendrigh, C.S. (1954). ON TEMPERATURE INDEPENDENCE IN THE CLOCK SYSTEM CONTROLLING EMERGENCE TIME IN DROSOPHILA. Proc. Natl. Acad. Sci. U. S. A. *40*, 1018–1029.

Plautz, J.D., Straume, M., Stanewsky, R., Jamison, C.F., Brandes, C., Dowse, H.B., Hall, J.C., and Kay, S.A. (1997). Quantitative analysis of Drosophila period gene transcription in living animals. J. Biol. Rhythms *12*, 204–217.

Portolés, S., and Más, P. (2010). The functional interplay between protein kinase CK2 and CCA1 transcriptional activity is essential for clock temperature compensation in Arabidopsis. PLoS Genet. *6*, e1001201.

Pruneda-Paz, J.L., Breton, G., Para, A., and Kay, S.A. (2009). A functional genomics approach reveals CHE as a component of the Arabidopsis circadian clock. Science *323*, 1481–1485.

Putterill, J., and Varkonyi-Gasic, E. (2016). FT and florigen long-distance flowering control in plants. Curr. Opin. Plant Biol. *33*, 77–82.

Putterill, J., Robson, F., Lee, K., Simon, R., and Coupland, G. (1995). The CONSTANS gene of Arabidopsis promotes flowering and encodes a protein showing similarities

to zinc finger transcription factors. Cell *80*, 847–857.

Raschke, A., Ibañez, C., Ullrich, K.K., Anwer, M.U., Becker, S., Glöckner, A., Trenner, J., Denk, K., Saal, B., Sun, X., et al. (2015). Natural variants of ELF3 affect thermomorphogenesis by transcriptionally modulating. BMC Plant Biol. *15*, 197.

Rim, Y., Huang, L., Chu, H., Han, X., Cho, W.K., Jeon, C.O., Kim, H.J., Hong, J.-C., Lucas, W.J., and Kim, J.-Y. (2011). Analysis of Arabidopsis transcription factor families revealed extensive capacity for cell-to-cell movement as well as discrete trafficking patterns. Mol. Cells *32*, 519–526.

Rizzini, L., Favory, J.-J., Cloix, C., Faggionato, D., O'Hara, A., Kaiserli, E., Baumeister, R., Schäfer, E., Nagy, F., Jenkins, G.I., et al. (2011). Perception of UV-B by the Arabidopsis UVR8 protein. Science *332*, 103–106.

Robinson, M.D., McCarthy, D.J., and Smyth, G.K. (2010). edgeR: a Bioconductor package for differential expression analysis of digital gene expression data. Bioinforma. Oxf. Engl. *26*, 139–140.

Rugnone, M.L., Faigón Soverna, A., Sanchez, S.E., Schlaen, R.G., Hernando, C.E., Seymour, D.K., Mancini, E., Chernomoretz, A., Weigel, D., Más, P., et al. (2013). LNK genes integrate light and clock signaling networks at the core of the Arabidopsis oscillator. Proc. Natl. Acad. Sci. U. S. A. *110*, 12120–12125.

Salisbury, F.J., Hall, A., Grierson, C.S., and Halliday, K.J. (2007). Phytochrome coordinates Arabidopsis shoot and root development. Plant J. Cell Mol. Biol. *50*, 429–438.

Salome, P.A., and McClung, C.R. (2005). PSEUDO-RESPONSE REGULATOR 7 and 9 are partially redundant genes essential for the temperature responsiveness of the Arabidopsis circadian clock. Plant Cell *17*, 791–803.

Sanchez, S.E., and Kay, S.A. (2016). The Plant Circadian Clock: From a Simple

Timekeeper to a Complex Developmental Manager. Cold Spring Harb. Perspect. Biol. *8*.

Sanchez, S.E., Rugnone, M.L., and Kay, S.A. (2020). Light Perception: A Matter of Time. Mol. Plant *13*, 363–385.

Schaffer, R., Ramsay, N., Samach, A., Corden, S., Putterill, J., Carré, I.A., and Coupland, G. (1998). The late elongated hypocotyl mutation of Arabidopsis disrupts circadian rhythms and the photoperiodic control of flowering. Cell *93*, 1219–1229.

Schibler, U., and Sassone-Corsi, P. (2002). A web of circadian pacemakers. Cell *111*, 919–922.

Schlaen, R.G., Mancini, E., Sanchez, S.E., Perez-Santángelo, S., Rugnone, M.L., Simpson, C.G., Brown, J.W.S., Zhang, X., Chernomoretz, A., and Yanovsky, M.J. (2015). The spliceosome assembly factor GEMIN2 attenuates the effects of temperature on alternative splicing and circadian rhythms. Proc. Natl. Acad. Sci. U. S. A. *112*, 9382–9387.

Schultz, T.F., Kiyosue, T., Yanovsky, M., Wada, M., and Kay, S.A. (2001). A role for LKP2 in the circadian clock of Arabidopsis. Plant Cell *13*, 2659–2670.

Seo, P.J., and Mas, P. (2014). Multiple layers of posttranslational regulation refine circadian clock activity in Arabidopsis. Plant Cell *26*, 79–87.

Seo, P.J., Park, M.-J., Lim, M.-H., Kim, S.-G., Lee, M., Baldwin, I.T., and Park, C.-M. (2012). A self-regulatory circuit of CIRCADIAN CLOCK-ASSOCIATED1 underlies the circadian clock regulation of temperature responses in Arabidopsis. Plant Cell *24*, 2427–2442.

Sharrock, R.A., and Clack, T. (2002). Patterns of expression and normalized levels of the five Arabidopsis phytochromes. Plant Physiol. *130*, 442–456.

Shibasaki, K., Uemura, M., Tsurumi, S., and Rahman, A. (2009). Auxin Response in Arabidopsis under Cold Stress: Underlying Molecular Mechanisms. Plant

Cell *21*, 3823.

Shikata, H., Hanada, K., Ushijima, T., Nakashima, M., Suzuki, Y., and Matsushita, T. (2014). Phytochrome controls alternative splicing to mediate light responses in Arabidopsis. Proc. Natl. Acad. Sci. U. S. A. *111*, 18781–18786.

Shimizu, H., Katayama, K., Koto, T., Torii, K., Araki, T., and Endo, M. (2015). Decentralized circadian clocks process thermal and photoperiodic cues in specific tissues. Nat. Plants *1*, 15163.

Shin, J., Anwer, M.U., and Davis, S.J. (2013). Phytochrome-interacting factors (PIFs) as bridges between environmental signals and the circadian clock: diurnal regulation of growth and development. Mol. Plant *6*, 592–595.

Silva, C.S., Nayak, A., Lai, X., Hutin, S., Hugouvieux, V., Jung, J.-H., López-Vidriero, I., Franco-Zorrilla, J.M., Panigrahi, K.C.S., Nanao, M.H., et al. (2020a). Molecular mechanisms of Evening Complex activity in Arabidopsis. Proc. Natl. Acad. Sci. U. S. A. *117*, 6901–6909.

Silva, C.S., Nayak, A., Lai, X., Hutin, S., Hugouvieux, V., Jung, J.-H., López-Vidriero, I., Franco-Zorrilla, J.M., Panigrahi, K.C.S., Nanao, M.H., et al. (2020b). Molecular mechanisms of Evening Complex activity in Arabidopsis. Proc. Natl. Acad. Sci. U. S. A. *117*, 6901–6909.

Singh, M., and Mas, P. (2018). A Functional Connection between the Circadian Clock and Hormonal Timing in Arabidopsis. Genes *9*.

Somers, D.E., Devlin, P.F., and Kay, S.A. (1998). Phytochromes and Cryptochromes in the Entrainment of the Arabidopsis Circadian Clock. Science *282*, 1488.

Somers, D.E., Schultz, T.F., Milnamow, M., and Kay, S.A. (2000). ZEITLUPE encodes a novel clock-associated PAS protein from Arabidopsis. Cell *101*, 319–329.

Song, Y.H., Shim, J.S., Kinmonth-Schultz, H.A., and Imaizumi, T. (2015). Photoperiodic

flowering: time measurement mechanisms in leaves. Annu. Rev. Plant Biol. *66*, 441–464.

Soy, J., Leivar, P., González-Schain, N., Martín, G., Diaz, C., Sentandreu, M., Al-Sady, B., Quail, P.H., and Monte, E. (2016). Molecular convergence of clock and photosensory pathways through PIF3-TOC1 interaction and co-occupancy of target promoters. Proc. Natl. Acad. Sci. U. S. A. *113*, 4870–4875.

Stahl, Y., and Simon, R. (2013). Gated communities: apoplastic and symplastic signals converge at plasmodesmata to control cell fates. J. Exp. Bot. *64*, 5237–5241.

Strayer, C., Oyama, T., Schultz, T.F., Raman, R., Somers, D.E., Más, P., Panda, S., Kreps, J.A., and Kay, S.A. (2000). Cloning of the Arabidopsis clock gene TOC1, an autoregulatory response regulator homolog. Science *289*, 768–771.

Takahashi, N., Hirata, Y., Aihara, K., and Mas, P. (2015). A hierarchical multi-oscillator network orchestrates the Arabidopsis circadian system. Cell *163*, 148–159.

Takeuchi, T., Newton, L., Burkhardt, A., Mason, S., and Farré, E.M. (2014). Light and the circadian clock mediate time-specific changes in sensitivity to UV-B stress under light/dark cycles. J. Exp. Bot. *65*, 6003–6012.

Tepperman, J.M., Zhu, T., Chang, H.S., Wang, X., and Quail, P.H. (2001). Multiple transcription-factor genes are early targets of phytochrome A signaling. Proc. Natl. Acad. Sci. U. S. A. *98*, 9437–9442.

Toledo-Ortiz, G., Johansson, H., Lee, K.P., Bou-Torrent, J., Stewart, K., Steel, G., Rodríguez-Concepción, M., and Halliday, K.J. (2014). The HY5-PIF regulatory module coordinates light and temperature control of photosynthetic gene transcription. PLoS Genet. *10*, e1004416.

Tong, M., Lee, K., Ezer, D., Cortijo, S., Jung, J., Charoensawan, V., Box, M.S., Jaeger, K.E., Takahashi, N., Mas, P., et al. (2020). The Evening Complex Establishes Repressive

Chromatin Domains Via H2A.Z Deposition. Plant Physiol. *182*, 612–625.

Turnbull, C.G.N., Booker, J.P., and Leyser, H.M.O. (2002). Micrografting techniques for testing long-distance signalling in Arabidopsis. Plant J. Cell Mol. Biol. *32*, 255–262.

Turner, S., and Sieburth, L.E. (2003). Vascular patterning. Arab. Book *2*, e0073.

Valverde, F., Mouradov, A., Soppe, W., Ravenscroft, D., Samach, A., and Coupland, G. (2004). Photoreceptor regulation of CONSTANS protein in photoperiodic flowering. Science *303*, 1003–1006.

Wang, H., and Wang, H. (2015). Phytochrome signaling: time to tighten up the loose ends. Mol. Plant *8*, 540–551.

Wang, Z.Y., and Tobin, E.M. (1998). Constitutive expression of the CIRCADIAN CLOCK ASSOCIATED 1 (CCA1) gene disrupts circadian rhythms and suppresses its own expression. Cell *93*, 1207–1217.

Wang, C.-Q., Sarmast, M.K., Jiang, J., and Dehesh, K. (2015). The Transcriptional Regulator BBX19 Promotes Hypocotyl Growth by Facilitating. Plant Cell *27*, 1128–1139.

Wang, Y., Wu, J.-F., Nakamichi, N., Sakakibara, H., Nam, H.-G., and Wu, S.-H. (2011). LIGHT-REGULATED WD1 and PSEUDO-RESPONSE REGULATOR9 form a positive feedback regulatory loop in the Arabidopsis circadian clock. Plant Cell *23*, 486–498.

Wang, Z.Y., Kenigsbuch, D., Sun, L., Harel, E., Ong, M.S., and Tobin, E.M. (1997). A Myb-related transcription factor is involved in the phytochrome regulation of an Arabidopsis Lhcb gene. Plant Cell *9*, 491–507.

Wigge, P.A., Kim, M.C., Jaeger, K.E., Busch, W., Schmid, M., Lohmann, J.U., and Weigel, D. (2005). Integration of spatial and temporal information during floral induction in Arabidopsis. Science *309*, 1056–1059.

Wu, S., and Gallagher, K.L. (2012). Transcription factors on the move. Curr. Opin. Plant

Biol. *15*, 645–651.

Wu, J.-F., Wang, Y., and Wu, S.-H. (2008). Two new clock proteins, LWD1 and LWD2, regulate Arabidopsis photoperiodic flowering. Plant Physiol. *148*, 948–959.

Wu, J.-F., Tsai, H.-L., Joanito, I., Wu, Y.-C., Chang, C.-W., Li, Y.-H., Wang, Y., Hong, J.C., Chu, J.-W., Hsu, C.-P., et al. (2016). LWD-TCP complex activates the morning gene CCA1 in Arabidopsis. Nat. Commun. *7*, 13181.

Xie, Q., Wang, P., Liu, X., Yuan, L., Wang, L., Zhang, C., Li, Y., Xing, H., Zhi, L., Yue, Z., et al. (2014). LNK1 and LNK2 are transcriptional coactivators in the Arabidopsis circadian oscillator. Plant Cell *26*, 2843–2857.

Yakir, E., Hilman, D., Kron, I., Hassidim, M., Melamed-Book, N., and Green, R.M. (2009). Posttranslational regulation of CIRCADIAN CLOCK ASSOCIATED1 in the circadian oscillator of Arabidopsis. Plant Physiol. *150*, 844–857.

Yamashino, T., Nomoto, Y., Lorrain, S., Miyachi, M., Ito, S., Nakamichi, N., Fankhauser, C., and Mizuno, T. (2013). Verification at the protein level of the PIF4-mediated external coincidence model for the temperature-adaptive photoperiodic control of plant growth in Arabidopsis thaliana. Plant Signal. Behav. *8*, e23390.

Yang, Z., Liu, B., Su, J., Liao, J., Lin, C., and Oka, Y. (2017). Cryptochromes Orchestrate Transcription Regulation of Diverse Blue Light Responses in Plants. Photochem. Photobiol. *93*, 112–127.

Yanovsky, M.J., Mazzella, M.A., Whitelam, G.C., and Casal, J.J. (2001). Resetting of the circadian clock by phytochromes and cryptochromes in Arabidopsis. J. Biol. Rhythms *16*, 523–530.

Yeom, M., Kim, H., Lim, J., Shin, A.-Y., Hong, S., Kim, J.-I., and Nam, H.G. (2014). How do phytochromes transmit the light quality information to the circadian clock in Arabidopsis? Mol. Plant *7*, 1701–1704.

Yoshida, R., Fekih, R., Fujiwara, S., Oda, A., Miyata, K., Tomozoe, Y., Nakagawa, M., Niinuma, K., Hayashi, K., Ezura, H., et al. (2009). Possible role of early flowering 3 (ELF3) in clock-dependent floral regulation by short vegetative phase (SVP) in Arabidopsis thaliana. New Phytol. *182*, 838–850.

Yu, J.-W., Rubio, V., Lee, N.-Y., Bai, S., Lee, S.-Y., Kim, S.-S., Liu, L., Zhang, Y., Irigoyen, M.L., Sullivan, J.A., et al. (2008a). COP1 and ELF3 control circadian function and photoperiodic flowering by regulating GI stability. Mol. Cell *32*, 617–630.

Yu, J.-W., Rubio, V., Lee, N.-Y., Bai, S., Lee, S.-Y., Kim, S.-S., Liu, L., Zhang, Y., Irigoyen, M.L., Sullivan, J.A., et al. (2008b). COP1 and ELF3 control circadian function and photoperiodic flowering by regulating GI stability. Mol. Cell *32*, 617–630.

Zagotta, M.T., Hicks, K.A., Jacobs, C.I., Young, J.C., Hangarter, R.P., and Meeks-Wagner, D.R. (1996). The Arabidopsis ELF3 gene regulates vegetative photomorphogenesis and the photoperiodic induction of flowering. Plant J. Cell Mol. Biol. *10*, 691–702.

Zha, P., Liu, S., Li, Y., Ma, T., Yang, L., Jing, Y., and Lin, R. (2020). The Evening Complex and the Chromatin-Remodeling Factor PICKLE Coordinately Control Seed Dormancy by Directly Repressing DOG1 in Arabidopsis. Winslow Briggs Spec. Issue Photobiol. *1*, 100011.

Zhang, H., He, H., Wang, X., Wang, X., Yang, X., Li, L., and Deng, X.W. (2011). Genome-wide mapping of the HY5-mediated gene networks in Arabidopsis that involve both transcriptional and post-transcriptional regulation. Plant J. Cell Mol. Biol. *65*, 346–358.

Zhu, J., Zhang, K.-X., Wang, W.-S., Gong, W., Liu, W.-C., Chen, H.-G., Xu, H.-H., and Lu, Y.-T. (2014). Low Temperature Inhibits Root Growth by Reducing Auxin Accumulation via ARR1/12. Plant Cell Physiol. *56*, 727–736.

Annexes

Annex Ⅰ : Detail protocol of micrografting assays with young seedlings in Arabidopsis

All processes for micrografting should be done in laminar flow cabinet.

Step 1: Preparation

Sterilize the laminar flow cabinet by UV light for 10 mins first. Then set up the dissecting microscope (Zeiss, Stemi SV6) in the cabinet and rinse the microscope and hands by standard surface sterilization procedures with ethanol.

Prepare 0.5 Murashige and Skoog agar medium with 0.5 sucrose (0.5^2 MS) and place strips of autoclaved filter paper (with sizes of 7cm*1cm) on the surface of the 0.5^2 medium plates (Figure1).

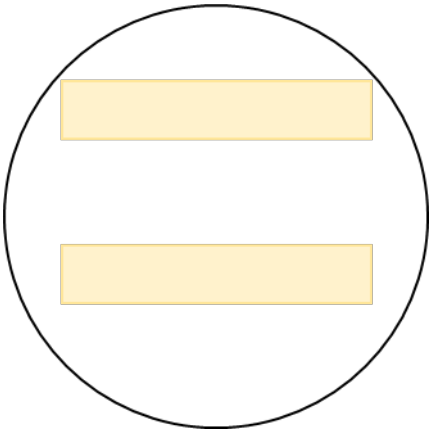

Figure 1. Place strips of filter paper on the medium plates.

Step 2: Remove seedlings to medium plates

Dip the tip of tweezers (with fine point, Dumont #55 Biology tweezers) with ethanol and flame sterilize with the alcohol lamp. Wait the cool down of the tweezers and press the tip of the tweezers into the agar medium and break the surface of the medium as picture shown (gray curves, Figure 2). Transfer the 5-7 days (vertically grown) old seedlings (used as rootstocks) to the surface of strips of filter paper gently by tweezers (Figure 3). Make sure the roots of seedlings bury in the medium and touch

the water from the medium.

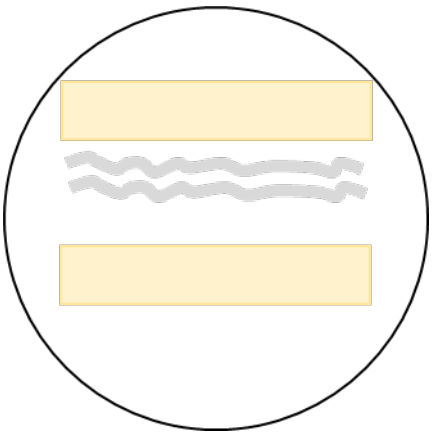

Figure 2. Break the surface of medium by tweezers (gray curves).

Transfer the 5-7 days (vertically grown) old seedlings (used as scions) to the surface of strips gently by tweezers (Figure 3).

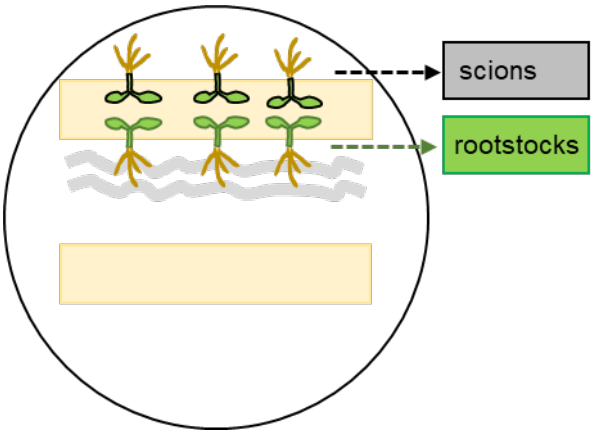

Figure 3. Place seedlings (used as scions and rootstocks) on the surface of strips. Seedlings on the top (with black cotyledon) will be used as scions whereas the seedlings on the bottom (with green cotyledon) will be used as rootstocks.

Step3: Cutting tissues

Using #11 sterile surgical blades (Swann-Morton) to remove the cotyledons from seedlings (used as scions) first. Then carefully cut off (clean fast and horizontal to the hypocotyls) the hypocotyls from scion seedlings with #11 blades (Figure 4).

Using #11 sterile surgical blades to cut off (clean fast and horizontal to the hypocotyls) the hypocotyls from seedlings (used as rootstocks) (Figure 5).

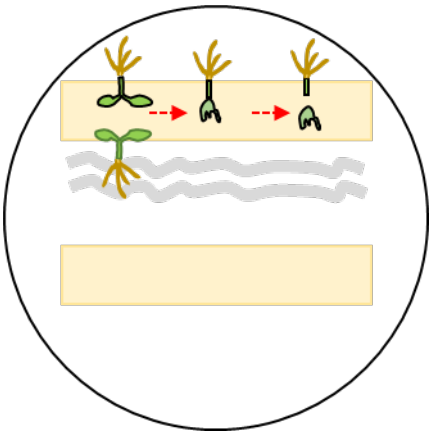

Figure 4. Cutting the scions from seedlings.

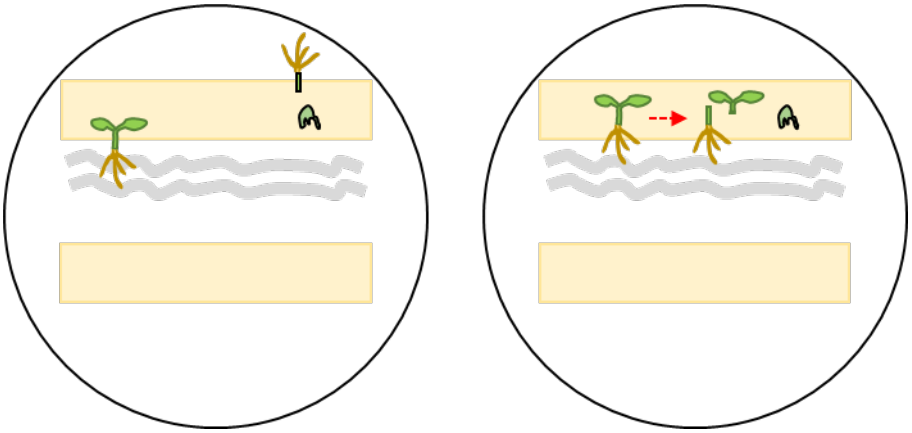

Figure 5. Cutting the rootstocks from seedlings.

Step 4: connecting scions with rootstocks after tissue cutting

Remove the strips of the filter paper upward a little bit by tweezers and let the top of the rootstocks drop on the medium (still make sure the roots of rootstocks bury in the medium after moving) (Figure 6).

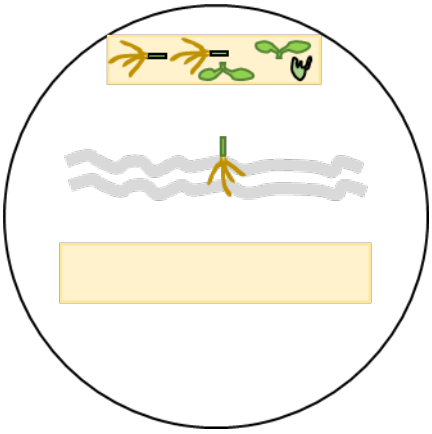

Figure 6. Remove the strips upward and rootstocks touch the medium.

Remove the scions (on the strips of filter paper) close to the rootstocks by tweezers (not grabbing or pinching, but gently touching and moving) (Figure 7). Make sure the bottom of scions closely touches the top of the rootstocks (move the scions and rootstocks gently by the tip of tweezers). Trash the rest tissues on the strips of filter paper and trash it. Incubate the plates to light chambers (12:12 (light: dark) chambers or 16:8(light: dark) long day chambers, with 22degree) vertically for 10 days.

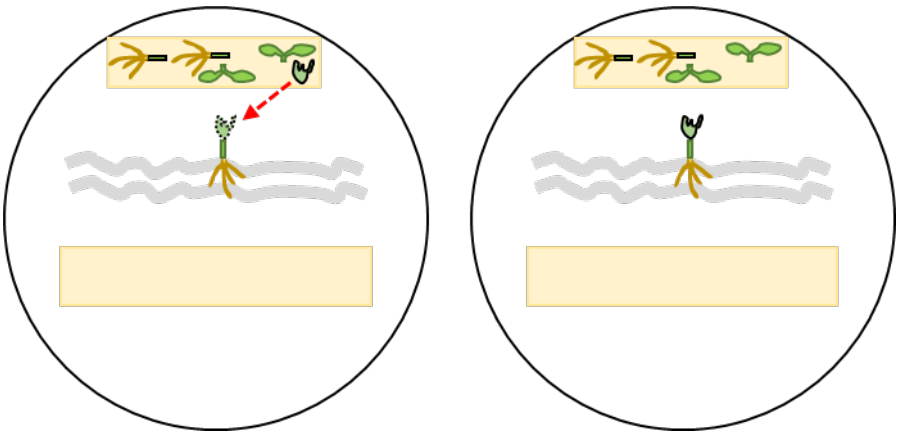

Figure 7. connecting scions with rootstocks.

Step5: Removing adventitious roots

Sometimes grafts emerge adventitious roots if the growth conditions are not very well. Remove the adventitious roots by sterilize tweezers and #11 blades under

dissecting microscope if the adventitious roots are observed (one week after grafting). Grab the tips of the adventitious roots by sterilize tweezers and cut as closer to the shoots as possible (with #11 blades).

References

Andersen, T. G., Liang, D., Halkier, B. A. and White, R. (2014). Grafting *Arabidopsis*. *Bio-protocol* 4(13): e1164. DOI: 10.21769/BioProtoc.1164.

Marsch-Martínez, N., Franken, J., Gonzalez-Aguilera, K.L. *et al.* An efficient flat-surface collar-free grafting method for *Arabidopsis thaliana* seedlings. *Plant Methods* **9,** 14 (2013). https://doi.org/10.1186/1746-4811-9-14

Notaguchi, M., Daimon, Y., Abe, M. *et al.* Adaptation of a seedling micro-grafting technique to the study of long-distance signaling in flowering of *Arabidopsis thaliana* . *J Plant Res* **122,** 201–214 (2009). https://doi.org/10.1007/s10265-008-0209-1

Turnbull, C.G.N., Booker, J.P. and Leyser, H.M.O. (2002), Micrografting techniques for testing long-distance signalling in *Arabidopsis*. The Plant Journal, 32: 255-262. doi:10.1046/j.1365-313X.2002.01419.x

Annex II

ARTICLES
https://doi.org/10.1038/s41477-020-0634-2

nature plants

A mobile ELF4 delivers circadian temperature information from shoots to roots

Wei Wei Chen[1,10], Nozomu Takahashi[1,10], Yoshito Hirata[2,3], James Ronald[4], Silvana Porco[5], Seth J. Davis[4,6], Dmitri A. Nusinow[7], Steve A. Kay[5,8] and Paloma Mas[1,9] ✉

The circadian clock is synchronized by environmental cues, mostly by light and temperature. Explaining how the plant circadian clock responds to temperature oscillations is crucial to understanding plant responsiveness to the environment. Here, we found a prevalent temperature-dependent function of the *Arabidopsis* clock component EARLY FLOWERING 4 (ELF4) in the root clock. Although the clocks in roots are able to run in the absence of shoots, micrografting assays and mathematical analyses show that ELF4 moves from shoots to regulate rhythms in roots. ELF4 movement does not convey photoperiodic information, but trafficking is essential for controlling the period of the root clock in a temperature-dependent manner. Low temperatures favour ELF4 mobility, resulting in a slow-paced root clock, whereas high temperatures decrease movement, leading to a faster clock. Hence, the mobile ELF4 delivers temperature information and establishes a shoot-to-root dialogue that sets the pace of the clock in roots.

Nearly all photosensitive organisms have evolved timing mechanisms or circadian clocks able to synchronize metabolism, physiology and development in coordination with the 24 h light–dark cycle[1]. In *Arabidopsis thaliana*, the molecular clockwork is based on complex regulatory networks of core clock components that generate rhythms in a myriad of biological outputs[2,3]. Appropriate phasing of biological processes relies on clock resetting by light and temperature cues; a mechanism that requires changes in the expression and activity of essential clock components[4]. Circadian clocks are also defined by a conserved feature known as temperature compensation[5]. In contrast to the temperature dependency of many physicochemical and biological activities, the circadian clock is able to maintain a constant period over a range of physiological temperatures. By using different transcriptional, post-transcriptional and post-translational mechanisms[6–9], the plant circadian system buffers the length of the circadian period. Thus, the circadian clock is able to sustain a period close to 24 h within a physiological range of temperatures. A diverse collection of light-related factors[10–14] and clock-associated components[9,15,16] has been shown to directly or indirectly regulate clock temperature compensation in plants.

Among the *Arabidopsis* clock components, ELF4 (EARLY FLOWERING 4) was initially identified by its role in photoperiod perception and circadian regulation[17]. Structural and functional studies provided a view of the multiple entry points of ELF4 function within the clock[18]. ELF4 protein assembles into the evening complex, a tripartite complex with ELF3 and LUX ARRHYTHMO (LUX) also known as PHYTOCLOCK1 (PCL1)[19,20]. The evening complex regulates growth and represses circadian gene expression[21,22]. ELF4 promotes the nuclear localization of ELF3[19], whereas LUX directly binds to the promoters of the target genes and thus facilitates the recruitment of ELF4 and ELF3[20,23]. Loss-of-function mutants of any of the evening complex components lead to arrhythmia[17,24–26]. Through multiple interactions with light, clock and photomorphogenesis related factors[27], the evening complex is able to coordinate plant responses to environmental cues including temperature[15,27–31], although ELF4, ELF3 and LUX also display functions independent from the evening complex[31–33].

Regarding the circadian structure and organization within the plant, it is broadly accepted that every plant cell harbours a circadian oscillator. However, circadian communication or coupling among cells and tissues varies among different parts of the plant[34–38]. For instance, whereas cotyledon cells present circadian autonomy[39], different degrees of cell-to-cell coupling have been reported in leaves[40–42], in the vasculature with neighbour mesophyll cells[43], in guard cells[44], in cells at the root tip[45,46] and within the shoot apex[47]. Long-distance shoot-to-root photosynthetic signalling is also important for clock entrainment in roots[48], and light piping down the root[49] contributes to this entrainment. Micrografting assays and shoot excision[47] suggest the existence of a long-distance mobile circadian signal from shoots to roots. Here we report that ELF4 moves from shoots to control the pace of the root clock in a temperature-dependent manner.

Results

Prevalent function of ELF4 sustaining rhythms in roots. We first approached the investigation of the circadian mobile signal by simultaneously following rhythms in shoots and roots of intact plants[47]. The waveforms of the morning-expressed *CIRCADIAN CLOCK ASSOCIATED 1* (*CCA1*) and *LATE ELONGATED HYPOCOTYL* (*LHY*) promoter activities displayed a long period, slightly reduced amplitude and phase delay in roots compared with shoots (Fig. 1a,b and Extended Data Fig. 1a). The rhythmic messenger RNA (mRNA) accumulation assayed by quantitative PCR with reverse transcription

[1]Centre for Research in Agricultural Genomics (CRAG), CSIC-IRTA-UAB-UB, Campus UAB, Bellaterra, Barcelona, Spain. [2]Mathematics and Informatics Center, The University of Tokyo, Tokyo, Japan. [3]Faculty of Engineering, Information and Systems, University of Tsukuba, Tsukuba, Japan. [4]Department of Biology, University of York, York, UK. [5]Keck School of Medicine, University of Southern California, Los Angeles, CA, USA. [6]Key Laboratory of Plant Stress Biology, School of Life Sciences, Henan University, Kaifeng, China. [7]Donald Danforth Plant Science Center, St. Louis, MO, USA. [8]Institute of Transformative Bio-Molecules, Nagoya University, Nagoya, Japan. [9]Consejo Superior de Investigaciones Científicas (CSIC), Barcelona, Spain. [10]These authors contributed equally: Wei Wei Chen, Nozomu Takahashi. ✉e-mail: paloma.mas@cragenomica.es

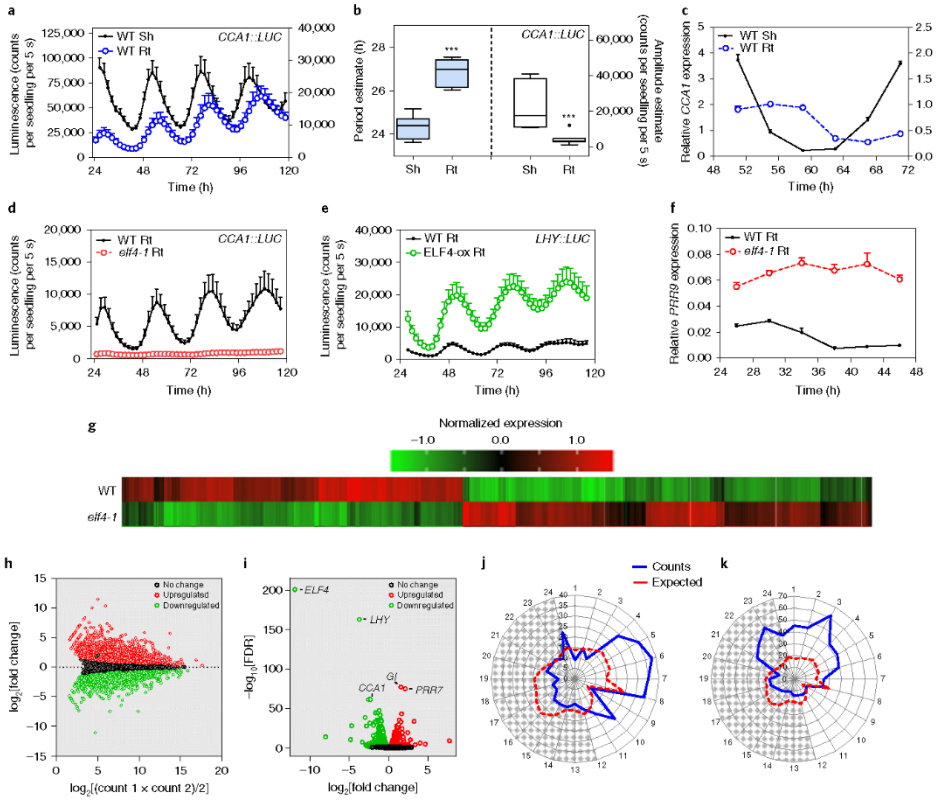

Fig. 1 | Prevalent function of ELF4 sustaining circadian rhythms in roots. a, Luminescence of *CCA1::luciferase* (*LUC*) oscillation simultaneously measured in shoots (Sh; left axis) ($n=9$) and roots (Rt; right axis) ($n=9$). **b**, Period (left *y* axis) estimates of *CCA1::LUC* rhythms in shoots and roots ($n=8$ for each) and amplitude (right *y* axis) estimates of *CCA1::LUC* rhythms in shoots ($n=7$) and roots ($n=8$). In box plots, the centre line is the median, box edges show 25th and 75th percentiles and whiskers extend to minimum and maximum values. ***$P<0.0001$; two-tailed *t*-tests with 95% confidence. **c**, Circadian time-course analyses of *CCA1* mRNA expression in wild-type (WT) shoots and roots. **d**, Luminescence of *CCA1::LUC* rhythms in WT ($n=9$) and *elf4-1* ($n=8$) roots. **e**, Luminescence of *LHY::LUC* rhythms in WT ($n=8$) and ELF4-ox root ($n=9$). **f**, Circadian time-course analyses of *PRR9* mRNA expression in roots of WT and *elf4-1* plants. Sampling was performed under constant light conditions following synchronization under light:dark cycles. In **a**,**c**–**f**, data are mean + s.e.m. **g**, Heat map of the median-normalized expression (*z*-scaled FPKM values) of DEGs following hierarchical clustering using the Euclidean distance. **h**, Relationship between average expression of WT (count 1) and *elf4-1* (count 2) and fold change for each gene. **i**, Volcano plot showing fold change versus significance of the differential-expression test. Black dots represent genes that are not differentially expressed, and red and green dots are genes that are significantly upregulated and downregulated, respectively. **j**,**k**, Circadian phases of upregulated (**j**) and downregulated (**k**) DEGs in *elf4-1* roots. The radial axis represents the subjective time (in units of h). White and grey areas represent subjective day and night, respectively. *n* refers to the number of independent samples. In **a**–**k**, data are representative of two biological replicates, with measurements taken from independent samples grown and processed at different times.

(RT–qPCR) followed the same trend (Fig. 1c). Similar patterns were observed for the promoter activity of the evening-expressed clock component *TIMING OF CAB EXPRESSION1* (TOC1) or *PSEUDO RESPONSE REGULATOR1* (*PRR1*) (Extended Data Fig. 1b,c). Therefore, the clock is fully operative in roots but its overall pace is slower and the phase is delayed compared with shoots.

Under free-running conditions (in the absence of environmental time cues), the circadian clock is unable to properly run in mutant plants of any of the evening complex components[17,24–26]. We therefore examined the roles of the evening complex components in the root clock, particularly focusing on ELF4. Circadian time-course analyses showed that although some very weak oscillations could be detected (Extended Data Fig. 1d), the *CCA1* and *LHY* promoter activities and their mRNA expression were suppressed in *elf4-1* mutant compared with WT roots (Fig. 1d and Extended Data Fig. 1e–g), following a similar trend to that described in shoots[22]

(Extended Data Fig. 1h–j). Overexpression of ELF4 (ELF4-ox) lengthened the period of *LHY::LUC* (Fig. 1e and Extended Data Fig. 1k), indicating that increased ELF4 activity in roots slows the clock. The expression of *PSEUDO RESPONSE REGULATOR 9* (*PRR9*), a previously described direct target of the evening complex in shoots, was upregulated in *elf4-1* mutant roots (Fig. 1f), suggesting that the evening complex also represses *PRR9* in roots. Thus, ELF4 has an important regulatory function in the root clock: mutation compromises rhythms, whereas overexpression lengthens the circadian period.

RNA-sequencing (RNA-seq) analyses of WT and *elf4-1* mutant roots provided a genome-wide view of ELF4 function in roots (Supplementary Table 1). We found that about 15% of the root genes were significantly misregulated in the absence of a functional ELF4, with a similar proportion of upregulated (1,297) and downregulated (1,555) genes (Fig. 1g,h and Extended Data Fig. 2a). The expression of core clock genes was among the most significantly misregulated (Fig. 1i and Extended Data Fig. 2b–i), with a substantial fraction of the misregulated genes being controlled by the clock, with phase enrichments during the subjective morning and subjective midday (Fig. 1j,k). Functional analyses showed that in addition to the enrichment of genes related to the circadian system and rhythmic processes, genes misexpressed in the *elf4-1* mutant were ascribed to several functional categories, including, among others, 'responses to stimuli' (Supplementary Table 1). Consistently, misexpression of ELF4 affected physiological outputs such as the number of lateral roots (Extended Data Fig. 2j). Together, the results indicate a prevalent function for ELF4 in sustaining rhythms in roots.

ELF4 moves from shoots to regulate oscillator gene expression in roots. Our previous study showed that a signal from shoots is important for circadian rhythms in roots[47]. Micrografting assays are a powerful tool to identify the nature of mobile signals. The grafting technique per se does not alter the rhythms in roots[47], as grafted WT scions into WT roots show similar rhythms as non-grafted WT plants (Extended Data Fig. 3a,b). By micrografting different genotypes, we found that grafts of ELF4-ox shoots into *elf4-1* rootstocks (ELF4-ox (Sh)/*elf4-1* (Rt)) (Extended Data Fig. 3c) were particularly efficient in recovering the rhythms in roots (Fig. 2a and Extended Data Fig. 3d). The results are noteworthy, as *CCA1::LUC* rhythms are affected in *elf4-1* mutant roots (Fig. 1d). Restoration of the rhythms reflected circadian function exclusively in roots, as water instead of luciferin was applied to shoots (ELF4-ox, Sh, H_2O) to avoid luminescence signals leaking from shoots into roots of adjacent wells. Rhythms in roots were also recovered when ELF4-ox scion was grafted into *elf4-2* mutant (Extended Data Fig. 3e) rootstocks (Fig. 2b). To exclude the possibility that the observed results were due to the high overexpression in ELF4-ox plants, we grafted WT shoots into *elf4-1* roots. Although the recovery of the rhythms was not as robust as with ELF4-ox grafts, a rhythmic pattern was observed in roots (Fig. 2c). Thus, ELF4 mRNA or protein is able to move from shoots to roots. This notion was reinforced by results showing the rhythmic recovery of *elf4-1* rootstocks grafted with ELF4 minigene scion (Fig. 2d and Extended Data Fig. 3f). These results rule out the possibility that the recovery of the rhythms was solely a result of the high overexpression of ELF4-ox scion. The influence of shoots as a driving rhythmic force of *elf4-1* rootstocks was also analysed mathematically with recurrence plots obtained by delay coordinates of the grafting time series. The waveforms of the driving rhythmic force reconstructed from the driven system and their autocorrelation analyses showed a strong periodicity after grafting (Extended Data Fig. 4a–h). We performed analyses with 10,000 randomly shuffled surrogates using a null hypothesis of no serial dependence; we obtained a P value of 0.2341 before grafting (black dashed line) (Extended Data Fig. 4f) and 0.0004 (grey dashed line) after grafting (Extended Data Fig. 4h). The statistics are therefore consistent with the notion that rhythms in roots are being forced by a signal from shoots.

To investigate whether the mRNA is the mobile signal, we performed RT–qPCR time-course analyses of roots from ELF4-ox (Sh)/*elf4-1* (Rt) grafts. Our results showed no detectable amplification of *ELF4* mRNA at any time point analysed (Fig. 2e), which suggests that *ELF4* mRNA did not move through the graft junctions. To confirm this notion, we injected purified ELF4 protein into *elf4-1* mutant (Extended Data Fig. 5a–c). Injection of ELF4 into shoots was able to restore rhythms in roots (Fig. 2f). The percentage of plants injected with ELF4 that recovered rhythms was low (5–8%) but the rhythmic recovery was observed reproducibly in different biological replicates. The restoration of root rhythms (relative amplitude error < 0.6) supports the notion that ELF4 protein moves from shoots to roots. Rhythmic recovery was not apparent when purified green fluorescent protein (GFP) was injected instead of ELF4 (Fig. 2f). The movement of ELF4 protein was further assayed by using shoots of plants overexpressing ELF4–GFP grafted into *elf4-1* mutant roots. Confocal imaging showed that ELF4–GFP fluorescent signals accumulated in the vasculature of *elf4-1* mutant rootstock, across the graft junctions (Fig. 2g,h and Extended Data Fig. 5d,e). Furthermore, western blot analyses of roots from ELF4–GFP (Sh)/*elf4-1* (Rt) grafts detected ELF4 protein as a band of the expected size (arrows in Fig. 2i) that was absent from protein extracts of *elf4-1* mutant roots (Fig. 2i). Grafting ELF4-ox fused to three GFPs (ELF4–3×GFP) scion into *elf4-2* mutant rootstock did not lead to an obvious recovery of rhythms (Fig. 2j and Extended Data Fig. 5f), suggesting that a mobile ELF4 protein is required. The ELF4–3×GFP is still functional, as its overexpression in the *elf4-1* mutant background restored the hypocotyl phenotypes of *elf4-1* mutant plants (Extended Data Fig. 5g) and repressed *PRR9* gene expression (Extended Data Fig. 5h, i). The functional relevance of ELF4 movement was also verified in *elf4-1* (Sh)/*elf4-1* (Rt) grafts, in which roots did not recover rhythms (Extended Data Fig. 5j,k). Therefore, multiple lines of evidence, including the ELF4 injection data, the grafting assays showing the recovery of the rhythms, the ELF4–GFP fluorescent signals across graft junctions, the detection of ELF4 protein in roots of the grafted plants, the lack of rhythmic recovery in roots of ELF4–3×GFP grafts and in *elf4-1* scion grafts, support the notion that ELF4 protein moves from shoots to regulate rhythms in roots. Other mobile proteins such as FLOWERING LOCUS T (FT) and LONG HYPOCOTYL 5 (HY5) share features with ELF4 protein in terms of low molecular weight and high isoelectric point (Fig. 2k).

Blocking ELF4 movement by shoot excision alters circadian rhythms in roots. We next aimed to identify the function of the mobile ELF4 by blocking ELF4 movement via shoot excision. Analyses of the rhythms showed that excised roots sustained robust oscillations (Extended Data Fig. 6a,b) confirming that the root clock is able to run in the absence of shoots. However, comparison of intact versus excised roots uncovered a shorter period in excised roots (Extended Data Fig. 6c,d). As accumulation of ELF4 results in long periods in shoots[22] and roots (Fig. 1e and Extended Data Fig. 1k), it is plausible that blocking ELF4 movement by shoot excision results in shorter periods in excised roots. If this is the case, blocking ELF4 movement should also affect ELF4 target-gene expression in excised roots. Time-course analyses by RT–qPCR revealed that the expression of *PRR9* and *PRR7* was upregulated in excised roots compared with intact roots (Extended Data Fig. 6e,f), which suggests that in the absence of ELF4 movement from shoots, repression of these genes is alleviated in roots. The use of ELF4-ox intact roots confirmed that *PRR9* and *PRR7* are targets of ELF4, as their expression was downregulated in intact ELF4-ox roots compared with WT intact roots (Extended Data Fig. 6g,h). Furthermore,

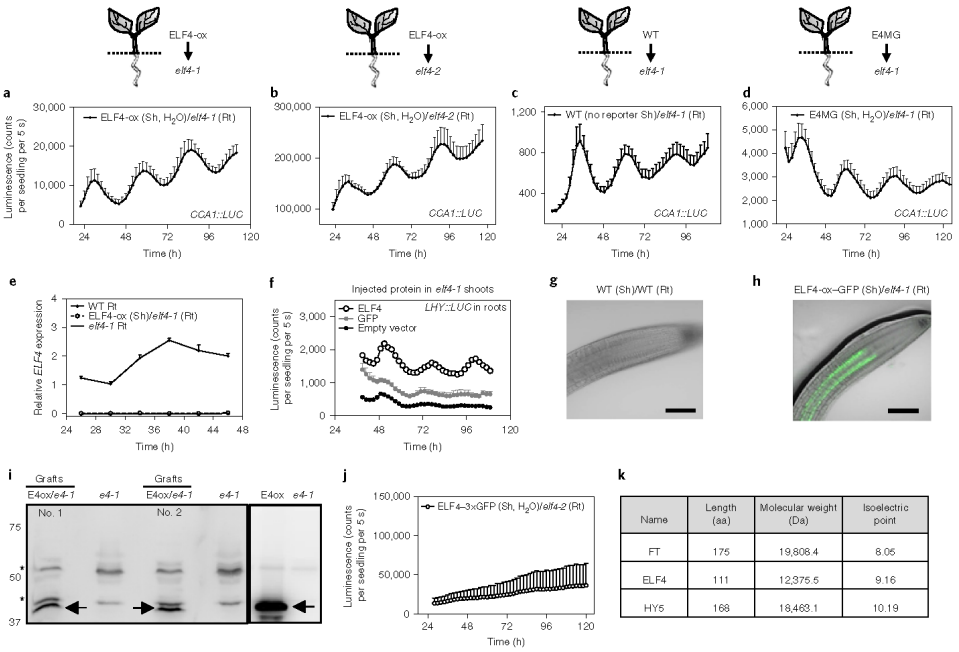

Name	Length (aa)	Molecular weight (Da)	Isoelectric point
FT	175	19,808.4	8.05
ELF4	111	12,375.5	9.16
HY5	168	18,463.1	10.19

Fig. 2 | ELF4 moves from shoots to regulate rhythms in roots. a,**b**, *CCA1::LUC* luminescence in roots of WT, ELF4-ox and ELF4 minigene (E4MG) scion grafts with *elf4-1* (**a**; $n=4$) and *elf4-2* (**b**; $n=3$) rootstocks. Water was added instead of luciferin to wells containing ELF4-ox shoots. **c**,**d**, *CCA1::LUC* luminescence in *elf4-1* rootstocks grafted with WT (**c**; $n=8$) and E4MG (**d**; $n=10$) scions. WT scions do not express reporters; water was added instead of luciferin to wells containing E4MG shoots. In **a**–**d**, schematics depict the different scion–rootstock combinations. **e**, Circadian time-course analyses of *ELF4* mRNA expression in roots of WT, *elf4-1* and ELF4-ox scion and *elf4-1* rootstocks. **f**, Luminescence of *LHY::LUC* rhythms in *elf4-1* roots after injection in shoots of purified ELF4 ($n=4$) or GFP ($n=8$) proteins, and *elf4-1* roots as a control ($n=6$). **g**, Representative image showing the lack of fluorescence signals in roots of WT scion grafts with WT rootstock. Scale bar, 100 µm. **h**, Representative image showing fluorescence signals in roots of ELF4-ox scion grafts with *elf4-1* rootstock. Scale bar, 100 µm. **i**, Western blot analysis of ELF4–GFP protein accumulation (arrows) in roots of ELF4-ox–GFP scion (E4ox) grafts with *elf4-1* rootstock (*e4-1*) (two pools of independent grafting assays—no. 1 and no. 2—are shown). Asterisks denote non-specific bands. **j**, *CCA1::LUC* luminescence in *elf4-2* rootstocks grafts with ELF4–3×GFP scions ($n=5$). Water was added instead of luciferin to wells containing ELF4–3×GFP shoots. In **a**–**f**,**j**, data are mean + s.e.m. **k**, Protein features of various plant mobile proteins. *n* refers to the number of independent samples. aa, amino acids. In **a**–**j**, two biological replicates were performed for all experiments, with measurements taken from independent samples grown and processed at different times.

ELF4-ox excised roots still showed repression of target-gene expression (Extended Data Fig. 6i,j) suggesting that excision per se is not responsible for the upregulation observed in WT excised roots.

To further reveal the function of ELF4 movement, we performed RNA-seq analyses of WT intact versus excised roots. Our results showed that, as expected, a substantial fraction of genes was affected by excision (Supplementary Table 2). Comparative analyses of *elf4-1* intact roots with WT excised roots enabled us to distinguish between effects due to excision from those due to the lack of ELF4 movement (Extended Data Fig. 7). Indeed, we focused on the differentially expressed genes (DEGs) present in both excised WT and intact *elf4-1* roots. As *elf4-1* mutant roots are intact, the overlapping DEGs are not affected by excision per se, but rather by the lack of ELF4 movement from shoots, which is shared by *elf4-1* intact roots and WT excised roots. Our comparative analyses of both datasets revealed that 67% of the DEGs in *elf4-1* intact roots were also differentially expressed in WT excised roots (Extended Data Fig. 7 and Supplementary Table 3). The proportion of overlapping DEGs (67%) is highly significant ($P<0.0001$, χ^2-test for equality of proportions) compared with the proportion of overlapping genes (26%) using a random gene list. The overlap is noteworthy due to the different genotypes (*elf4-1* mutant versus WT), and most notably, the different conditions (intact versus excised). As WT excised roots and *elf4-1* intact roots both lack of ELF4 movement from shoots, the overlapping DEGs provides the genes that directly or indirectly require ELF4 movement for proper expression in roots. Consistently, the overlapping DEGs included nearly all of the core oscillator genes (Extended Data Fig. 6k and Supplementary Table 3). A significant fraction of overlapping DEGs also exhibited circadian oscillation with phase enrichments during the subjective morning and subjective midday (Extended Data Fig. 6l). Therefore, ELF4 movement appears to be important for a fully functional clock in roots.

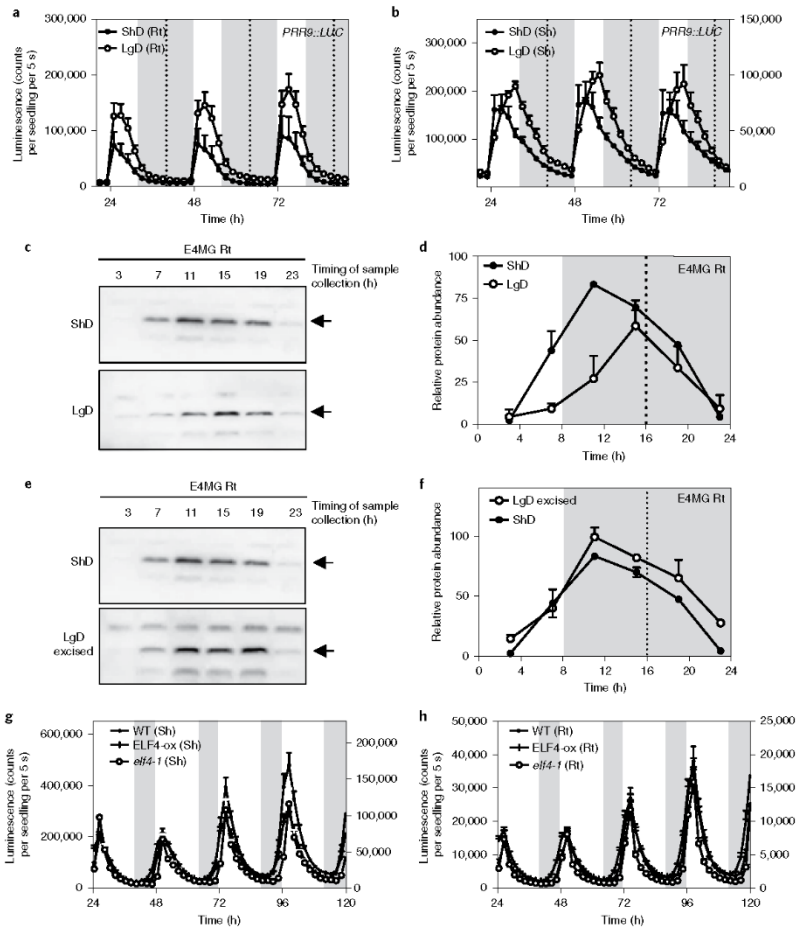

Fig. 3 | Mobile ELF4 does not regulate the photoperiod-dependent phase in roots. a,**b**, Luminescence analyses of *PRR9::LUC* rhythms in roots (**a**; $n=5$ for ShD, $n=6$ for LgD) and shoots (**b**; $n=6$ for ShD, $n=4$ for LgD) of plants grown under ShD or LgD conditions. Shaded areas indicate dark periods. **c**,**d**, Western blot analyses (**c**) and quantification (**d**) of ELF4 protein accumulation in ELF4 minigene roots (E4MG Rt) of plants grown under ShD and LgD (also in Extended Data Fig. 8a–d). **e**,**f**, Western blot analyses (**e**) and quantification (**f**) of ELF4 protein accumulation in ELF4 minigene (E4MG) roots of plants grown under ShD and excised roots grown under LgD (also in Extended Data Fig. 8a–f). In **c**–**f**, Arrows indicate the ELF4 protein. **g**,**h**, Luminescence of *LHY::LUC* oscillation in WT, ELF4-ox and *elf4-1* plants measured in shoots (**g**; $n=12$) and roots (**h**; $n=12$) under LgD conditions. In **a**,**b**,**d**,**f**–**h**, data are mean + s.e.m. Dashed lines indicate dusk under LgD. *n* refers to the number of independent samples. In **a**–**h**, two biological replicates were performed for all experiments, with measurements taken from independent samples grown and processed at different times.

Mobile ELF4 does not regulate the photoperiod-dependent phase in roots. In aerial tissues, the circadian clock controls the photoperiodic regulation of growth and development[20]. To determine whether ELF4 movement is important to deliver photoperiodic information, we analysed rhythms under short day (ShD) and long day (LgD) conditions. In roots, *PRR9::LUC* waveforms displayed a subtle phase delay under LgD compared to ShD (Fig. 3a) following a similar trend to that observed in shoots (Fig. 3b). Time-course analyses by western blot of roots of ELF4 minigene plants[30] confirmed the phase delay of ELF4 protein accumulation under LgD compared with ShD (Fig. 3c,d). We reasoned that if ELF4 movement is correlated with the photoperiodic-dependent phase delay, then excision of shoots might affect the phase shift in roots. In agreement with the oscillations in promoter activity (Extended Data Fig. 6c,d), the phase of ELF4 protein accumulation was advanced following excision under both LgD and ShD (Extended Data Fig. 8a–d).

Of note, under LgD conditions, excision resulted in a similar pattern of ELF4 accumulation than in intact roots under ShD (Fig. 3e,f). Thus, excision abolished the phase delay observed in intact root under LgD (compare Fig. 3c,d with Fig. 3e,f). The results suggest that the photoperiod-dependent phase shift in roots is hampered by blocking ELF4 movement. However, excised roots still showed the phase delay under LgD compared with excised roots under ShD (Extended Data Fig. 8e,f). Furthermore, analyses of rhythms under LgD conditions showed that plants misexpressing ELF4 (ELF4-ox and *elf4-1* mutant) displayed very similar rhythms to WT plants both in shoots and roots (Fig. 3g,h) suggesting that ELF4 function is not essential to sustain rhythms under entraining conditions. Together, the results suggest that blocking ELF4 movement by excision advances the phase of the root clock, but the mobile ELF4 does not directly regulate the photoperiod-dependent phase shift in roots.

ELF4 movement contributes to the temperature-dependent changes in circadian period of the root clock. As the evening complex also coordinates temperature responses, we examined whether a mobile ELF4 can convey temperature information from shoots to roots. We first examined the effect of different temperatures (28 °C, 18 °C and 12 °C) on circadian rhythms in roots. We found that the circadian period of *LHY::LUC* was shorter at higher temperatures (Extended Data Fig. 9a,b). Shortening of period length with increasing temperature was also observed for other circadian reporter lines (Extended Data Fig. 9c–f), indicating that at this developmental stage and under our experimental conditions, the circadian clock in roots is not able to sustain circadian period length within a range of temperatures.

As ELF4 accumulation increases period length, we next examined the possible contribution of ELF4 to the long period phenotype at low temperatures. Changes in period length could be mediated by increased ELF4 activity and/or by increased protein movement from shoots to roots. To examine these possibilities, we compared the effects of blocking ELF4 movement by excision at low and high temperatures. Essentially, if the long period in roots at 12 °C is independent of movement but results from the increased activity of ELF4, blocking movement from shoots by excision should not have a major effect on period length. However, if ELF4 movement contributes to the period regulation, abolishing ELF4 traffic should lead to an observable and differential effect on period length at different temperatures.

Our results showed that excision shortened the period length at 12 °C but not so markedly at 28 °C (Extended Data Fig. 10a–d). Therefore, blocking ELF4 movement by excision shortens the period of WT roots at 12 °C. Analyses of other circadian reporter lines and at 18 °C also showed that excision shortened period length compared to intact roots (Extended Data Fig. 10e,f). The results suggest a temperature-dependent control of ELF4 movement that regulates period length in roots. To further verify this notion, we examined the rhythmic recovery in grafts of ELF4-ox scion into *elf4-1* rootstock at low and high temperatures. Our results showed an evident rhythmic recovery at 12 °C but not at 28 °C (Fig. 4a,b). Furthermore, grafts of E4MG scion into *elf4-1* rootstock also efficiently recovered rhythms at 12 °C but not at 28 °C (Fig. 4c,d). ELF4 was still able to delay the phase and lengthen the period at 28 °C (Fig. 4e and Extended Data Fig. 10g), suggesting that movement, rather than changes in activity, were responsible for the observed effects. ELF4 protein accumulation in roots of ELF4-ox scion into *elf4-1* rootstock was higher at 12 °C than at 28 °C (Fig. 4f and Extended Data Fig. 10h,i) but ELF4 protein accumulation in shoots was similar at different temperatures[31] (Extended Data Fig. 10j). Therefore, ELF4 movement, rather than protein accumulation or activity, appears to be regulated by temperature, contributing to the temperature-dependent control of circadian period in roots.

We propose a model by which mobile ELF4 (MbE4) from shoots to roots defines a pool of active ELF4 protein that is competent to repress target circadian gene expression in roots. ELF4 trafficking is favoured at low temperatures, resulting in a slow-paced clock (Fig. 4g), whereas high temperatures decrease the movement, leading to a faster root clock (Fig. 4h). The temperature-dependent movement of ELF4 enables a shoot-to-root dialogue that controls the pace of the clock and provides a mechanism by which temperature cues from shoots set the circadian period length in roots.

Discussion

The simultaneous examination of rhythms in shoots and roots of single individual plants shows that the promoter activities and mRNA accumulation of clock genes in roots display a longer period and delayed phase compared with shoots. A similar trend was observed for morning- and evening-expressed key oscillator genes, suggesting that the overall circadian system in roots is not as precise as in other parts of the plant (for example, the shoot apex)[47]. Despite the long period, the rhythms persist in roots for several days under constant light conditions, which is reminiscent of a fully functional clock. The lack of precision might provide circadian flexibility for rapid adjustments and improved responses in roots. Previous studies have reported spatial waves of clock gene expression within and among different organs[40,42,45] that might be due to differences in period length and variable local coupling.

The evening complex directly represses the expression of *PRR9* and *PRR7*[19,23,29,51,52] and indirectly promotes the expression of the morning-expressed oscillator genes *CCA1* and *LHY*[51–54]. Our analyses with *elf4-1* mutant and ELF4-ox plants demonstrate that ELF4 function in roots is also important for proper repression of *PRR9* and *PRR7* and activation of *CCA1* and *LHY*. ELF4 regulatory function in roots appears to be similar to that previously described for the evening complex using whole plants. Overexpression of ELF4 lengthens the period of the root clock, suggesting that ELF4 slows the circadian period in roots, as in shoots[22]. The lengthening of the period on accumulation of ELF4 is in agreement with the results showing that blocking ELF4 movement by shoot excision shortens the period. RNA-seq analyses revealed that the expression of oscillator genes as well as genes involved in other pathways, including responses to stimuli are affected in *elf4-1* roots. These pathways are also consistent with the function of the evening complex in responses to environmental cues[55]. The misregulated genes in *elf4-1* roots might be direct targets of ELF4 and/or indirect outputs of the clock in roots. One of these outputs might be lateral root emergence, as the number of lateral roots is affected in *elf4-1* and ELF4-ox plants compared with WT plants. Future studies are necessary to uncover the molecular and cellular mechanisms by which ELF4 regulates the number of lateral roots in *Arabidopsis*.

Micrografts of ELF4-ox scion into *elf4-1* or *elf4-2* rootstocks enable a recovery of rhythms that is not observed when seedlings expressing ELF4–3×GFP are used as scion. These results suggest that ELF4 movement is indeed important for the rhythmic recovery. Fluorescent signals accumulating in the vasculature of *elf4-1* mutant rootstock grafted with ELF4–GFP scion and the detection of the ELF4 protein in roots of the micrografted plants also suggest that ELF4 moves from shoots to roots. This conclusion is complemented by the grafting assays of *elf4-1* (Sh)/*elf4-1* (Rt) showing the lack of rhythmic recovery in roots, and by ELF4 protein-injection assays in shoots and the subsequent rhythmic recovery in roots. Micrografts of E4MG and WT plants are also able to recover the rhythms of the *elf4-1* mutant roots, indicating that the effects are not due to excess accumulation of ELF4-ox. The results suggest that small amounts of mobile ELF4 might be required to regulate the rhythms. Our experiments in which we added water to the scion or used WT scion without LUC reporter exclude the possibility that rhythms in grafted roots are due to leakage from the adjacent well containing the shoot.

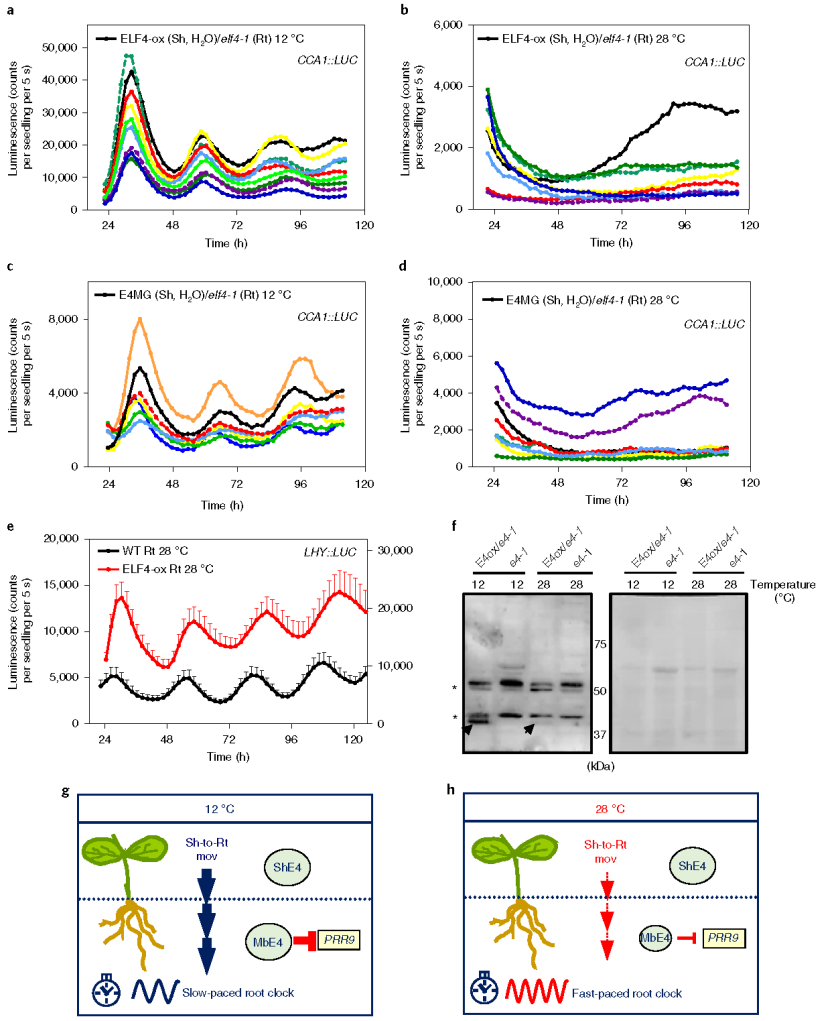

Fig. 4 | Mobile ELF4 sets the temperature-dependent pace of the root clock. a,**b**, Individual luminescence waveforms of *CCA1::LUC* rhythmic oscillation in ELF4-ox scion into *elf4-1* rootstocks at 12 °C (**a**; $n=10$) and 28 °C (**b**; $n=8$). **c**,**d**, Individual luminescence waveforms of *CCA1::LUC* rhythmic oscillation in E4MG scion into *elf4-1* rootstocks at 12 °C (**c**; $n=7$) and 28 °C (**d**; $n=8$). Water was added instead of luciferin to wells containing ELF4-ox and E4MG scions. **e**, Luminescence of *LHY::LUC* rhythmic oscillation in WT and ELF4-ox roots at 28 °C ($n=8$ for WT, $n=5$ for ELF4-ox). Data are mean + s.e.m. **f**, Left: western blot analysis of ELF4–GFP protein accumulation (arrows) in roots of ELF4-ox–GFP scion (E4ox) grafted into *elf4-1* rootstock (*e4-1*) at 12 °C and 28 °C. *elf4-1* mutant protein extracts were used as a control. Asterisks denote non-specific bands. Right: Ponceau S staining of the membrane. **g**,**h**, Schematic of the increased shoot-to-root movement of ELF4 (Sh-to-Rt mov; thick blue vertical arrows) increased *PRR9* repression and the slow pace of the root clock at low temperatures (**g**), and the decreased shoot-to-root movement (thin red vertical arrows) decreased *PRR9* repression and fast-paced root clock at high temperature (**h**). *n* refers to the number of independent samples. In **a**–**f**, Two biological replicates were performed for all experiments, with measurements taken from independent samples grown and processed at different times.

ELF4 protein shows similar properties in terms of length, molecular weight and isoelectric point to other mobile proteins[55–59], which also supports the notion of ELF4 movement. We postulate that following movement, the complex regulatory feedback loops at the core of the oscillator are reset to control the pace of the clock. Further experiments at different developmental stages and under various growing

conditions (for example, different light and temperature conditions) will be required to confirm whether the long-distance movement of ELF4 contributes to the spatial waves of clock gene expression observed in roots[42].

Excision blocks ELF4 movement from shoots and consequently, we observe that oscillator gene expression and other output genes are affected in WT excised roots. Previous studies have also used excision to define properties of the circadian function in roots[42]. Although many genes are affected by excision, it is noteworthy that 67% of the genes misregulated in *elf4-1* intact roots are also misexpressed in WT excised roots. Both conditions have in common a lack of ELF4 movement, suggesting that the overlapping DEGs are due to the lack of mobile ELF4 (note that the RNA-seq studies with *elf4-1* mutant were performed with intact roots). The phase shifts observed following excision prompted us to examine whether ELF4 movement contributed to the photoperiodic-dependent phase shift. However, excised roots still sustained the phase delay under LgD, suggesting that other factors are responsible for this regulation. Light piping down the root[49] might be also important for synchronization. Regardless the mechanism, it is able to overcome the misexpression of ELF4 in shoots and roots, as ELF4-ox and *elf4-1* mutant plants displayed similar rhythms to WT. Clear alteration of circadian expression under contant light but not under entraining conditions has been reported for other clock mutant plants and plants overexpressing clock genes[60].

Evening complex activity is downregulated at high temperatures in whole seedlings[29,31]. Shoot excision shortened the period, suggesting that ELF4 movement is important in the control of circadian period length. Period shortening is more significant at low temperatures than at high temperatures, confirming that ELF4 movement is favoured at low temperatures. The temperature-dependent control of ELF4 movement is also supported by the increased accumulation of ELF4 protein in grafted roots at 12 °C compared to 28 °C. As ELF4 accumulation results in a longer period, the increased movement leads to a clock that runs slower at low temperatures than at high temperatures. It would be interesting to elucidate whether period sensitivity to temperature might provide an advantage for optimal root responsiveness to temperature variations.

Methods

Plant material, growth conditions, constructs and physiological assays. *A. thaliana* seedlings were stratified at 4 °C in the dark for 2–3 d on Murashige and Skoog agar medium with 3% sucrose (MS3). Plates were transferred to chambers with controlled light and temperature conditions with 25–50 μmol m^{-2} s^{-1} of cool-white fluorescent light. Seedlings were synchronized under 12:12 h light:dark cycles at 22 °C. For experiments with different temperatures, seedlings were analysed under constant light conditions at 12 °C, 18 °C, 22 °C or 28 °C following synchronization under 12:12 h light:dark cycles at 22 °C. For experiments with different photoperiods, seedlings were grown under ShD (8:16 h light:dark) or LgD (16:8 h light:dark) conditions. Reporter lines *CCA1::LUC*[61], *LHY::LUC*[59], *PRR9::LUC*[62], *TOC1::LUC*[6] and *elf4-1*[17], *elf4-2*[17], ELF4 minigene[20] and ELF4–GFP-ox[19,20] plants have been described elsewhere. The ELF4–3×GFP construct was generated by PCR amplification of the *ELF4* coding sequence and subsequent subcloning into the PGWB514 gateway vector[63,64]. The resulting plasmid was digested with PacI and SacI restriction enzymes and ligated with the 3×GFP insert from the pBS-x3GFP vector (Addgene). The construct was transformed into *elf4-1* mutant plants. Plants were transformed using *Agrobacterium tumefaciens* (GV2260)-mediated DNA transfer[65]. For in vitro protein-injection assays, the ELF4 coding sequence was subcloned into the pET MBP_1a vector (Novagen) after removing the GFP by digestion with NcoI and XhoI.

For lateral root analyses, WT, *elf4-1* and ELF4-ox seeds were surface-sterilized and plated onto Murashige and Skoog medium supplemented with 0.25% w/v sucrose and 1.5% agar. The top quarter of the agar was removed and seeds were pipetted evenly along this line. Plants were then grown vertically for 12 d before lateral roots were measured. Lateral roots were manually counted using a Nikon SMZ800 dissecting microscope. Statistical analysis was completed using R (v.3.6), within R Studio (v.1.1.4). For hypocotyl elongation measurements, WT, *elf4-1*, ELF4–GFP-ox and ELF4–3×GFP-ox seeds transformed into the *elf4-1* mutant background were stratified on MS3 medium in the dark for 4 d at 4 °C, exposed to white light (40 μmol m^{-2} s^{-1}) for 6 h and maintained in the dark (22 °C) for 18 h before transferring to chambers under ShD conditions. Hypocotyl length was measured using ImageJ (v.1.48 v) (https://imagej.nih.gov/ij/) 7 d after stratification. Each experiment was repeated at least twice using 20–50 seedlings per genotype. Statistical analyses were performed using GraphPad Prism (v.5.01) using two-tailed *t*-tests with 95% confidence interval.

In vivo luminescence assays. In vivo luminescence assays were performed as previously described[47]. In brief, 7- to 15-d-old seedlings synchronized under light:dark cycles at 22 °C were transferred to 96-well plates and released into the different conditions specific for each experiment. Analyses were performed with a LB960 luminometer (Berthold Technologies) using Microwin (v.4.41; Mikrotek Laborsysteme). The period, phase and amplitude were estimated using the fast Fourier transform–non-linear least squares (FFT-NLLS) suite 63[66] using the biological rhythms analysis software system (BRASS; v.3.0; http://www.amillar.org). For simultaneous analysis of rhythms of shoots and roots from the same plant, the connection between the two adjacent wells of the 96-well plates was serrated. Seedlings were then horizontally positioned so the shoot was placed in one well and the roots were placed in the contiguous well. For excision analyses, roots were excised from shoots and placed into the 96-well plates for luminescence analyses. Data from samples that appeared damaged or contaminated were excluded from the analysis. For analyses of grafted samples, water was applied instead of luciferin to the wells containing shoots to avoid possible leaking signals from shoots to roots, as specified. At least two biological replicates were performed per experiment, with measurements taken from independent samples grown and processed at different times. Each biological replicate included 6 to 12 independent seedlings per condition and/or genotype. Statistical analyses were performed using GraphPad Prism (v.5.01) using two-tailed *t*-tests with 95% confidence interval.

Protein purification and injection analyses. *Escherichia coli* cells (BL21, Dh5α) were transformed and grown in LB medium (10 g l^{-1} tryptone, 5 g l^{-1} yeast extract and 10 g l^{-1} NaCl, pH 7.5) until optical density (OD_{600}) values of 0.8–1.0. Isopropyl-β-D-1-thiogalactopyranoside (IPTG)-mediated induction of maltose-binding protein (MBP)–ELF4 and MBP–GFP was performed at 28 °C for 6 h. Bacteria resuspended in lysis buffer (50 mM Tris-HCl, pH 7–8, 5% glycerol, 50 mM NaCl) were lysed by sonication for 2–3 min (30 s on, 30 s off, high intensity) using a sonicator (Bioruptor, Diagnode). Recombinant proteins were purified using gravity-flow columns with amylose resin (New England Biolabs). MBP cleavage was performed by incubation in cleavage buffer (50 mM Trizma-HCl, pH 8.0, 0.5 mM EDTA, and 1 mM DTT) for 2 h at 30 °C with native tobacco etch virus protease (Sigma-Aldrich). The purified recombinant proteins were concentrated using Amicon centrifugal filters (Millipore) following the manufacturer's recommendations. Protein yield was estimated by measuring absorbance at 595 nm using a spectrophotometer (UV-2600, Shimadzu). Proteins were also examined by Coomassie brilliant blue staining of polyacrylamide gels to confirm protein size and integrity. Purified ELF4 was injected into leaves of 10 d old *elf4-1* mutant seedlings harbouring the *LHY::LUC* reporter line. Similar concentration of GFP protein was also injected as a negative control. Rhythms were subsequently examined in a LB960 luminometer (Berthold Technologies) as described above.

Time-course analyses of gene expression by RT–qPCR. Seedlings were synchronized under light:dark cycles in MS3 medium plates for 12–14 d and subsequently transferred to constant light. Shoots and roots from intact plants were taken every 4 h over the circadian cycle. For excised roots, shoots and roots were carefully separated with a sterile razor blade and the excised roots were deposited on MS3 agar medium plates for 2 or 3 d as specified. RNA was purified using a Maxwell RSC Plant RNA kit (Promega) following the manufacturer's recommendations. Single-stranded cDNA was synthesized using iScript Reverse Transcription Supermix for RT–qPCR (Bio-Rad). qPCR analyses were performed with cDNAs diluted 50-fold with nuclease-free water using Brilliant III Ultra-Fast SYBR Green qPCR Master Mix (Agilent) with a 96-well CFX96 Touch Real-Time PCR detection system (Bio-RAD CFX96 Manager v.3.1, Bio-Rad). Each sample was run in technical triplicates. The expression of *PP2AA3* (*PROTEIN PHOSPHATASE 2A SUBUNIT A3*, AT1G13320) or *MON1* (*MONENSIN SENSITIVITY1*, AT2G28390)[67] was used as a control. Crossing point (Cp) calculation was used for quantification using absolute quantification analysis by the second-derivative maximum method. At least two biological replicates were performed, with measurements taken from independent samples grown and processed at different times.

RNA-seq analyses. Roots from 14-d-old intact WT, *elf4-1* mutant and excised WT plants synchronized under light:dark cycles in MS3 medium plates were transferred to constant light conditions for 3 d. Roots were excised just before transferring to constant light. Samples were collected on the fourth day under constant light at circadian time 75 (CT75). Total RNA was isolated using a Maxwell RSC Plant RNA kit. RNA sequencing was performed by IGATech. About 1–2 μg of high quality RNA (RNA integrity number > 7) was used for library preparation with a TruSeq Stranded mRNA Sample Prep kit (Illumina). Poly-A mRNA was fragmented for 3 min at 94 °C. Purification was performed with 0.8× Agencourt AMPure XP beads. RNA samples and final libraries were quantified using the Qubit 2.0 Fluorometer (Invitrogen). Quality was tested using the Agilent 2100

Table 1 | List of primers

Name	Sequence	Experiment
REF1(PP2A_A3)_EXP_F	AAGCGGTTGTGGAGAACATGATACG	Expression analysis
REF1(PP2A_A3)_EXP_R	TGGAGAGCTTGATTTGCGAAATACCG	Expression analysis
MON1_EXP_F	AACTCTATGCAGCATTTGATCCACT	Expression analysis
MON1_EXP_R	TGATTGCATATCTTTATCGCCATC	Expression analysis
PRR7_EXP_F	AAGTAGTGATGGGAGTGGCG	Expression analysis
PRR7_EXP_R	GAGATACCGCTCGTGGACTG	Expression analysis
PRR9_EXP_F	ACCAATGAGGGGATTGCTGG	Expression analysis
PRR9_EXP_R	TGCAGCTTCTCTCTGGCTTC	Expression analysis
ELF4_EXP_F	GACAATCACCAATCGAGAAT	Expression analysis
ELF4_EXP_R	ATGTTTCCGTTGAGTTCTTG	Expression analysis
CCA1_EXP_F	TCGAAAGACGGGAAGTGGAACG	Expression analysis
CCA1_EXP_R	GTCGATCTTCATTGGCCATCTCAG	Expression analysis
LHY_EXP_F	AAGTCTCCGAAGAGGGTCGT	Expression analysis
LHY_EXP_R	GGCGAAAAGCTTTGAGGCAA	Expression analysis
ELF4_CLN_F	CACCATGAAGAGGAACGGCGA	Cloning
ELF4_CLN_R	AGCTCTAGTTCCGGCAGCACCA	Cloning
MBP-ELF4_CLN_F	CATGCCATGGGCATGAAGAGGAACGGCGAG	Cloning
MBP-ELF4_CLN_R	CCGCTCGAGTTAAGCTCTAGTTCCGGCAGCAC	Cloning
PacI-pBS3xGFP-F	GGTTAATTAACGCTGGAGGATCCATGTCTA	Generation of pGWB-c3xGFP
SacI-pBS3xGFP-R	TCGAGCTCTCTAGAACTAGTGGATCTTTA	Generation of pGWB-c3xGFP

Bioanalyzer RNA Nano assay (Agilent). Libraries were then processed with Illumina cBot for cluster generation on the flow cell, following the manufacturer's instructions, and sequenced in paired-end mode at the multiplexing level requested on HiSeq2500 (Illumina). CASAVA (v.1.8.2) in the Illumina pipeline was used to process raw data for both format conversion and de-multiplexing.

Sequence analysis was performed using AIR software (v.1.0) (Sequentia Biotech). In brief, raw sequence files were first subjected to quality control analysis using FastQC (v.0.10.1) before trimming and removal of adapters with BBDuk (https://jgi.doe.gov/data-and-tools/bbtools/). Reads were then mapped against the *A. thaliana* genome (TAIR10 Genome Release) with STAR (v.2.6)[68]. FeatureCounts (v.1.6.1)[69] was then used to obtain raw expression counts for each annotated gene. The differential-expression analysis was conducted with edgeR (v.3.18.1)[70] using the TMM normalization method. Fragments per kilobase of transcript per million mapped reads (FPKM) were obtained with edgeR.

The Integrative Genomics Viewer (v.2.4.13) (https://software.broadinstitute.org/software/igv/) was used to visualize the data[71,72]. The circadian phases were analysed using the publicly available Gene Phase Analysis Tool 'PHASER' from the DIURNAL database (http://diurnal.mocklerlab.org/)[73,74]. Phase overrepresentation is calculated as the number of genes with a given phase divided by the total number of genes over the number of genes called rhythmic and divided by the total number of genes in the dataset. Functional categories of the DEGs were obtained using the web tool BIOMAPS (VirtualPlant, v.1.3)[75], which renders overrepresented and significant functional terms (Gene Ontology or MIPS) compared with the frequency of the term in the whole genome.

Western blot assays. Approximately 50–100 mg of roots from plants grown under the specified photoperiodic condition were sampled every 4 h over a 24 h cycle. Samples were rapidly frozen with liquid nitrogen and grounded with stainless steel beads (Millipore) in a TissueLyser II (QIAGEN). Tissue was subsequently resuspended in protein extraction buffer (50 mM Tris-HCl pH 7.5, 150 mM NaCl, 0.5% NP40, 1 mM EDTA, protease inhibitor cocktail (1:100) and PMSF (1:1,000)). Protein extracts were centrifuged at 4 °C, measured for protein concentration using Bradford reagent (Bio-Rad) and normalized to 2 mg ml^{-1} in 4× SDS loading buffer (250 mM Tris-HCl, pH 6.8, 8% SDS, 0.08% bromophenol blue and 40% glycerol). Samples were run on a 12% gel and analysed by immunoblotting, fixed 30 min with 0.4% glutaraldehyde solution (Sigma-Aldrich) and detected with a haemagglutinin (HA) antibody (Roche) (1:2,000 dilution) and a goat anti-rat horseradish peroxidase-conjugated secondary antibody (Sigma-Aldrich) (1:4,000 dilution). For analyses of the grafted plants, roots from plants synchronized under light:dark cycles were subsequently transferred to constant light for 3 d at 12 °C, 22 °C or 28 °C. Samples were collected at CT81, rapidly frozen with liquid nitrogen and grounded with stainless steel beads (Millipore) in a TissueLyser II (QIAGEN). Powder extracts were subsequently resuspended in protein extraction buffer with 100 μM MG132. Protein extracts were centrifuged at 4 °C, measured for protein concentration using Bradford reagent (Bio-Rad) and normalized to 2 μg μl^{-1} in 4× SDS loading buffer with 5 mM β-mercaptoethanol. For detection of ELF4 protein fused to GFP, samples were run on a 10% gel and detected using a GFP antibody (ab290, Abcam) (1:5,000) and goat anti-rabbit IgG (H + L chains) secondary antibody, horseradish peroxidase conjugate (Thermo Fisher Scientific, 31460 lot OG188649) (1:5,000 dilution). For detection of ELF4 protein fused to HA (ELF4 minigene) in shoots, samples were resuspended in protein extraction buffer with 100 μM MG132. Protein extracts in 4× SDS loading buffer with 5 mM β-mercaptoethanol were run on a 12% gel and analysed by immunoblotting, fixed for 30 min with 0.4% glutaraldehyde solution (Sigma-Aldrich) and detected with a HA antibody from rat IgG1 (11867423001, Sigma-Aldrich) (1:2,000) and a goat anti-rat horseradish peroxidase-conjugated secondary antibody (A9037, Sigma-Aldrich) (1:4000). Image Lab (v.5.2.1; Bio-Rad) was used to image the western blots. Membranes were stained with a Ponceau S solution following the manufacturer's recommendations (Sigma). Proteins were also run on a 10% SDS–PAGE gel and stained with Coomassie brilliant blue. At least two biological replicates were performed per experiment and/or condition, with measurements taken from independent samples grown and processed at different times.

Micrografting assays. Micrografting was performed essentially as described[47]. Data from unsuccessful grafted seedlings that failed to properly join together or grafts that were insufficiently clear to be successful were discarded. Approximately 100–150 grafting events were performed for every combination of grafts. The percentage of successfully micrografted plants was about 30–50% (possibly higher but only the clearly successful grafted plants were taken into account). From the successfully grafted plants, 30–60% showed different degrees of recovered rhythms. For in vivo luminescence assays, shoots and roots of grafted plants were simultaneously examined using the protocol described above. Water was added instead of luciferin to wells containing shoots to exclude the possibility that recovery of rhythms in roots was due to leaking signals from shoots. As specified, some grafted shoots contained no reporter.

Reconstruction of driving forces by recurrence plots. Common driving forces were estimated following a multistep procedure. Suppose that we have K simultaneous time-series measurements $\{s_i(t)|i = 1, 2, \ldots, K, t = 1, 2, \ldots, T\}$. First, we took time differences $\tilde{s}_i(t) = s_i(t+1) - s_i(t)$ $(i = 1, 2, \ldots, K, t = 1, 2, \ldots, T-1)$ of consecutive measurements and removed trends. Second, we used delay coordinates[76,77] $\vec{s}_i(t) = [\tilde{s}_i(t), \tilde{s}_i(t+1), \tilde{s}_i(t+2), \tilde{s}_i(t+3), \tilde{s}_i(t+4)]$ of five-dimensional space $(i = 1, 2, \ldots, K, t = 1, 2, \ldots, T-4)$ to obtain a recurrence plot[78]. A recurrence plot is a two-dimensional figure proposed originally for visualizing time-series data. Both axes are the same time axis. If the Euclidean distance $\|\vec{s}_i(t_1) - \vec{s}_i(t_2)\| < \varepsilon_i$, where ε_i is a threshold and $t_1, t_2 \in \{1, 2, \ldots, T-4\}$, then we plot a point at (t_1, t_2). We denote this as $R_i(t_1, t_2) = 1$. Otherwise, we do not plot a point at (t_1, t_2). We denote this state as $R_i(t_1, t_2) = 0$. We controlled the value of the threshold ε_i for each component $i \in \{1, 2, \ldots, K\}$ so that 5% of points, except

for the central diagonal line, have points plotted. Third, we took the union for the recurrence plots to infer the recurrence plot of the common driving force[79]. Namely we declare $R(t_1, t_2)=1$ if we have $R_i(t_1, t_2)=1$ for at least one of $i \in \{1, 2, \ldots, K\}$. Otherwise, we have $R(t_1, t_2)=0$. In each of the original recurrence plots, points are plotted where the driving force and the driven system are both similar. By taking their union, we can extract pairs of times where only the driving force is similar. Fourth, we applied the assumption of continuity and supplied the points at $(t, t+1)$ and $(t+1, t)$ for each i (ref. [80]). Namely, we forcefully declare $R(t, t+1)=R(t+1, t)=1$ for $t=1, 2, \ldots, T-5$. Fifth, we applied the method described[79] to convert the recurrence plot of the common driving force into time series. Here we describe the detail for this step: (1) we construct a network where each node correspond to a time point and we connect two nodes t_1 and t_2 if $R(t_1, t_2)=1$; (2) we assign a distance for each edge as $1-\frac{\#\{k-1,2,\ldots,T-4|R(k,t_1)=1 \text{ and } R(k,t_2)=1\}}{\#\{k-1,2,\ldots,T-4|R(k,t_1)=1 \text{ or } R(k,t_2)=1\}}$ (where the # symbol refers to the operator returning the number of elements in a set after the symbol #); (3) we obtain the shortest distance for each pair of nodes on this graph (this process approximates the geodesic distance between two time points); and (4) we apply the multi-dimensional scaling to convert the distance matrix to a time series. This fifth step works as the inverse transform of a recurrence plot and we can reproduce a rough shape for the original time series. This fifth step has two mathematical proofs[81,82]. Lastly, we extracted the component corresponding to the largest eigenvalue. The periodicity of the reconstructed common driving force $X(t)$ was evaluated using the autocorrelation function and 10,000 random shuffle surrogates[83], for each of which the order of time points is randomly exchanged. Here, the null hypothesis was that there was no serial dependence. The autocorrelation with time difference k is the correlation coefficient between $X(t)$ and $X(t+k)$. Thus, it is close to 1 if $X(t)$ and $X(t+k)$ are similar, and it is close to 0 if they are not related to each other. If there is a 24 h periodicity in the driving force, the autocorrelation with 24 h time difference should be a value close to 1.

Confocal imaging. For in vivo confocal imaging, the roots of WT and ELF4-ox–GFP-grafted shoots into *elf4-1* mutants were placed on microscope slides (Sigma). Fluorescent signals were imaged with an argon laser (transmissivity 40%; excitation 515 nm; emission range 530–630 nm) in a FV-1000 confocal microscope (Olympus) using FV-10-ASW4.2 Viewer Manager software (Olympus) with a 40× 1.3 numerical aperture oil-immersion objective. Image sizes were about 640×640 pixels (0.497 μm per pixel) and sampling speed was 4 μs per pixel. The results are representative of at least three biological replicates for grafting and about three to four images per grafts.

Primers. The primers used for expression analyses, cloning and generation of 3×GFP construct are shown in Table 1.

Reporting Summary. Further information on research design is available in the Nature Research Reporting Summary linked to this article.

Data availability

Data and materials generated in this study are available without restriction upon request from the corresponding author. Next-generation sequencing data are deposited in NCBI BioProject with accession code PRJNA610472 (BioSample accessions SAMN14299292, SAMN14299293 and SAMN14299294). Source data for all figures are provided with the paper.

Received: 10 May 2019; Accepted: 11 March 2020;
Published online: 13 April 2020

References

1. Zhang, E. E. & Kay, S. A. Clocks not winding down: unravelling circadian networks. *Nat. Rev. Mol. Cell Biol.* **11**, 764–776 (2010).
2. Greenham, K. & McClung, C. R. Integrating circadian dynamics with physiological processes in plants. *Nat. Rev. Genet.* **16**, 598–610 (2015).
3. Nagel, D. H. & Kay, S. A. Complexity in the wiring and regulation of plant circadian networks. *Curr. Biol.* **22**, R648–R657 (2012).
4. Oakenfull, R. J. & Davis, S. J. Shining a light on the *Arabidopsis* circadian clock. *Plant Cell Environ.* **40**, 2571–2585 (2017).
5. Hogenesch, J. B. & Ueda, H. R. Understanding systems-level properties: timely stories from the study of clocks. *Nat. Rev. Genet.* **12**, 407 (2011).
6. Portolés, S. & Más, P. The functional interplay between protein kinase CK2 and CCA1 transcriptional activity is essential for clock temperature compensation in *Arabidopsis*. *PLoS Genet.* **6**, e1001201 (2010).
7. Hansen, L. L., van den Burg, H. A. & van Ooijen, G. Sumoylation contributes to timekeeping and temperature compensation of the plant circadian clock. *J. Biol. Rhythms* **32**, 560–569 (2017).
8. Marshall, C. M., Tartaglio, V., Duarte, M. & Harmon, F. G. The *Arabidopsis sickle* mutant exhibits altered circadian clock responses to cool temperatures and temperature-dependent alternative splicing. *Plant Cell* **28**, 2560–2575 (2016).
9. Salomé, P., Weigel, D. & McClung, C. The role of the *Arabidopsis* morning loop components CCA1, LHY, PRR7, and PRR9 in temperature compensation. *Plant Cell* **22**, 3650–3661 (2010).
10. Edwards, K. D., Lynn, J. R., Gyula, P., Nagy, F. & Millar, A. J. Natural allelic variation in the temperature-compensation mechanisms of the *Arabidopsis thaliana* circadian clock. *Genetics* **170**, 387–400 (2005).
11. Edwards, K. D. et al. *FLOWERING LOCUS C* mediates natural variation in the high-temperature response of the *Arabidopsis* circadian clock. *Plant Cell* **18**, 639–650 (2006).
12. Ito, S. et al. FLOWERING BHLH transcriptional activators control expression of the photoperiodic flowering regulator *CONSTANS* in *Arabidopsis*. *Proc. Natl Acad. Sci. USA* **109**, 3582–3587 (2012).
13. Gould, P. D. et al. Network balance via CRY signalling controls the *Arabidopsis* circadian clock over ambient temperatures. *Mol. Syst. Biol.* **9**, 650 (2013).
14. Nagel, D. H., Pruneda-Paz, J. L. & Kay, S. A. FBH1 affects warm temperature responses in the *Arabidopsis* circadian clock. *Proc. Natl Acad. Sci. USA* **111**, 14595–14600 (2014).
15. Jones, M. A., Morohashi, K., Grotewold, E. & Harmer, S. L. *Arabidopsis* JMJD5/JMJ30 acts independently of LUX ARRHYTHMO within the plant Circadian clock to enable temperature compensation. *Front. Plant Sci.* **10**, 57 (2019).
16. Gould, P. D. et al. The molecular basis of temperature compensation in the *Arabidopsis* circadian clock. *Plant Cell* **18**, 1177–1187 (2006).
17. Doyle, M. R. et al. The *ELF4* gene controls circadian rhythms and flowering time in *Arabidopsis thaliana*. *Nature* **419**, 74–77 (2002).
18. Kolmos, E. et al. Integrating *ELF4* into the circadian system through combined structural and functional studies. *HFSP J.* **3**, 350–366 (2009).
19. Herrero, E. et al. EARLY FLOWERING4 recruitment of EARLY FLOWERING3 in the nucleus sustains the *Arabidopsis* circadian clock. *Plant Cell* **24**, 428–443 (2012).
20. Nusinow, D. A. et al. The ELF4–ELF3–LUX complex links the circadian clock to diurnal control of hypocotyl growth. *Nature* **475**, 398–402 (2011).
21. Khanna, R., Kikis, E. A. & Quail, P. H. *EARLY FLOWERING 4* functions in phytochrome B-regulated seedling de-etiolation. *Plant Physiol.* **133**, 1530–1538 (2003).
22. McWatters, H. G. et al. *ELF4* is required for oscillatory properties of the circadian clock. *Plant Physiol.* **144**, 391–401 (2007).
23. Helfer, A. et al. *LUX ARRHYTHMO* encodes a nighttime repressor of circadian gene expression in the *Arabidopsis* core clock. *Curr. Biol.* **21**, 126–133 (2011).
24. Onai, K. & Ishiura, M. *PHYTOCLOCK 1* encoding a novel GARP protein essential for the *Arabidopsis* circadian clock. *Genes Cells* **10**, 963–972 (2005).
25. Hazen, S. P. et al. *LUX ARRHYTHMO* encodes a Myb domain protein essential for circadian rhythms. *Proc. Natl Acad. Sci. USA* **102**, 10387–10392 (2005).
26. Hicks, K. A. et al. Conditional circadian dysfunction of the *Arabidopsis early-flowering 3* mutant. *Science* **274**, 790–792 (1996).
27. Huang, H. et al. Identification of Evening Complex associated proteins in *Arabidopsis* by affinity purification and mass spectrometry. *Mol. Cell. Proteomics* **15**, 201–217 (2016).
28. Li, G. et al. Coordinated transcriptional regulation underlying the circadian clock in *Arabidopsis*. *Nat. Cell Biol.* **13**, 616–622 (2011).
29. Mizuno, T. et al. Ambient temperature signal feeds into the circadian clock transcriptional circuitry through the EC night-time repressor in *Arabidopsis thaliana*. *Plant Cell Physiol.* **55**, 958–976 (2014).
30. Siddiqui, H., Khan, S., Rhodes, B. M. & Devlin, P. F. PHY3 and FAR1 act downstream of light stable phytochromes. *Front. Plant Sci.* **7**, 175 (2016).
31. Ezer, D. et al. The evening complex coordinates environmental and endogenous signals in *Arabidopsis*. *Nat. Plants* **3**, 17087 (2017).
32. Kim, Y. et al. ELF4 regulates GIGANTEA chromatin access through subnuclear sequestration. *Cell Rep.* **3**, 671–677 (2013).
33. Nieto, C., López-Salmerón, V., Davière, J.-M. & Prat, S. ELF3–PIF4 interaction regulates plant growth independently of the evening complex. *Curr. Biol.* **25**, 187–193 (2015).
34. Sai, J. & Johnson, C. H. Different circadian oscillators control Ca^{2+} fluxes and *lhcb* gene expression. *Proc. Natl Acad. Sci. USA* **96**, 11659–11663 (1999).
35. Thain, S. C., Murtas, G., Lynn, J. R., McGrath, R. B. & Millar, A. J. The circadian clock that controls gene expression in *Arabidopsis* is tissue specific. *Plant Physiol.* **130**, 102–110 (2002).
36. Michael, T. P., Salome, P. A. & McClung, C. R. Two *Arabidopsis* circadian oscillators can be distinguished by differential temperature sensitivity. *Proc. Natl Acad. Sci. USA* **100**, 6878–6883 (2003).
37. Bordage, S., Sullivan, S., Laird, J., Millar, A. J. & Nimmo, H. G. Organ specificity in the plant circadian system is explained by different light inputs to the shoot and root clocks. *New Phytol.* **212**, 136–149 (2016).
38. Muranaka, T. & Oyama, T. Heterogeneity of cellular circadian clocks in intact plants and its correction under light-dark cycles. *Sci. Adv.* **2**, e1600500 (2016).
39. Thain, S. C., Hall, A. & Millar, A. J. Functional independence of circadian clocks that regulate plant gene expression. *Curr. Biol.* **10**, 951–956 (2000).

40. Fukuda, H., Nakamichi, N., Hisatsune, M., Murase, H. & Mizuno, T. Synchronization of plant circadian oscillators with a phase delay effect of the vein network. *Phys. Rev. Lett.* **99**, 098102 (2007).
41. Wenden, B., Toner, D. L. K., Hodge, S. K., Grima, R. & Millar, A. J. Spontaneous spatiotemporal waves of gene expression from biological clocks in the leaf. *Proc. Natl Acad. Sci. USA* **109**, 6757–6762 (2012).
42. Greenwood, M., Domijan, M., Gould, P. D., Hall, A. J. W. & Locke, J. C. W. Coordinated circadian timing through the integration of local inputs in *Arabidopsis thaliana*. *PLoS Biol.* **17**, e3000407 (2019).
43. Endo, M., Shimizu, H., Nohales, M. A., Araki, T. & Kay, S. A. Tissue-specific clocks in *Arabidopsis* show asymmetric coupling. *Nature* **515**, 419–422 (2014).
44. Yakir, E. et al. Cell autonomous and cell-type specific circadian rhythms in *Arabidopsis*. *Plant J.* **68**, 520–531 (2011).
45. Gould, P. D. et al. Coordination of robust single cell rhythms in the *Arabidopsis* circadian clock via spatial waves of gene expression. *eLife* **7**, e31700 (2018).
46. Fukuda, H., Ukai, K. & Oyama, T. Self-arrangement of cellular circadian rhythms through phase-resetting in plant roots. *Phys. Rev. E* **86**, 041917 (2012).
47. Takahashi, N., Hirata, Y., Aihara, K. & Mas, P. A hierarchical multi-oscillator network orchestrates the *Arabidopsis* circadian system. *Cell* **163**, 148–159 (2015).
48. James, A. B. et al. The circadian clock in *Arabidopsis* roots is a simplified slave version of the clock in shoots. *Science* **322**, 1832–1835 (2008).
49. Nimmo, H. G. Entrainment of *Arabidopsis* roots to the light:dark cycle by light piping. *Plant Cell Environ.* **41**, 1742–1748 (2018).
50. de Montaigu, A., Tóth, R. & Coupland, G. Plant development goes like clockwork. *Trends Genet.* **26**, 296–306 (2010).
51. Kolmos, E. et al. A reduced-function allele reveals that EARLY FLOWERING3 repressive action on the circadian clock is modulated by phytochrome signals in *Arabidopsis*. *Plant Cell* **23**, 3230–3246 (2011).
52. Dixon, L. E. et al. Temporal repression of core circadian genes is mediated through EARLY FLOWERING 3 in *Arabidopsis*. *Curr. Biol.* **21**, 120–125 (2011).
53. Kikis, E., Khanna, R. & Quail, P. ELF4 is a phytochrome-regulated component of a negative feedback loop involving the central oscillator components CCA1 and LHY. *Plant J.* **44**, 300–313 (2005).
54. Lu, S. X. et al. CCA1 and ELF3 interact in the control of hypocotyl length and flowering time in *Arabidopsis*. *Plant Physiol.* **158**, 1079–1088 (2012).
55. Huang, H. & Nusinow, D. A. Into the evening: complex interactions in the *Arabidopsis* circadian clock. *Trends Genet.* **32**, 674–686 (2016).
56. Corbesier, L. et al. FT protein movement contributes to long-distance signaling in floral induction of *Arabidopsis*. *Science* **316**, 1030–1033 (2007).
57. Jaeger, K. E. & Wigge, P. A. FT protein acts as a long-range signal in *Arabidopsis*. *Curr. Biol.* **17**, 1050–1054 (2007).
58. Mathieu, J., Warthmann, N., Küttner, F. & Schmid, M. Export of FT protein from phloem companion cells is sufficient for floral induction in *Arabidopsis*. *Curr. Biol.* **17**, 1055–1060 (2007).
59. Chen, X. et al. Shoot-to-root mobile transcription factor HY5 coordinates plant carbon and nitrogen acquisition. *Curr. Biol.* **26**, 640–646 (2016).
60. Flis, A. et al. Defining the robust behaviour of the plant clock gene circuit with absolute RNA timeseries and open infrastructure. *Open Biol.* **5**, 150042 (2015).
61. Salomé, P. A. & McClung, C. R. *PSEUDO-RESPONSE REGULATOR 7* and *9* are partially redundant genes essential for the temperature responsiveness of the *Arabidopsis* circadian clock. *Plant Cell* **17**, 791–803 (2005).
62. Edwards, K. D. et al. Quantitative analysis of regulatory flexibility under changing environmental conditions. *Mol. Syst. Biol.* **6**, 424 (2010).
63. Nakagawa, T. et al. Development of series of gateway binary vectors, pGWBs, for realizing efficient construction of fusion genes for plant transformation. *J. Biosci. Bioeng.* **104**, 34–41 (2007).
64. Nakagawa, T. et al. Improved gateway binary vectors: high-performance vectors for creation of fusion constructs in transgenic analysis of plants. *Biosci. Biotechnol. Biochem.* **71**, 2095–2100 (2007).
65. Clough, S. J. & Bent, A. F. Floral dip: a simlified method for *Agrobacterium*-mediated transformation of *Arabidopsis thaliana*. *Plant J.* **16**, 735–743 (1998).
66. Plautz, J. D. et al. Quantitative analysis of *Drosophila* period gene transcription in living animals. *J. Biol. Rhythms* **12**, 204–217 (1997).
67. Czechowski, T., Stitt, M., Altmann, T., Udvardi, M. K. & Scheible, W.-R. Genome-wide identification and testing of superior reference genes for transcript normalization in *Arabidopsis*. *Plant Physiol.* **139**, 5–17 (2005).
68. Dobin, A. et al. STAR: ultrafast universal RNA-seq aligner. *Bioinformatics* **29**, 15–21 (2013).
69. Liao, Y., Smyth, G. K. & Shi, W. featureCounts: an efficient general purpose program for assigning sequence reads to genomic features. *Bioinformatics* **30**, 923–930 (2014).
70. Robinson, M. D., McCarthy, D. J. & Smyth, G. K. edgeR: a Bioconductor package for differential expression analysis of digital gene expression data. *Bioinformatics* **26**, 139–140 (2010).
71. Robinson, J. T. et al. Integrative genomics viewer. *Nat. Biotech.* **29**, 24–26 (2011).
72. Thorvaldsdóttir, H., Robinson, J. T. & Mesirov, J. P. Integrative Genomics Viewer (IGV): high-performance genomics data visualization and exploration. *Brief. Bioinform.* **14**, 178–192 (2013).
73. Michael, T. P. et al. Network discovery pipeline elucidates conserved time-of-day-specific *cis*-regulatory modules. *PLoS Genet.* **4**, e14 (2008).
74. Mockler, T. et al. The Diurnal project: Diurnal and circadian expression profiling, model-based pattern matching, and promoter analysis. *Cold Spring Harb. Symp. Quant. Biol.* **72**, 353–363 (2007).
75. Katari, M. S. et al. VirtualPlant: A software platform to support systems biology research. *Plant Physiol.* **152**, 500–515 (2010).
76. Takens, F. in *Dynamical Systems and Turbulence* (eds Rand, D. & Young, L. S.) 366–381 (Springer, 1981).
77. Stark, J. Delay embeddings for forced systems I. Deterministic forcing. *J. Nonlinear Sci.* **9**, 255–332 (1999).
78. Marwan, N., Romano, C. M., Thiel, M. & Kurths, J. Recurrence plots for the analysis of complex systems. *Phys. Rep.* **438**, 237–329 (2007).
79. Hirata, Y., Horai, S. & Aihara, K. Reproduction of distance matrices and original time series from recurrence plots and their applications. *Eur. Phys. J.* **164**, 13–22 (2008).
80. Tanio, M., Hirata, Y. & Suzuki, H. Reconstruction of driving forces through recurrence plots. *Phys. Lett. A* **373**, 2031–2040 (2009).
81. Hirata, Y., Komuro, M., Horai, S. & Aihara, K. Faithfulness of recurrence plots: a mathematical proof. *Int. J. Bifurcation Chaos* **25**, 1550168 (2015).
82. Khor, A. & Small, M. Examining k-nearest neighbour networks: superfamily phenomena and inversion. *Chaos* **26**, 043101 (2016).
83. Small, M. *Applied Nonlinear Time Series Analysis: Applications in Physics, Physiology and Finance* (World Scientific, 2005).

Acknowledgements

We thank members of the Mas laboratory for helpful discussion and suggestions; T. Nakagawa and M. Seika Kaisha for the Gateway vectors; J. E. Salazar-Henao for tips on the western blot protocol in roots; and I. Rubio-Somoza for sharing the GFP antibody. Research in the Y.H. laboratory is supported by JSPS KAKENHI (Grant Number JP18K11461). The S.J.D. laboratory is funded by the Biotechnology and Biological Sciences Research Council (BB/N018540/1). S.A.K. acknowledges support from the National Institutes of Health (GM067837). The Mas laboratory is funded by the FEDER/Spanish Ministry of Economy and Competitiveness, the Ramon Areces Foundation and the Generalitat de Catalunya (AGAUR). The P.M. laboratory also acknowledges financial support from the CERCA Program, Generalitat de Catalunya and by the Spanish Ministry of Economy and Competitiveness through the Severo Ochoa Program for Centers of Excellence in R&D 2016–2019 (SEV-2015-0533). W.W.C. is a recipient of a Chinese Scholarship Council (CSC) fellowship.

Author contributions

W.W.C, N.T. and I.R. performed the biological experiments. Y.H. performed the mathematical analysis. S.P., S.J.D., D.A.N. and S.A.K. contributed reagents and comments. P.M. designed the experiments and wrote the manuscript. All authors read, revised and approved the manuscript.

Competing interests

The authors declare no competing interests.

Additional information

Extended data is available for this paper at https://doi.org/10.1038/s41477-020-0634-2.

Supplementary information is available for this paper at https://doi.org/10.1038/s41477-020-0634-2.

Correspondence and requests for materials should be addressed to P.M.

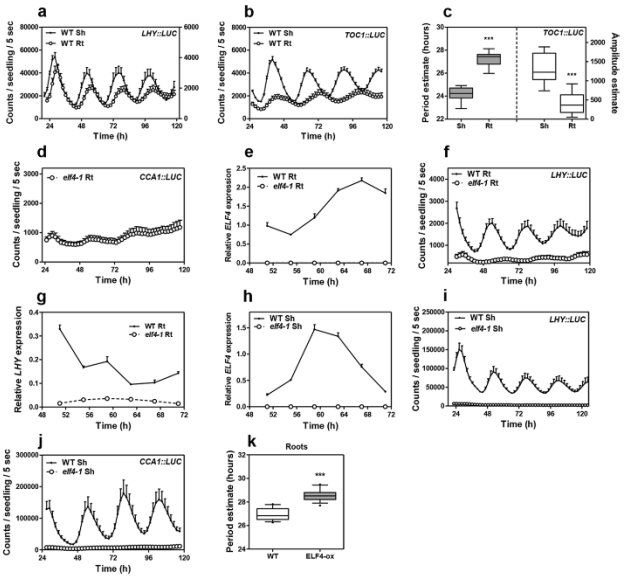

Extended Data Fig. 1 | Comparative analyses of rhythmic circadian oscillation in shoots and roots. Luminescence of **a**, *LHY::LUC* (n=6 for Sh, n=6 for Rt), and **b**, *TOC1::LUC* (n=16 for Sh, n=15 for Rt) rhythms simultaneously measured in shoots (Sh) and roots (Rt). Root luminescence signals in **a**, are represented in the right Y-axis. **c**, Circadian period (left Y-axis, n=16 for Sh, n=14 for Rt) and amplitude (right Y-axis, n=16 for Sh, n=15 for Rt) estimates of *TOC1::LUC* luminescence signals (data are represented as the median ± max and min; 25-75 percentile). *** p-value<0.0001; two-tailed t-tests with 95% of confidence. **d**, Luminescence of *CCA1::LUC* rhythms in *elf4-1* Rt (n=8) (from Fig. 1d) showing the weak rhythms of the mutant. **e**, Circadian time course analyses of *ELF4* mRNA expression in WT and *elf4-1* mutant Rt. **f**, Luminescence of *LHY::LUC* rhythms in WT (n=6) and *elf4-1* mutant Rt (n=6). **g**, Circadian time course analyses of *LHY* mRNA expression in roots of WT and *elf4-1*. **h**, Circadian time course analyses of *ELF4* mRNA expression in WT and *elf4-1* mutant Sh (also in Extended Data Fig. 3c). **i**, Luminescence of *LHY::LUC* (n=6) and **j**, *CCA1::LUC* (n=9) rhythms in WT and *elf4-1* mutant Sh. **k**, Circadian period estimates of *LHY::LUC* in WT (n=12) and ELF4-ox (n=14) roots; data are represented as the median ± max and min; 25-75 percentile). *** p-value<0.0001; two-tailed t-tests with 95% of confidence. **a-b, d-j,** Data are represented as the means + SEM. The mRNA expression and promoter activity analyses were performed under constant light conditions previous synchronization of plants under LD cycles at 22°C. The "n" values refer to independent samples. **a-k**, Two biological replicates were performed for all experiments, with measurements taken from distinct samples grown and processed at different times.

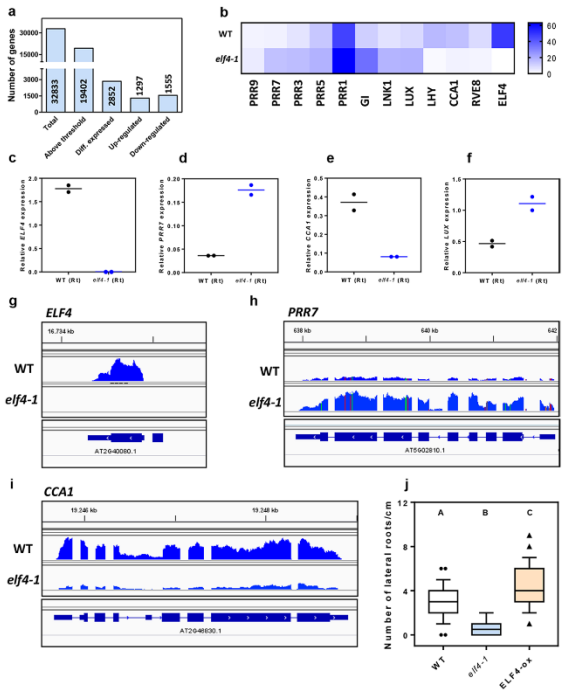

Extended Data Fig. 2 | RNA-Seq analyses of WT and *elf4-1* mutant roots. a, Quantitative analysis of DEGs in *elf4-1* versus WT roots. The statistical analyses of the DEGs are detailed in Materials and Methods. **b**, Heatmap of the median-normalized expression (Z-scaled FPKM values) of the oscillator genes in WT and *elf4-1* roots. Analyses by RT-QPCR of **c**, *ELF4*, **d**, *PRR7*, **e**, *CCA1* and **f**, *LUX* mRNA expression in roots at CT75 after three days in LL. Visualization of RNA-seq reads by using the Integrative Genomics Viewer (IGV) browser for **g**, *ELF4*, **h**, *PRR7*, **i**, and *CCA1*. **j**, Number of lateral roots per cm in the Ws-2 (WT, n=86), *elf4-1* (n=28) or ELF4-ox lines (n=48). Plants were grown for 12 days under short day (8h light:/16h darkness) photoperiod with a constant temperature of 22°C. Letters signify significant difference ($p<0.01$) as determined by a one-way ANOVA with a Tukey HSD post hoc test. Data is represented as the median ± max and min; 25-75 percentile). Data represents an average of two independent experiments.

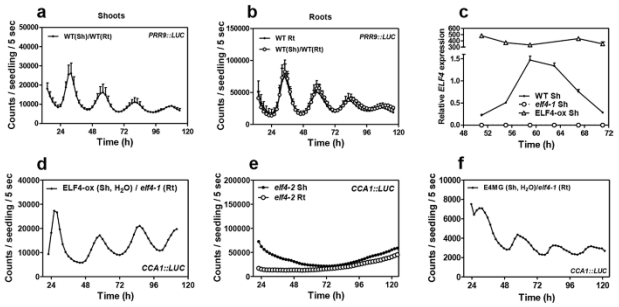

Extended Data Fig. 3 | Analyses of circadian rhythmicity of the micrografting assays. Luminescence of *PRR9::LUC* in **a**, shoots (n=3) and **b**, roots (n=3) of WT scion into WT rootstocks and its comparison with luminescence in (non-grafted) WT roots (n=4). **c**, Circadian time course analyses of *ELF4* mRNA expression in shoots of WT, *elf4-1* and ELF4-ox (also in Extended Data Fig. 1h). **d** Individual waveform of *CCA1::LUC* rhythmic recovery in roots of ELF4-ox scion and *elf4-1* rootstocks. Water instead of luciferin was added to the wells containing ELF4-ox shoots. **e**, *CCA1::LUC* luminescence in shoots and roots of *elf4-2* mutant plants (n=5 for each). **f**, Individual waveform of *CCA1::LUC* rhythmic recovery in roots of E4MG scion into *elf4-1* rootstocks. Water instead of luciferin was added to the wells containing E4MG shoots. **a–f**, Data are represented as the means + SEM. The mRNA expression and promoter activity analyses were performed under constant light conditions previous synchronization of plants under LD cycles at 22°C. The "n" values refer to independent samples. **a–f**, Two biological replicates were performed for all experiments, with measurements taken from distinct samples grown and processed at different times.

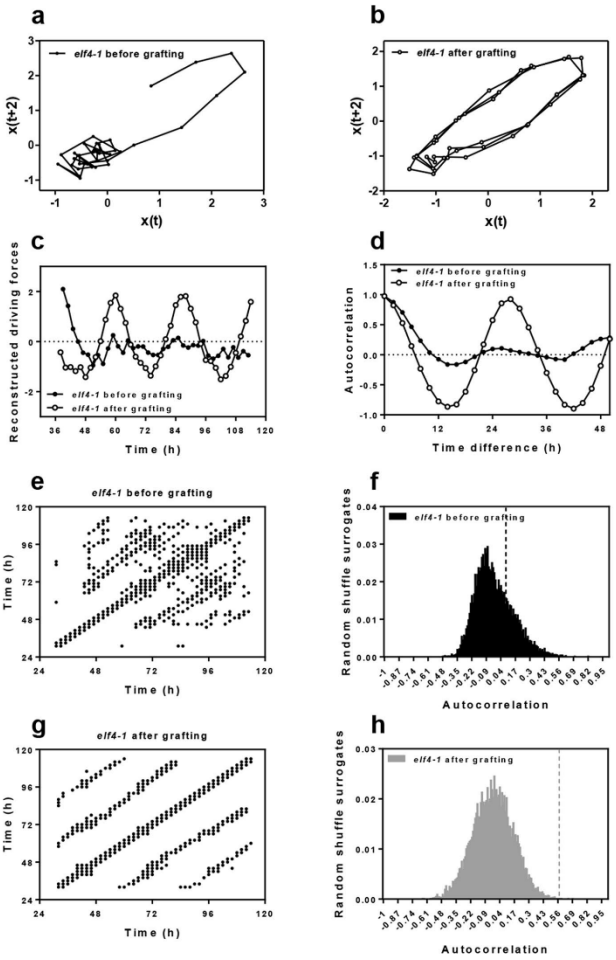

Extended Data Fig. 4 | Mathematical analyses of the micrografting effects on rhythms. Two-dimensional plots of *CCA1::LUC* rhythms in roots **a**, before and **b**, after grating ELF4-ox scion into *elf4-1* rootstocks. **c**, Reconstructed waveforms and **d**, autocorrelation analyses in roots before and after grafting. **e**, **g**, Recurrence plots for the driver obtained by delay coordinates and autocorrelation analyses **f**, before and **h**, after ELF4-ox scion grafting into *elf4-1* rootstock. Number of surrogates for each test: 10000. Before grafting: 95% confidence interval: [−1 0.2932]; effect size: 0.0975; p-value: 0.2339. After grafting: 95% confidence interval: [−1 0.2720]; effect size: 0.5752; p-value: 0.00045.

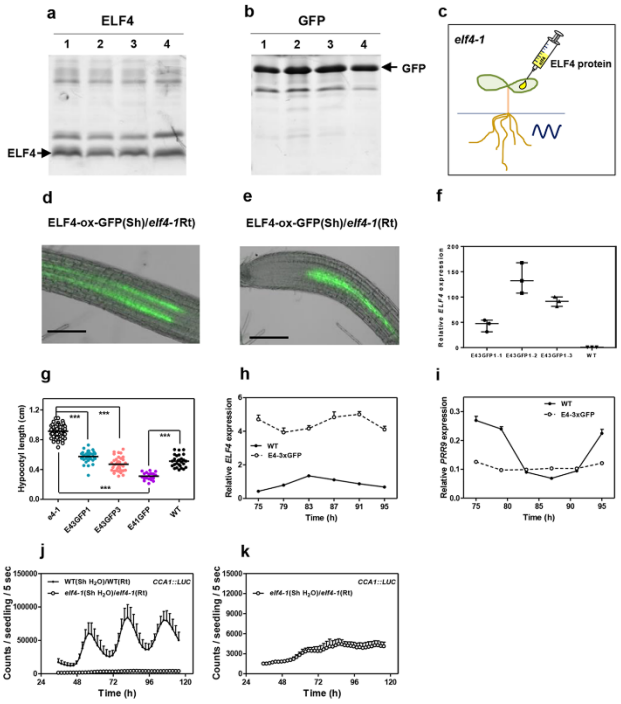

Extended Data Fig. 5 | Analyses of ELF4 movement from shoots to roots. a, ELF4 and **b**, GFP proteins purified from bacteria and **c**, injected in shoots of *elf4-1* mutant plants to examine rhythmic recovery in roots. **d, e**, Representative images showing fluorescence signals in roots of ELF4-ox-GFP scion and *elf4-1* rootstock. Scale bars: 100µm. **f**, Gene expression analyses of *ELF4* mRNA expression in WT and different ELF4-x3GFPs lines. Data are represented as the median ± max and min; 25-75 percentile. **g**, Hypocotyl length of different lines expressing ELF4-x3GFPs (E43GFP) (E43GFP1 n=34; E43GFP3 n=35) transformed into *elf4-1* mutant plants. Hypocotyl length was also assayed for WT (n=27), *elf4-1* (n=48) and plants over-expressing ELF4 fused to 1 GFP (E41GFP) (n=19). *** p-value<0.0001; two-tailed t-tests with 95% of confidence. Data are represented as the median ± max and min; 25-75 percentile. Circadian time course analyses of **h**, *ELF4*, and **i**, *PRR9* mRNA expression by RT-QPCR in shoots of WT and ELF4-x3GFPs. **j**, Luminescence of *elf4-1* scion into *elf4-1* rootstocks *elf4-1* (Sh)/*elf4-1*(Rt) (n=4) and its comparison with luminescence in WT (Sh)/WT(Rt) roots (n=5). **k**, Luminescence signals of *elf4-1* (Sh)/*elf4-1*(Rt) from **j**, shown in a separate graph. Water instead of luciferin was added to the wells containing WT and *elf4-1* shoots. **h-k**, Data are represented as the means + SEM. **a-k**, At least two biological replicates were performed for all experiments, with measurements taken from distinct samples grown and processed at different times.

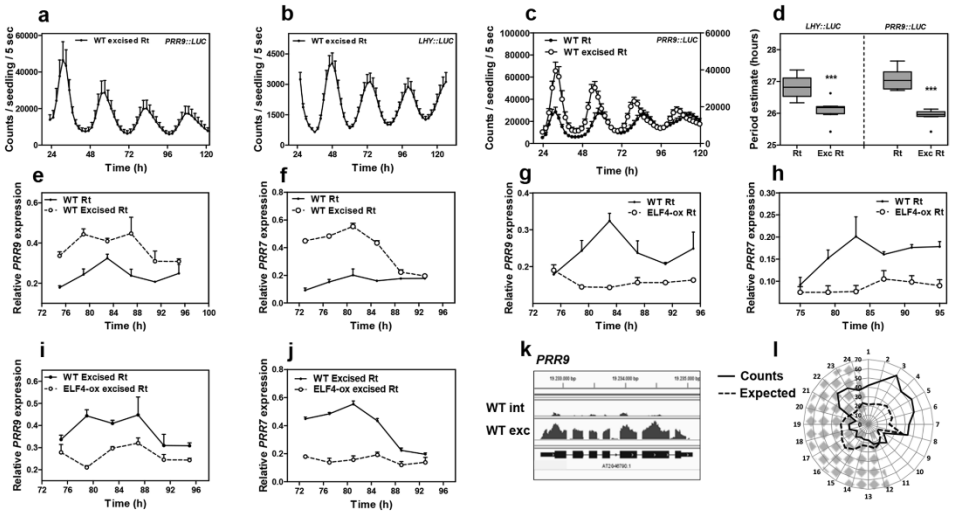

Extended Data Fig. 6 | Shoot excision advances the phase and shortens the circadian period in roots. Luminescence of **a**, *PRR9::LUC* (n=5) and **b**, *LHY::LUC* (n=8) circadian rhythms in WT excised roots. **c**, Comparison of *PRR9::LUC* circadian rhythms in WT intact (n=6) versus excised roots (n=6). **d**, Period estimates of *LHY::LUC* (left graph) (n=8) and *PRR9::LUC* (right graph) (n=8) rhythms in WT intact versus excised roots. Data are represented as the median ± max and min; 25-75 percentile. *** p-value<0.0001; two-tailed t-tests with 95% of confidence. Circadian time course analyses of **e**, *PRR9* and **f**, *PRR7* mRNA expression in WT intact versus excised roots. Circadian time course analyses of **g**, *PRR9* and **h**, *PRR7* mRNA expression in WT and ELF4-ox intact roots. Circadian time course analyses of **i**, *PRR9* and **j**, *PRR7* mRNA expression in WT excised and ELF4-ox excised roots. **a-c, e-j**, Data are represented as the means + SEM. **k**, Visualization of *PRR9* RNA-seq reads by using the Integrative Genomics Viewer (IGV) browser. **l**, Circadian phases of overlapped DEGs in *elf4-1* and WT excised roots relative to WT intact roots. Radial axis represents the subjective time (hours). White and gray areas represent subjective day and night, respectively. The mRNA expression and promoter activity analyses were performed under constant light conditions previous synchronization of plants under LD cycles at 22°C. The "n" values refer to independent samples. **a-l**, Two biological replicates were performed for all experiments, with measurements taken from distinct samples grown and processed at different times.

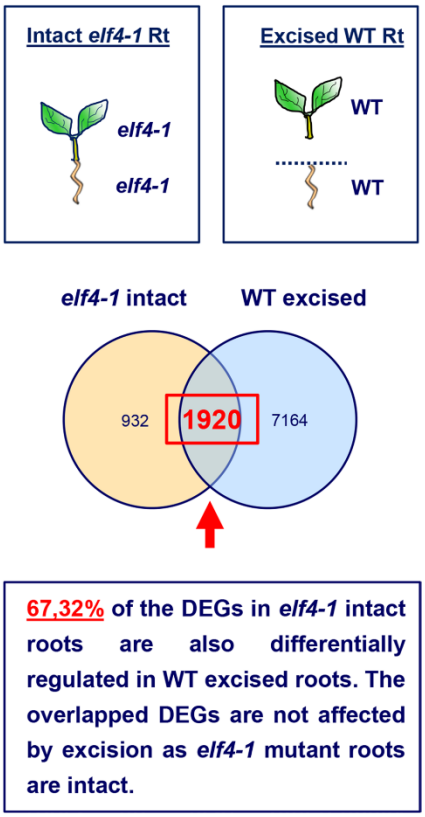

Extended Data Fig. 7 | The lack of ELF4 movement affects gene expression in roots. Schematic drawing depicting the RNA-Seq comparison of different root genotypes (*elf4-1* mutant versus WT) and conditions (intact versus excised). The proportion of overlapped DEGs (67%) is highly significant (P-value < 0.0001, chi-square test for equality of proportions) compared to the overlapped proportion of genes (30%) using random gene lists with the same counts as the DEGs in WT excised roots. The overlapped genes cannot be the result of excision because the data of *elf4-1* mutant roots come from intact roots.

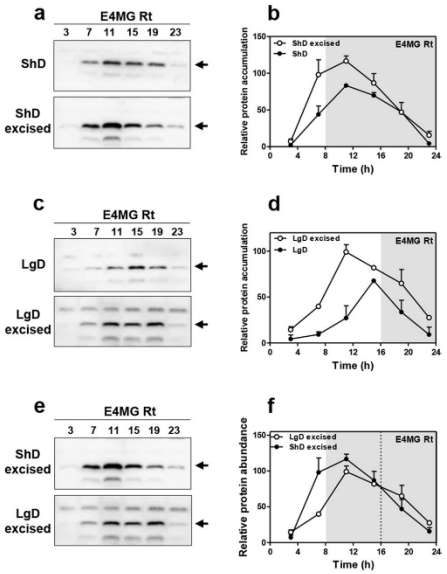

Extended Data Fig. 8 | Excision advances the phase of ELF4 protein accumulation in roots under entraining conditions. a, Western-blot analysis and **b**, quantification of ELF4 protein accumulation in ELF4 minigene (E4MG) intact and excised roots under ShD (also in Fig. 3c, d). **c**, Western-blot analysis and **d**, quantification of ELF4 protein accumulation in E4MG intact and excised roots under LgD (also in Fig. 3e, f). **e**, Western-blot analysis and **f**, quantification of ELF4 protein accumulation in E4MG excised roots under ShD and LgD (also in Fig. 3e, f). **b, d, f**, Data are represented as the means + SEM. **a–f**, Two biological replicates were performed for all experiments, with measurements taken from distinct samples grown and processed at different times.

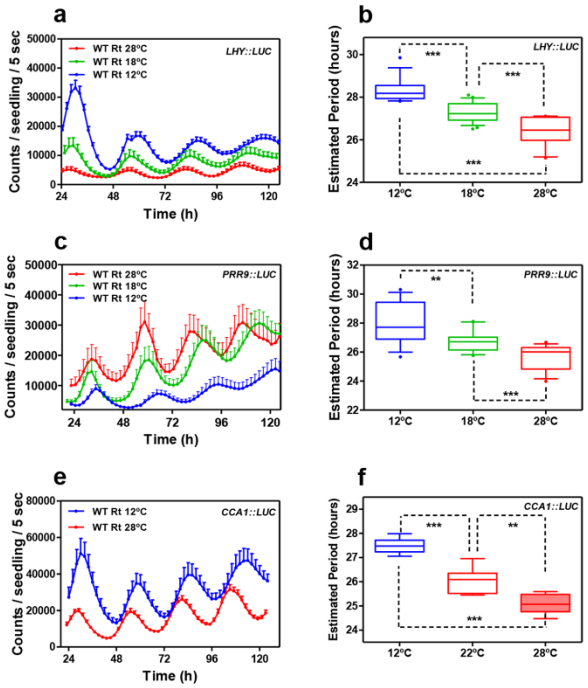

Extended Data Fig. 9 | The root clock is not temperature-compensated. a, Luminescence waveforms of *LHY::LUC* rhythmic oscillation in WT roots at 28°C (n=8), 18°C (n=8) and 12°C (n=8) and **b**, circadian period estimates of *LHY::LUC* rhythmic oscillation in WT roots at 28°C (n=12), 18°C (n=23) and 12°C (n=14). Data are represented as the median ± max and min; 25-75 percentile. **c**, Luminescence waveforms of *PRR9::LUC* rhythmic oscillation in roots at 28°C (n=8), 18°C (n=16) and 12°C (n=8) and **d**, circadian period estimates of *PRR9::LUC* rhythmic oscillation in roots at 28°C (n=14), 18°C (n=16) and 12°C (n=12). Data are represented as the median ± max and min; 25-75 percentile. **e**, Luminescence waveforms and **f**, circadian period estimates of *CCA1::LUC* rhythmic oscillation in roots at 28°C (n=6), 22°C (n=6) and 12°C (n=6) Data are represented as the median ± max and min; 25-75 percentile. **b d, f**, *** p-value<0.0001; ** p-value<0.005; two-tailed t-tests with 95% of confidence. **a, c, e**, Data are represented as the means + SEM. The "n" values refer to independent samples. **a-f**, Two biological replicates were performed for all experiments, with measurements taken from distinct samples grown and processed at different times.

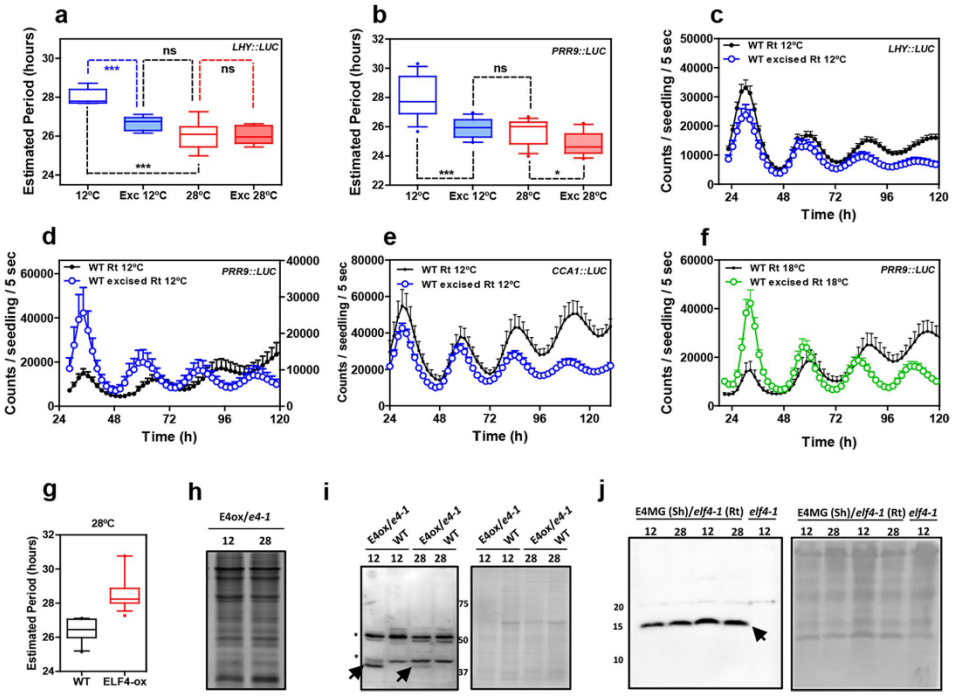

Extended Data Fig. 10 | Circadian rhythms in excised roots at various temperatures. Circadian period estimates of **a**, *LHY::LUC* in intact (n=8) versus excised WT roots (n=7) at 12°C and 28°C (n=8 for intact and n=8 for excised) and **b**, *PRR9::LUC* in intact (n=12) versus excised WT roots (n=13) at 12°C and 28°C (n=14 for intact and n=16 for excised). Data are represented as the median ± max and min; 25-75 percentile. *** p-value<0.0001; * p-value<0.05; ns: non-significant p=0.369; two-tailed t-tests with 95% of confidence. Luminescence rhythmic oscillation in WT intact and excised roots (n=8 for each) at 12°C of **c**, *LHY::LUC*, **d**, *PRR9::LUC* (n=8 for each) and **e**, *CCA1::LUC* (n=4 for excised, n=5 for intact). **f**, Luminescence of *PRR9::LUC* rhythmic oscillation in WT intact and excised roots at 18°C (n=16 for each). **c-f**, Data are represented as the means + SEM. **g**, Circadian period estimates of *LHY::LUC* in WT (n=12) and ELF4-ox (n=17) at 28°C. Data are represented as the median ± max and min; 25-75 percentile. Promoter activity analyses were performed under constant light conditions previous synchronization of plants under LD cycles at 22°C. **h**, Coomassie Blue staining of protein extracts from roots of ELF4-ox-GFP scion (E4-ox) grafted into *elf4-1* rootstock (*e4-1*) at 12°C and 28°C. **i**, Western-blot analyses of ELF4-GFP protein accumulation (arrows) in roots of ELF4-ox-GFP scion (E4-ox) grafted into *elf4-1* rootstock (*e4-1*) at 12°C and 28°C. WT protein extracts were used as a control. Asterisks denote non-specific bands. Ponceau S staining of the membrane is shown in the right panel. **j**, Western-blot analyses of ELF4 protein accumulation (arrow) in shoots of ELF4 minigene (E4MG) grafted into *elf4-1* rootstock (*e4-1*) at 12°C and 28°C. *elf4-1* protein extracts were used as a control. Ponceau S staining of the membrane is shown in the right panel. The "n" values refer to independent samples. **a-j**, Two biological replicates were performed for all experiments, with measurements or analyses taken from distinct samples grown and processed at different times.